Aeroelastic Analysis of Multi-Rotor System Wind Turbines

アムル, モハメド, メトワッリ, イスマイル

https://doi.org/10.15017/2534483

出版情報：Kyushu University, 2019, 博士（学術）, 課程博士
バージョン：
権利関係：

九州大学

Aeroelastic Analysis of Multi-Rotor System Wind Turbines
マルチロータ風力発電システムの空力弾性解析

by

Amr Mohamed Metwally Ismaiel

アムル　モハメド　メトワッリ　イスマイル

Submitted to the Earth System Science and Technology Department

In partial fulfillment of the requirements for the degree of

Doctor of Philosophy in Engineering

at

Kyushu University

September 2019

This page is intentionally left blank.

Aeroelastic Analysis of Multi-Rotor System Wind Turbines

by

Amr Mohamed Metwally Ismaiel

Submitted to the Earth System Science and Technology Department

On July 2019

In partial fulfillment of the
requirements for the degree of

Doctor of Philosophy in Engineering

Abstract

The approach to increase the harvested power out of wind in the past few decades, was by increasing the size of the rotor of a wind turbine. Multi-rotor system (MRS) wind turbines can be a competitive alternative to large-scale wind turbines.

MRS are superior to large-scale wind turbines from the aspect of less weight/power ratio, ease of transportation and maintenance. However, one of the main challenges of MRS wind turbines is the

complex supporting structure. The tower of MRS is subject to complex dynamic loads and coupled vibrational modes which are difficult to model, and hence manufacture.

The aim of this thesis is to address the structural behaviour of the MRS turbine tower. In order to do this, an in-house aeroelastic tool has been developed to study the dynamic responses of a MRS configuration wind turbine consisting of multiplicands of the NREL 5MW rotor. The developed tool has been verified by comparing the results of a single-rotor configuration to a FAST analysis for the same simulation conditions.

Steady flow and turbulent load cases were investigated for the twin-rotor configuration. The results of the simulations have shown that the elasticity of the tower should be considered for studying tower dynamic responses. The tower loads, and deformations are not straightforward with the number of rotors added. For an equivalent tower, an additional rotor will increase the tower-top deflection, and the tower-base bending moment both in the fore-aft direction to be more than doubled. The tower torsional stiffness becomes a crucial factor in the case of the twin-rotor tower to avoid severe torsional deflection. Tower natural frequencies are dominant over the flow conditions regarding the loads and deflections.

Furthermore, Three-Rotor and Four-Rotor configurations were modeled. Dynamic responses for each configurations' tower have been studied. The results showed that severer loads appear on the tower, although a stiffer tower was used to support those configurations. It also showed that the effect of a single-rotor in a MRS

configuration on the torsional stresses are reduced compared to the twin-rotor configuration

Thesis Supervisor: Dr. Shigeo Yoshida
Title: Professor
Date: 31/7/2019

This page is intentionally left blank.

Declaration

No portion of the work referred to in the thesis has been submitted in support of an application for another degree or qualification of this or any other university or other institute of learning.

This page is intentionally left blank.

Dedication

With all love and respect, I dedicate this work to the soul of my father, whom without I wouldn't be a responsible person capable of learning and benefiting myself, and I wouldn't be able to achieve any of my dreams.

This page is intentionally left blank.

Acknowledgments

First of all, I would like to express my deepest gratitude to my supervisor; **Prof. Shigeo Yoshida** for his continuous support, technical guidance, and providing the perfect work environment. Your precious comments and mentoring have improved the quality and output of this work throughout the whole three years. I am so grateful and so proud to be a member of the laboratory of Professor Yoshida.

Prof. Changhong Hu and **Prof. Nobuhide Uda**; thank you so much for your precious time reviewing my thesis. Your valuable comments and suggestions have enhanced the quality of my work.

I should also thank the Ministry of Education, Culture, Sports, Science, and Technology (**MEXT**), Japan government, for completely funding my PhD research and degree. Also, I should thank the Interdisciplinary Graduate School of Engineering Sciences (**IGSES**) for funding the expenses of my internships and scientific conferences.

I must thank the student support center and the support section in IGSES. You have been of great help during all the three years. I would like to specially thank **Ms. Kojima**, **Ms. Akiko**, **Ms. Nagamine**, **Ms. Nishiyama**, and everyone else in this amazing and professional place.

I would also like to thank all the staff of Yoshida-lab. Academic staff; specially **Dr Yingyi Liu**, technical staff; **Mr. Masahiro Hamasaki**, and administrative staff**; Ms. Sakura Kawasaki**, and **Ms. Yukiko Matsuse**, for

all your kind help and support in all aspects during my 3 years PhD program.

A major role in the achievement of this thesis was due to the efforts of **Prof. Taeseong Kim**, and **Prof. Martin Hansen** of the Technical University of Denmark (**DTU**). My three months internship in DTU was the main reason I was able to complete my work and have a better understanding of the theory I used in accomplishing this thesis. The technical help I got from Prof. Hansen and Prof. Kim was the cornerstone of my code, thank you a lot. Also, thanks to all the staff of DTU university for your kind welcoming in your community and helping me in the social life during my stay. Thanks to my friend **Ayman Nassar**.

A million thank you to **Benny**, **Laura**, **Freja**, and **Wilma** for your kind hospitality while hosting me during my stay in Denmark. Your kindness has made me feel like I'm home and a member of the family. This has made my life a lot easier while in Denmark. I will be forever grateful to you. I wish we will meet again one day.

My friends in the KU IGSES International Students Association (KIISA), since day one in Japan, I've been a member of your amazing community. Your efforts in supporting international students' lives are so impressive. I have shared a lot of fun times with you, thank you a lot for that. Special thank you to my dear friends; **John**, **Alisa**, **Alicia**, and **Moses**.

My **classmates of the 3rd batch of the IEI** PhD program, thank you for everything. We have been working together as a team specially in

organizing the IEICES conference. You have been amazing friends and the best team I could ever work with. Thank you so much.

My friend and mentor **Dr. Mohamed Kamra**, you have been my tutor one day, and yet you have come to be a friend who has helped me a lot during my study whether in the undergraduate or the post graduate studies. Thank you so much.

My dear friends **Ibrahim**, **Nassef**, **Ali**, **Islam**, **Sameh**, **Egiza**, **Abdelrahman**, **Hatem**, **Omar**, **Tarek Attia**, **Tarek Amen**, **Ramadan**, **Sami**, **Jabir**, and many more, thank you guys for all the awesome events we had. My life in Japan was made enjoyable by all of you.

Thanks to Future University in Egypt (FUE), for allowing me to travel and pursue the PhD degree. Thanks to the faculty and department board members. Specially **Prof. Mohamed Badr**, **Prof. Mohamed Aboelela**, **Prof. Mostafa Zidan**, **Prof. Rafat Okelah**, **Prof. Yehia Hendawy**, and **Prof. Sayed Atta**. Also thank you to my colleagues and friends who have been supporting me overseas, specially **Dr. Hassan**, **Rana**, **Anas**, **Ahmed Adel**, **Amira**, **Mostafa**, **Abdelbarr**, **Zakaria**, **Dr. Samah**, **Essam**, **Doaa**, **Aya**, **Nada**, and many more. Also, my friends from the administrative staff **Doaa**, **Mona**, and **Ali**.

My wonderful friends in Egypt who has been in contact with me all the time, encouraging me and checking up on me. I would like to thank you all. Especially **Passant**, **Mohab**, **Omar**, **Sami**, **Mostafa**, **Ahmed**, **Behery**, and many more. Thank you so much.

My dearest friends, the companions of my journey; **Tarek Dief**, **Amr Halawa**, and **Mostafa Rushdi**. We have started this journey about 12 years ago since the undergraduate studies, and yet we continued together till we achieved the PhD. We have been together through ups and downs, through happiness and sorrow, and you have been always of great support to me when I feel down or insecure about my progress in study or any other aspect. No words can describe how grateful I am to you.

Last but not least, my family, my source of power, who has sacrificed a lot so that I can achieve this degree. My mother **Nabila**, my sister **Injy**, my best friend and brother-in-law **Basem**. You have supported me by all means, you have waited and have borne my absence for 3 years. However, you have been with me for all my steps despite the distance, you have taken care of me while I'm away, and I wish I can pay back your sacrifices after my return.

Amr Ismaiel

Kyushu University

August 2019

Nomenclature

Abbreviations

3D	Three Dimensional
BEM	Blade Element Momentum
CFD	Computational Fluid Dynamics
DOF	Degrees of Freedom
DTU	Technical University of Denmark
FAST	Fatigue-Aerodynamics-Structure-Turbulence
FFT	Fast Fourier Transform
FSI	Fluid Structure Interaction
GM	Generalized Mass
HAWT	Horizontal Axis Wind Turbines
IEC	International Electrotechnical Commission
MRS	Multi-Rotor System
NREL	National Renewable Energy Laboratory
RK	Runge-Kutta

SRS	Single-Rotor System
VSC	Variable Speed Control

Greek Symbols

α	Angle of Attack
β	Twist Angle
δ	Logarithmic Decrement for Damping
θ_p	Pitch Angle
ρ	Air Density
φ	Flow Angle
ω	Rotational Speed
ω_{e1}	Blade 1st Edge-wise Natural Frequency
ω_{f1}	Blade 1st Flap-wise Natural Frequency
ω_{f2}	Blade 2nd Flap-wise Natural Frequency
ω_{fa1}	Tower 1st Fore-Aft Natural Frequency
ω_{fa2}	Tower 2nd Fore-Aft Natural Frequency
ω_{ss1}	Tower 1st Side-Side Natural Frequency

θ_A	Rotor Azimuth Angle
θ_c	Rotor Cone Angle
θ_t	Rotor Tilt Angle

Roman Symbols

B	Number of Blades
c	Chord Length
$\boldsymbol{C}$	Damping Matrix
C_D	Drag Coefficient
C_L	Lift Coefficient
D	Drag Force
F	Prandtl's Tip-Loss Factor
f_g	Glauert Correction Factor
$\boldsymbol{F_g}$	Generalized Forces Array
$\boldsymbol{K}$	Stiffness Matrix
L	Lift Force
L_{aero}	Aerodynamic Force/Load

$\boldsymbol{M}$	Mass Matrix
m'	Mass Density
$\boldsymbol{r}$	Blade-Section Position
u	Blade/Tower Deformation
$\dot{u}$	Blade/Tower Vibrational Velocity
$\ddot{u}$	Blade/Tower Vibrational Acceleration
u^{e1}	1st Edge-Wise Mode Shape
u^{f1}	1st Flap-Wise Mode Shape
u^{f2}	2nd Flap-Wise Mode Shape
u^{fa1}	1st Fore-Aft Mode Shape
u^{fa2}	2nd Fore-Aft Mode Shape
u^{ss1}	1st Side-Side Mode Shape
$\boldsymbol{V_0}$	Inflow Velocity
$\boldsymbol{V_{rel}}$	Relative Velocity
w	Induced Velocity
$\boldsymbol{x}$	Degrees of Freedom Array
$\dot{\boldsymbol{x}}$	DOF 1st Time-Derivative Array

$\ddot{\boldsymbol{x}}$	DOF 2nd Time-Derivative Array

Subscripts/Superscripts/Accents

$\dot{}$	1st Time-Derivative
$\ddot{}$	2nd Time-Derivative
‘	Quantity Per Unit Length
e1	1st Edge-Wise Component
f1	1st Flap-Wise Component
f2	2nd Flap-Wise Component
fa1	1st Fore-Aft Component
fa2	2nd Fore-Aft Component
ss1	1st Side-Side Component
XB	Component in X_B axis direction
YB	Component in Y_B axis direction

This page is intentionally left blank.

Contents

Nomenclature XV

List of Figures XXV

List of Tables XXIX

1. Introduction 1

1.1. Historical Background 1

1.2. Global Wind Energy Status 6

1.3. Advantages of MRS 8

1.4. State of the Art Research on MRS 10

1.5. Problem Statement and Objective 13

1.6. Methodology 13

1.7. Novelty 16

1.8. Thesis Overview 16

2. Mathematical Model 19

2.1. Chapter Overview 19

2.2. Aerodynamic Model 20

2.3. Structure Model 23

2.4. Aeroelastic Coupling 27

2.5. NREL Aeroelastic Tools 28
2.5.1. Modes 29
2.5.2. TurbSim 29
2.5.3. FAST 32
3. Verification with a Single-Rotor Model 35
3.1. Chapter Overview 35
3.2. Model Outline 36
3.3. Rotor Aerodynamics 38
3.4. Modal Analysis 40
3.4.1. Blades 40
3.4.2. Tower 42
3.5. Aeroelastic Analysis 43
3.5.1. Blades 44
3.5.2. Tower 46
3.6. Chapter Summary 47
4. Simulation of Twin-Rotor Model 49
4.1. Chapter Overview 49
4.2. Twin-Rotor Wind Turbine Model 50
4.3. Tower Analysis 53
4.3.1. Steady Flow Condition 53

4.3.2. Turbulent Flow Condition....58
4.4. Side-Boom Analysis....65
4.5. Chapter Summary....72
5. Simulation of Multi-Rotor Configurations....73
5.1. Chapter Overview....73
5.2. Three-Rotor Configuration....73
5.2.1. Three-Rotor Tower Analysis....76
5.3. Four-Rotor Configuration....81
5.2.2. Four-Rotor Tower Analysis....84
5.4. Chapter Summary....89
6. Conclusions....91
6.1. Main Findings....91
6.2. Future Work....94
Bibliography....95
Appendix A: FAST Input Files....103
A.1 FAST Primary Input File....103
A.2 Elastodyn Input File....105
A.3 Wind File....110
A.4 AeroDyn Input File....112

A.5 Blade Input File 115

A.6 Tower Input File 118

A.7. Airfoil-Data Input File 120

A.7.1. Cylinder 1 120

A.7.2. Cylinder 2 121

A.7.3. DU21-A17 123

A.7.4. DU25-A17 128

A.7.5. DU30-A17 132

A.7.6. DU35-A17 136

A.7.7. DU40-A17 140

A7.8. NACA64-A17 145

A.8. ServoDyn Input File 149

7. List of Publications 153

List of Figures

Figure 1.1. Pharaonic sail boat [2] 2
Figure 1.2. Heron's wind powered Machine 3
Figure 1.3. Medieval photograph of a windmill 3
Figure 1.4. The world's first Mega-Watt sized wind turbine 5
Figure 1.5. Global cumulative installed wind capacity 2001-2017 [10] 6
Figure 1.6. World's top 10 cumulative wind capacity [10] 7
Figure 1.7. World's largest wind turbines [13] 8
Figure 1.8. Conceptual MRS made by Honnef on 1930 [15] 9
Figure 1.9. 4R-V29 wind turbine located at the Risø campus, DTU [20] 12

Figure 2.1. Analysis flow chart 20
Figure 2.2. Blade coordinates system [27] 21

Figure 3.1. NREL 5MW wind turbine blade [32] 36
Figure 3.2. Blade mass density distribution 37
Figure 3.3. Blade stiffness distribution 37
Figure 3.4. Tower mass density distribution 38
Figure 3.5. Tower stiffness distribution 38
Figure 3.6. Steady state responses for different wind speeds [31] 39
Figure 3.7. Steady state responses - Comparison between results of the developed tool to NREL reference file 39
Figure 3.8. Blade flap-wise mode shapes 41
Figure 3.9. Blade edge-wise mode shape 41

Figure 3.10. Tower fore-aft mode shapes - Single rotor configuration 42
Figure 3.11. Tower side-side mode shape - Single rotor configuration 43
Figure 3.12. Blade-root, flap-wise bending moment 44
Figure 3.13. Blade-root, edge-wise bending moment.....45
Figure 3.14. Blade-tip, flap-wise deflection.....45
Figure 3.15. Blade-tip, edge-wise deflection 45
Figure 3.16. Tower-base, fore-aft bending moment 46
Figure 3.17. Tower-top, fore-aft deflection.....47

Figure 4.1. Sketch of the twin-rotor configuration 50
Figure 4.2. Tower mass density distribution – Single-rotor Vs. Twin-rotor 52
Figure 4.3. Tower stiffness distribution – Single-rotor Vs. Twin-rotor.....52
Figure 4.4. Tower-base fore-aft bending moment - Stiff Vs. Elastic Tower54
Figure 4.5. Tower-base, fore-aft bending moment 55
Figure 4.6. Tower-top, fore-aft deflection 55
Figure 4.7. Tower-base, fore-aft bending moment - Single-rotor Vs Twin-rotor 56
Figure 4.8. Tower-top, fore-aft deflection - Single-rotor Vs Twin-rotor 56
Figure 4.9. Tower-base, fore-aft bending moment 57
Figure 4.10. Tower-top, fore-aft deflection.....57
Figure 4.11. Tower top yawing deflection – 60^0 phase difference.....58
Figure 4.12. Average wind speed at hub height.....59
Figure 4.13. Tower-base fore-aft bending moment – Turb. Class A 59
Figure 4.14. Tower-top fore-aft deflection – Turb. Class A 60
Figure 4.15. Tower-top yawing deflection – Turb. Class A 60

Figure 4.16. Tower-base fore-aft bending moment – Turb. Class B.....61
Figure 4.17. Tower-top fore-aft deflection – Turb. Class B.....61
Figure 4.18. Tower-top yawing deflection – Turb. Class B.....62
Figure 4.19. Tower-base fore-aft bending moment – Turb. Class C.....62
Figure 4.20. Tower-top fore-aft deflection – Turb. Class C.....62
Figure 4.21. Tower-top yawing deflection – Turb. Class C.....63
Figure 4.22. Frequency analysis, tower-base bending moment - Turb. Class A.....63
Figure 4.23. Frequency analysis, tower-base bending moment - Turb. Class B.....64
Figure 4.24. Frequency analysis, tower-base bending moment - Turb. Class C.....64
Figure 4.25 Side-boom mass density distribution.....66
Figure 4.26. Side-boom stiffness distribution.....67
Figure 4.27. Fore-aft tip deflection - Side-boom 1 - Turb. Class A.....67
Figure 4.28. Side-side tip deflection - Side-boom 1 - Turb. Class A.....68
Figure 4.29. Fore-aft tip deflection - Side-boom 1 - Turb. Class B.....68
Figure 4.30. Side-side tip deflection - Side-boom 1 - Turb. Class B.....68
Figure 4.31. Fore-aft tip deflection - Side-boom 1 - Turb. Class C.....69
Figure 4.32. Side-side tip deflection - Side-boom 1 - Turb. Class C.....69
Figure 4.33. Fore-aft tip deflection - Side-boom 2 - Turb. Class A.....70
Figure 4.34. Side-side tip deflection - Side-boom 2 - Turb. Class A.....70
Figure 4.35. Fore-aft tip deflection - Side-boom 3 - Turb. Class A.....70
Figure 4.36. Side-side tip deflection - Side-boom 3 - Turb. Class A.....71
Figure 4.37. Side-boom stiffness vs. mean deflection.....71

Figure 5.1 Three-rotor configuration sketch 74

Figure 5.2. Tower mass density distribution – Single-rotor Vs. Three-rotor 75

Figure 5.3. Tower stiffness distribution – Single-rotor Vs. Three-rotor.....76

Figure 5.4. 3R Tower-top fore-aft deflection – Turb. Class A 77

Figure 5.5. 3R Frequency analysis, tower-top deflection – Turb. Class A ..77

Figure 5.6. 3R Tower-top yawing deflection – Turb. Class A.....78

Figure 5.7. 3R Tower-top fore-aft deflection – Turb. Class B.....79

Figure 5.8. 3R Frequency analysis, tower-top deflection – Turb. Class B...79

Figure 5.9. 3R Tower-top yawing deflection – Turb. Class B 79

Figure 5. 10. 3R Tower-top fore-aft deflection – Turb. Class C 80

Figure 5.11. 3R Frequency analysis, tower-top deflection – Turb. Class C 80

Figure 5. 12. 3R Tower-top yawing deflection – Turb. Class C 80

Figure 5.13. Four-rotor configuration sketch 82

Figure 5.14. Tower mass density distribution – Single-rotor Vs. Four-rotor 83

Figure 5.15. Tower stiffness distribution – Single-rotor Vs. Four-rotor.....83

Figure 5.16. 4R Tower-top fore-aft deflection – Turb. Class A 84

Figure 5.17. 4R Frequency analysis, tower-top deflection – Turb. Class A 85

Figure 5.18. 4R Tower-top yawing deflection – Turb. Class A.....85

Figure 5.19. 4R Tower-top fore-aft deflection – Turb. Class B.....86

Figure 5.20. 4R Frequency analysis, tower-top deflection – Turb. Class B.86

Figure 5.21. 4R Tower-top yawing deflection – Turb. Class B 87

Figure 5.22. 4R Tower-top fore-aft deflection – Turb. Class C 87

Figure 5.23. 4R Frequency analysis, tower-top deflection – Turb. Class C 87

Figure 5.24. 4R Tower-top yawing deflection – Turb. Class C 88

List of Tables

Table 3.1. Natural frequencies of the blade 41

Table 3.2. Natural frequencies for the tower - Single rotor configuration .42

Table 4.1. Tower geometry – Single-rotor compared to twin-rotor configuration.....51

Table 4.2. Natural frequencies of the tower – Single Vs. Twin rotor configuration.....52

Table 4.3. Statistical Analysis for Tower-Base Bending Moment in Turbulent Cases.....65

Table 5.1. Tower geometry – Single-rotor compared to three-rotor configuration.....75

Table 5.2. Natural frequencies of the tower – Single Vs. Three-rotor configuration.....76

Table 5.3. Statistical analysis for tower-top deflection in turbulent cases – 3R 81

Table 5.4. Tower geometry – Single-rotor compared to four-rotor configuration.....81

Table 5.5. Natural frequencies of the tower – Single Vs. Four-rotor configuration.....84

Table 5.6. Statistical analysis for tower-top deflection in turbulent cases – 4R 88

This page is intentionally left blank.

Chapter 1

Introduction

Contents

1.1. Historical Background 1

1.2. Global Wind Energy Status 6

1.3. Advantages of MRS 8

1.4. State of the Art Research on MRS 10

1.5. Problem Statement and Objective 13

1.6. Methodology 13

1.7. Novelty 16

1.8. Thesis Overview 16

1.1. Historical Background

The use of wind energy dates to thousands of years back in the world's earliest recorded history. It has been recorded that the first use of wind power in history was as early as 3100 BC by the Ancient Egyptians,

who used crafts sailed with papyrus and linen for transport in the Nile River. Architects have used concepts of natural ventilation in buildings around the same time by wind-driven techniques [1].

Figure 1.1. Pharaonic sail boat [2]

Later on, wind power being converted to mechanical power has been developed. The earliest instance recorded of this conversion was in the 1st century AD by the Greek engineer Heron of Alexandria. He designed a wind-driven wheel to power a machine. Another early example of a wind-driven wheel was the prayer wheel, which has been used in ancient India, Tibet, and China since the 4th century [3].

The first windmills were used in Iran on the borders with Afghanistan as early as the 7th century. These windmills, called "Panemone windmills", had long vertical driveshafts with rectangular sails covered in cloth or reed matting. The main use of these windmills was to pump water,

and in the grist grinding and sugarcane industries. The widespread use of windmills across the Middle East and Central Asia, led to the spread of their use to China and India. Later, horizontal windmills were used widely in northwestern Europe for flour grinding starting from the 1180s, many examples still exist [4].

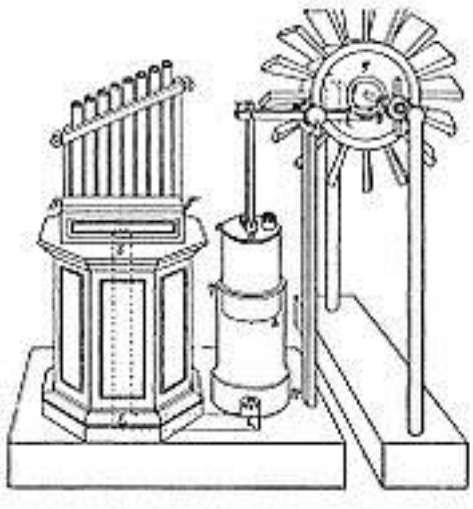

Figure 1.2. Heron's wind powered Machine [3]

Figure 1.3. Medieval photograph of a windmill [4]

The first use of windmills for electricity production was in Scotland in 1887 by James Blyth [5]. The 10 m high, sailed wind turbine was installed at Marykirk in Kincardineshire in the garden of his holiday cottage and was used to charge accumulators, to power the cottage lighting, to be the first house to have wind powered supplied electricity in the world. Later, he built another wind turbine to provide emergency power to the dispensary

of Montrose, the technology was not economically viable, and so the invention was never really established.

With the evolution of electric power, wind power was used for new applications, such as lighting buildings far from central power generators. During the 20th century parallel paths developed small wind machines to satisfy the needs of farms or residences, and large-scale wind generators that could be linked to electricity networks for remote use of power.

By the 1930s wind turbines were vastly used on farms in the United States to generate electricity, where there was no connection to electricity networks. Used to supplement battery storage collectors, the generating capacities of these machines are typically between few hundred watts up to several kilowatts. They were also used for separate applications besides providing farm power, such as preventing corrosion on bridge structures by electrifying it [6].

The Darrieus vertical axis wind turbine was invented in 1931, providing different design trade-offs from the traditional horizontal axis wind turbine. The vertical orientation of the axis of rotation needs no adjustments to wind. Another advantage is that instead of a top tower, the heavy gearbox and generator equipment can rest on the ground [7].

The world's first Mega Watt size wind turbine was linked to the local electrical allocation system on the mountain Grandpa's Knob in Castleton, Vermont, USA, in 1941. The design was made by Palmer Putnam and produced by the S. Morgan Smith Company. This Smith-Putnam turbine, producing 1.25 MW power, operated for about 1100 hours before failure of a blade at a known weak point, not being reinforced due to shortage in materials during wartime. For about forty years, no similar-sized turbines were to repeat this enterprising experiment. The short lifetime of the wind turbine emphasized the idea of considering dynamic analysis during the design process to avoid failure due to fatigue [8].

Chapter 1. Introduction

After World War II, when the petroleum products were cheap and plentiful, the interest in wind power stopped. This was due to the high cost and the uncertainty of wind. Then, when the Arab Nations held an embargo on petroleum products in 1973, petroleum was no cheaper nor plentiful. People then realized that the world's reserves of oil will not last forever, so, other energy sources were developed [9].

Figure 1.4. The world's first megawatt sized wind turbine [8]

This was like a turning point in the use of wind power. Continuous development in this field started that time and till these days. Now wind powered generators operate in a wide range of sizes between tiny battery-charging plants at isolated residences, up to Giga Watt sized offshore wind farms that provide electricity to electric grids.

1.2. Global Wind Energy Status

With the world's high demand of energy, and the limitation of the amount of fossil fuels, renewable energies have become a field of interest for many researchers. Sustainable and renewable energy sources are widely used in many countries as a very important source of power. Wind energy is one of the most growing renewable sources of energy, in terms of usage and research topics. According to the Global Wind Energy Council (GWEC) [10], the wind market's growth has been stable since 2014, installing more than 50 Giga Watts of new capacity every year.

The global cumulative installed wind capacity has increased 2,200% from the year 2001 to 2017.

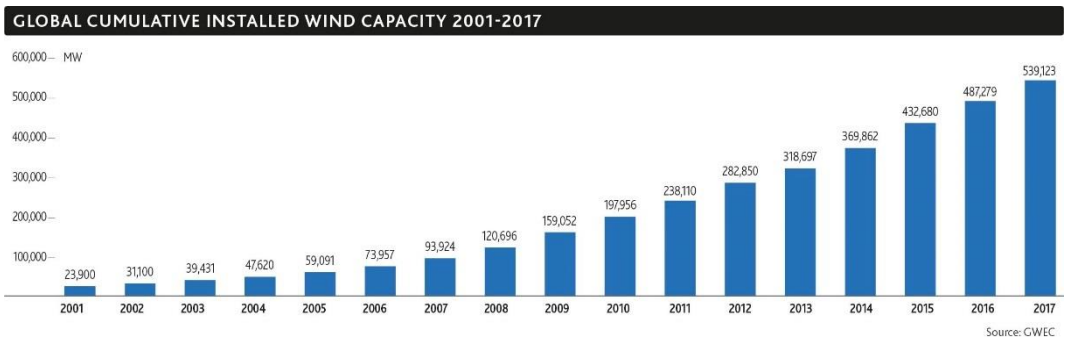

Figure 1.5. Global cumulative installed wind capacity 2001-2017 [10]

Countries around the world are competing to increase their installed capacity. The world's top 10 countries with installed wind capacity by the end of 2017 according to the same report by GWEC are shown in Figure 1.6.

Not only the total wind capacity of wind energy is increasing with time, but also the capacity of a single wind turbine has been increasing by the advanced technology and research year by year. This is necessary to improve the efficiency and cost of energy of a wind turbine. The conventional trend for increasing capacity over the past few decades, was increasing the size of the rotor.

Chapter 1. Introduction

The world's current largest capacity wind turbine in actual operation is the Vestas V164, with a rotor diameter of 164m and a capacity of 8MW [11]. However, General Electric has announced an even larger capacity wind turbine, the GE Haliade-X. With a 107m length of only the blade, and a capacity of 12 MW. Nonetheless, it's still a prototype [12].

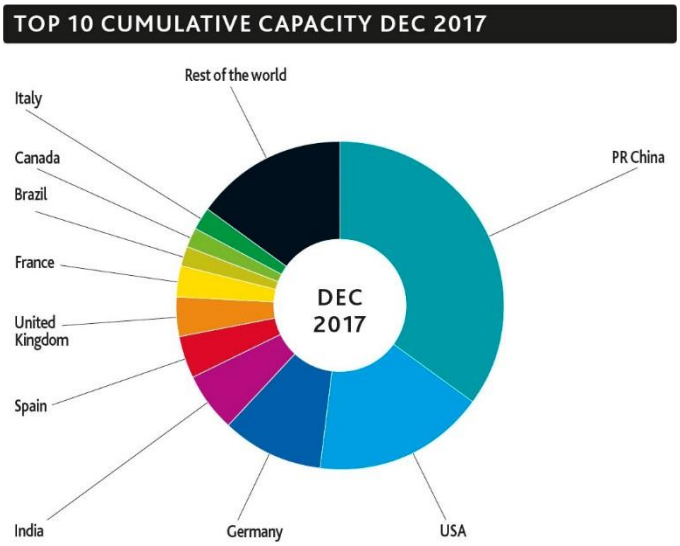

Country	MW	% Share
PR China	188,392	35
USA	89,077	17
Germany	56,132	10
India	32,848	6
Spain	23,170	4
United Kingdom	18,872	4
France	13,759	3
Brazil	12,763	2
Canada	12,239	2
Italy	9,479	2
Rest of the world	82,391	15
Total TO P10	456,732	85
World Total	539,123	100

Source: GWEC

Figure 1.6. World's top 10 cumulative wind capacity [10]

Figure 1.7 shows the size of the Haliade-X compared to other wind turbines and high buildings.

However, upscaling of the rotor size is not the only way of increasing the total capacity of a wind turbine. An alternative which can be

competitive with the large-scale wind turbine, is the Multi Rotor Systems (MRS) wind turbines.

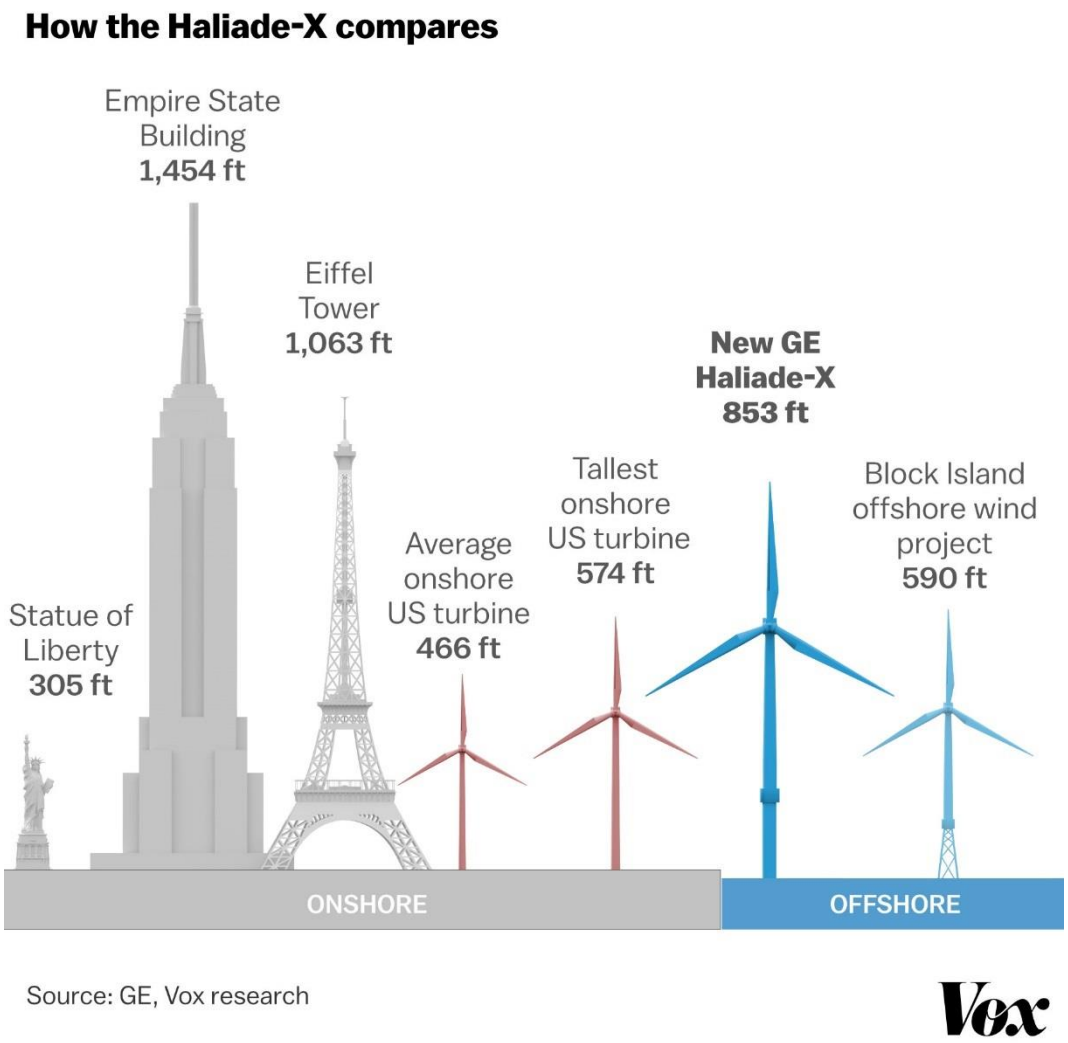

Figure 1.7. World's largest wind turbines [13]

1.3. Advantages of MRS

With the large-scale wind turbines comes big challenges, for instance, the huge transportation and installation cost of extremely large wind turbines, and the severe structure dynamic loads on the blades and

the tower. As well as the need develop each component, including the blade, bearing, generator, gearbox, …etc. which are suitable for the large-scale single rotor turbines, which includes risk in cost and quality. Also, the risk it includes if a failure occurs, then the whole wind turbine will shut down and no power will be produced until the failed part is fixed or replaced [14].

The concept of multi-rotor systems (MRS) is a technology which has a long history, goes back to 1930, but it has fallen out of consideration for its complexity while large scale single rotor wind turbines became technically feasible [15].

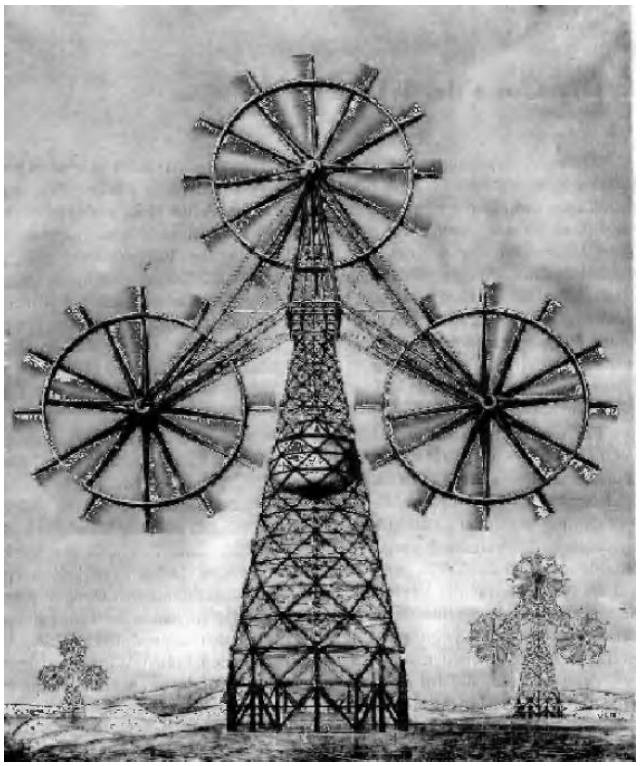

Figure 1.8. Conceptual MRS made by Honnef on 1930 [15]

The concept of MRS was proposed at a time when steel was the material used for constructing rotor blades. With the huge weight accompanied with steel, MRS were found unfeasible. However, with advanced materials and technology nowadays, MRS can be a promising alternative to large-scale wind turbines.

The main advantages of MRS are;

- Standardization of the wind turbine components in terms of cost and reliability,
- Ease of transportation since the rotors are of a small scale compared to large-scaled wind turbines,
- Ease of installation, and the cost and the reliability of wind turbines since multi rotors insures if there is a failure in one rotor, then the other rotors are still producing power.

But the most beneficial advantage, is the cost effectiveness of MRS. The reason for that is the surface area to volume ratio. For a MRS with n number of rotors, the total mass and cost has a ratio of $1/\sqrt{n}$ compared to a single rotor of the same capacity.

The major challenges in a MRS are the complexity of the supporting structure, the yawing system, and the aerodynamic interaction between rotors placed closely to each other. Which are if addressed effectively, MRS can be an alternative to large-scale single-rotor turbines.

1.4. State of the Art Research on MRS

While MRS has become an interesting field of research, researchers from many countries had attempted to issue very interesting research points. Some attempts were interested in studying aerodynamics and the aerodynamic interaction between the rotors of a MRS. Experiments made by Goltenbott et al. [16] has shown that two and three diffuser augmented rotor configurations have increased the power produced per rotor by 5% and 9% respectively, compared to a single rotor.

Also, the computational fluid dynamics (CFD) simulations made by Chasapogiannis et al. [17] has proven the same point. Simulations made for a 7-rotor system has shown a power increase per rotor by 3%. This proves

that not only MRS can improve the total mass and cost, but also the power production has increased.

The coherence effect on the produced power and tower loads on a 7 rotor MRS has been studied by Yoshida et al. [18]; Wind models with three different coherences were used in the simulation and it showed that larger coherence implies higher power production yet increases the collective loads. Which can be a challenge which needs to be addressed while the support structure is designed.

MRS was also found to improve the wake recovery; the wakes were found to recover faster for MRS as compared to a single-rotor configuration, as well as smaller turbulence intensity in the wake [19].

One of the leading research institutes who are having great interest in MRS is the Technical University of Denmark (DTU), they constructed a 4-rotor wind turbine in Risø campus. They conducted experiments as well as simulations for the 4-rotor wind turbine, and they both agreed that the interaction between the rotors improve the power performance by 1.8±0.2%, which can increase the annual power production by 1.5±0.2% [20].

Downscaling for design and cost of wind turbine rotors to replace a single large rotor with multiple smaller rotors has been made by Verma et al. [21]. A 5 x 1MW multi-rotor turbine was compared to the NREL 5MW single rotor turbine. The scaled down multi-rotor configuration has shown 37% reduction in weight, and 25% reduction in cost compared to a single rotor producing the same amount of power.

As an extension to Verma's work, Mate et al. [22] have designed a support structure for the 5-rotor configuration proposed in his colleague's work, in addition to other configurations Gaurav proposed himself. A finite element approach was used for modelling the support structure. However, these simulations did not include the study of the aeroelastic behaviour of either the blades or the support structure, and the wind conditions.

Overall, the research attempts on MRS is still limited. It is necessary to have an aeroelastic simulation tool or code in order to understand the dynamic behaviour of the support structure.

Figure 1.9. 4R-V29 wind turbine located at the Risø campus, DTU *[20]*

1.5. Problem Statement and Objective

As has been mentioned before, the major challenges in MRS systems are the complexity of the supporting structure, the yawing system, and anticipating the aerodynamic interference between the rotors.

The concern of this thesis is the support structure of a MRS. In order to address the structural problems correctly, it should be analysed in an aeroelastic way. So that the effect of aerodynamic and inertial loading on the structure can be understood, anticipated, and taken into consideration in the design process.

So far there is no research proposed or an open-source tool which introduced an aeroelastic analysis for the multi-rotor concept. In this thesis, the support structure of a MRS is being aero-elastically analysed, by an in-house tool developed for the modelling of MRS, so that structural problems can be addressed in further researches.

It is the first attempt to develop an in-house aeroelastic tool for MRS support structure. In this work, the present tool is used to model a twin-rotor wind turbine, with two coplanar rotors placed on a T-shaped tower, and it can be later extended to model support structures for different configurations of MRS.

1.6. Methodology

Prediction of the aerodynamic properties of a wind turbine is more difficult and challenging than that of a fixed wing, because in wind turbines, the blade encounters large fluctuations in the aerodynamic forces due to changes in wind directions, changes in the angle of attack with large gusts, boundary layer effects, and the interaction with the unsteady wakes from

the tower. Tower wake interaction with the blade can result in impulsive load changes and dynamic stall over the rotating blades.

There are various methods to compute the aerodynamic loads on the blades of a wind turbine, such as Computational Fluid Dynamics (CFD), Blade Element Momentum theory (BEM) theory, and singularity methods. The criteria of comparison between the different methods are;

- How accurate they are,
- How much time does it consume,
- How much does it cost, and
- How it is flexible to make modifications to the model.

Wind turbines design and evaluation tools are based on BEM theory. The main advantage that makes BEM is preferable to CFD, is that BEM is very cost efficient and can count for fluctuating loads. Wind turbine blades are subject to unsteady, turbulent, 3D, incompressible flow and is affected by far field conditions. This means that to make a good simulation, it needs a large domain and a fine spatial resolution as well. Full CFD analysis that satisfies these requirements is very expensive and time consuming. That is the main reason BEM model is superior in this field and it is the model used for the design of most modern HAWTs

Aeroelastic analyses for wind turbines are doable for single rotors using either CFD models or deterministic models. Hansen introduced a tool to study the Aeroelastic stability of wind turbines with an eigenvalue approach [23]. In that tool, the finite beam element method is used for the structure modelling, while blade element momentum is used for the aerodynamic load calculation. The results of the eigenvalue approach showed good agreement between the measured and predicted aeroelastic damping. This work was later extended to study instability problems for wind turbines such as stall-induced vibrations and flutter [24].

Lee et al. made an analysis of structural dynamics of HAWTs using a methodology that represents the turbine as a multi-flexible-body system

[25]. Aeroelastic simulation tools can also be extended to include offshore wind turbines, in that case additional models for the hydrodynamic loads should be considered [26]. Offshore wind turbines induce more aeroelastic instabilities since it is more flexible, studies have been made to model those kind of instabilities [27] [28] [29].

Computational Fluid Dynamics (CFD) approach was also used to model aeroelastic behaviour of wind turbines like the work done by Bazilevs et al. [30] or Halawa et al. [31]. However, a fully coupled aeroelastic simulation for a wind turbine will include a lot of challenges, like a dynamic mesh to adapt to the structural deformations of the wind turbine parts [32] [33] [34]. A comparison between deterministic models and CFD methods has been made by MOL Hansen et al. [35].

NREL's tool, FAST, is one of the most used aeroelastic tools for modelling wind turbines, it is based on models derived from the fundamental theory of aerodynamics and structure analysis, which are more time-efficient compared to CFD models [36].

The theory used in this work is the Blade Element Momentum (BEM) theory which is used to calculate the aerodynamic loads, and Virtual work method with a modal approach to calculate the structural deformations of blades and tower, then coupling of the two theory results to create an aeroelastic interface between the blades and tower on one hand, and wind on the other.

The approach of verifying the results of the present tool is by comparing results of a single rotor wind turbine, to NREL's FAST results of the same turbine model, then the results of the twin-rotor configuration are introduced.

1.7. Novelty

The work done in this thesis is the first approach to model the supporting structure of a multi-rotor system wind turbines. As mentioned before, research approaches in multi-rotor systems were solely concerned with aerodynamics and performances. In addition, aeroelastic tools available commercially or in academia can only model single-rotor configurations or in the best-case wind field.

The current tool developed in this thesis is the first to achieve aeroelastic modelling of a tower supporting more than one rotor. Accordingly, all the findings and outcomes of that tool results are all novel and the first in the academic field.

1.8. Thesis Overview

This thesis is structured into 5 chapters. They include the following;

- **Chapter 1**: Gives an introduction about the wind energy, its history, current status of its usage, introduces MRS and why they are superior over single-rotor wind turbines, the objective of the thesis and finally the methodology followed to achieve it.

- **Chapter 2**: Describes the mathematical model used for building the in-house tool. Governing equations of the blade element momentum (BEM) theory, as well as the virtual work method used for the structure analysis as explained. Finally, the

aeroelastic coupling between the two theories needed to create an aeroelastic simulation.

- **Chapter 3**: Includes verification of the developed in-house tool. The approach for validation is by comparing the results of the present tool to a similar FAST simulation. The verification process goes step by step from the aerodynamics of the rotor, through the modal analysis, and finally to the aeroelastic analysis. The blades' loads, and deformations are compared, then the same is done to the tower.

- **Chapter 4**: Includes simulation for the twin-rotor configuration. The T-shaped tower of the twin-rotor configuration is modelled. Load cases for steady and turbulent wind conditions were studied, and the main tower and side booms' loads and deformations are introduced.

- **Chapter 5:** Simulation is extended to include three-rotor and four-rotor configurations. Turbulent load cases were studied, and dynamic behaviour of the main tower is introduced. Comparison between performance of three-rotor and four-rotor configurations is introduced.

- **Chapter 6**: Concludes the thesis, to point the main findings of this work. Finally, it proposes the future work planned to improve the in-house tool and make it more reliable for more simulation conditions and parameters.

This page is intentionally left blank.

Chapter 2

Mathematical Model

Contents

2.1. Chapter Overview 19

2.2. Aerodynamic Model 20

2.3. Structure Model 23

2.4. Aeroelastic Coupling 27

2.5. NREL Aeroelastic Tools 28

2.5.1. Modes 29

2.5.2. TurbSim 29

2.5.3. FAST 32

2.1. Chapter Overview

In this chapter, the theory used for developing the present aeroelastic tool will be explained. First, the aerodynamic model; unsteady blade element momentum (BEM) theory was used to obtain the

aerodynamic loads affecting the wind turbine blades for different wind conditions. Then the mathematical model of the structure, where the virtual work method with a modal approach was used to calculate the deformations and vibrations for both the blades and the tower. Finally, the aeroelastic coupling between the two theories, where the vibrations of the blade and the tower, as well as the turbine components' displacements and inertial loads affect the dynamics. Figure 2.1 shows the analysis flow chart.

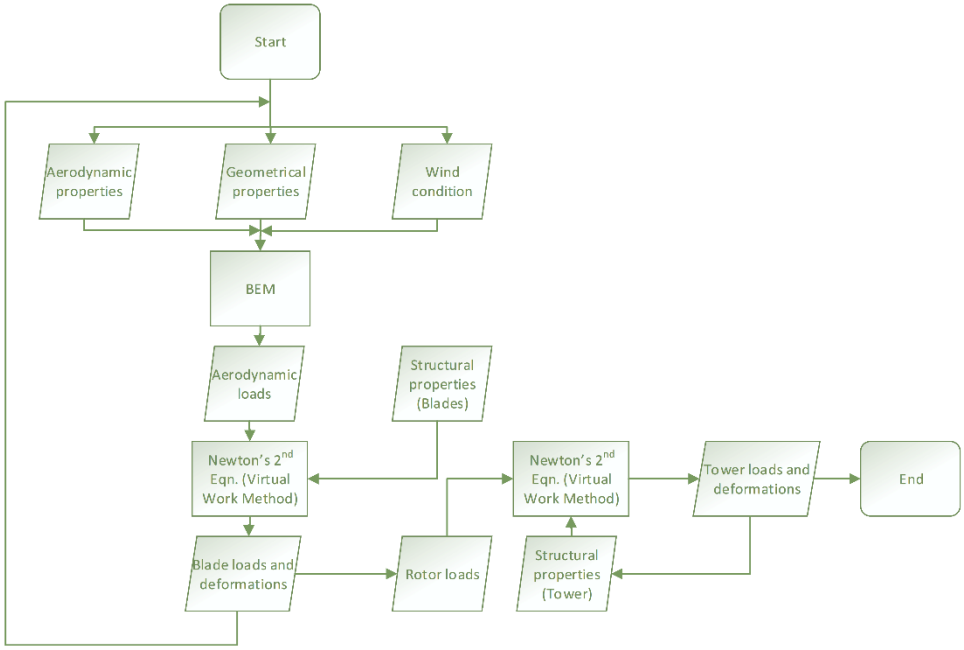

Figure 2.1. Analysis flow chart

2.2. Aerodynamic Model

Classical blade element momentum method, also known as steady BEM, is enough to calculate steady loads on a wind turbine for different conditions of wind speed, rotational speed, or different blade pitch angles. It can accordingly calculate the thrust and power for a rotor. However, it can only be acceptable for estimation of the annual energy production from

a wind turbine by computing the steady power curve. In reality, the wind has an unsteady nature. Many factors affect the unsteadiness of the wind, for instance, wind shear or atmospheric turbulence [37].

In this work, unsteady BEM was used where the loads change with time, based on the blade positions, rotor rotational speed, and wind conditions. The coordinate system used for the model is the blade coordinate system, shown in Figure 2.1.

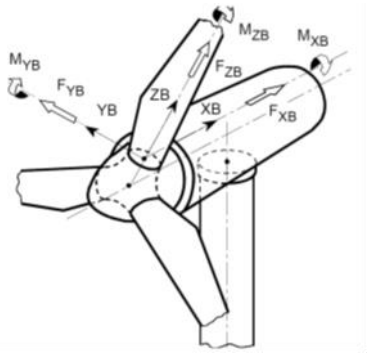

Figure 2.2. Blade coordinates system *[38]*

Initially, the blades are in an undeformed status, so the initial relative velocity components in the blade's cross-section coordinates, y_B tangential to the blade width and x_B normal to the blade, are as follows;

$$V_{rel,x_B} = V_{0,x_B} + w_{x_B} \quad (1)$$

$$V_{rel,y_B} = V_{0,y_B} - \omega r + w_{y_B} \quad (2)$$

Where;

V_0 is the inflow velocity,

ω is the rotational speed of the rotor,

r is the blade section position,

w_{xB} is the induced velocity in the x_B axis, and

w_{yB} is the induced velocity in the y_B axis.

The apparent angle of attack relative to each blade section is then calculated to deduce the coefficients of lift and drag for each section, for each time step as follows;

$$V_{rel} = \sqrt{V_{rel,y_B}^2 + V_{rel,x_B}^2} \tag{3}$$

$$tan(\phi) = -\frac{V_{rel,x_B}}{V_{rel,y_B}} \tag{4}$$

$$AoA = \phi - \theta_p - \beta \tag{5}$$

Where;

φ is the flow angle,

α is the angle of attack,

θ_p is the pitch angle, and

β is the twist angle.

When the lift and drag coefficients are known, the lift and drag forces are then calculated.

$$L = \frac{1}{2}\rho V_{rel}^2 c C_L \tag{6}$$

$$D = \frac{1}{2}\rho V_{rel}^2 c C_D \tag{7}$$

Where;

L and D are the lift and drag forces of the blade section,

ρ is the air density at rotor height,

c is the chord length of each blade section,

C_L and CD are the lift and drag coefficients of the blade section,

Prandtl's tip loss factor and Glauert correction are used in the calculation of the induced velocities which were initially assumed to be zero, then recalculated after the lift and drag forces are calculated, in an iterative manner.

$$w_{x_B} = -\frac{BLcos(\phi)}{4\rho\pi rF\left|V_0 + f_g w_{x_B}\right|} \tag{8}$$

$$w_{y_B} = -\frac{BLsin(\phi)}{4\rho\pi rF\left|V_0 + f_g w_{y_B}\right|} \tag{9}$$

Where;

B is the number of blades.

F is Prandtl's tip loss factor, and

f_g is the Glauert correction.

After enough iterations, the lift and drag forces on each blade section are known, hence the aerodynamic loads in the tangential and normal to blade directions, $L_{yB,aero}$ and $L_{xB,aero}$ respectively, can finally be calculated.

$$L_{x_B,aero} = Lcos(\phi) + Dsin(\phi) \tag{10}$$

$$L_{y_B,aero} = Lsin(\phi) - Dcos(\phi) \tag{11}$$

2.3. Structure Model

The virtual work method is a principle which can be used to formulate the mass, damping, and stiffness matrices for a mechanical system, such as the Newton's second law [39];

Chapter 2. Mathematical Model

$$\boldsymbol{M\ddot{x} + C\dot{x} + Kx = F_g} \tag{12}$$

Where;

M, C, *and* ***K*** are the mass, damping and stiffness matrices,

$\boldsymbol{F_g}$ is the generalized forces array,

$\boldsymbol{x}$ is the degrees of freedom array,

$\boldsymbol{\dot{x}}$ and $\boldsymbol{\ddot{x}}$ are the first and second time-derivative, and

$\boldsymbol{\ddot{x}}$ is the second time-derivative.

The uncoupled modal shapes were used as the degrees of freedom for the formulation of the model. The use of modal shape functions is advantageous for the following reasons; First, it reduces the number of degrees of freedom, which reduces the size of the matrices and hence the computational time for each time step. Second, the uncoupled modes have orthogonality constraint which eliminates many terms from the matrices as will be shown later.

For the blades, the first and second flap-wise, and the first edge-wise modes are used, denoted by u^{f1}, u^{f2}, and u^{e1} respectively. And hence, the size of the matrices is 3x3. The mass matrix's first column is as follows;

$$\begin{bmatrix} m_{11} \\ m_{21} \\ m_{31} \end{bmatrix} = \begin{bmatrix} \int u_{x_B}^{f1}(r)m'(r)u_{x_B}^{f1}(r)dr + u_{y_B}^{f1}(r)m'(r)u_{y_B}^{f1}(r)dr \\ \int u_{x_B}^{f1}(r)m'(r)u_{x_B}^{e1}(r)dr + u_{y_B}^{f1}(r)m'(r)u_{y_B}^{e1}(r)dr \\ \int u_{x_B}^{f1}(r)m'(r)u_{x_B}^{f2}(r)dr + u_{y_B}^{f1}(r)m'(r)u_{y_B}^{f2}(r)dr \end{bmatrix} = \begin{bmatrix} GM_1 \\ 0 \\ 0 \end{bmatrix} \tag{13}$$

Where;

m' is the mass density along the blade length,

u_{xB} is the normal to blade component of the mode shape, and

u_{yB} is the tangential to blade component.

For simplicity, the first component is denoted by GM_1. The other two components equal 0 due to the orthogonality between the uncoupled mode shapes. Similarly, the other off-diagonal components of the mass matrix will be zeroes. The mass matrix will consist of three values on the diagonal as follows;

$$\boldsymbol{M} = \begin{bmatrix} GM_1 & 0 & 0 \\ 0 & GM_2 & 0 \\ 0 & 0 & GM_3 \end{bmatrix} \tag{14}$$

And the generalized masses GM_2 and GM_3 can be calculated in the same manner;

$$GM_2 = \int u_{x_B}^{e1}(r)m'(r)u_{x_B}^{e1}(r)dr + u_{y_B}^{e1}(r)m'(r)u_{y_B}^{e1}(r)dr \tag{15}$$

$$GM_3 = \int u_{x_B}^{f2}(r)m'(r)u_{x_B}^{f2}(r)dr + u_{y_B}^{f2}(r)m'(r)u_{y_B}^{f2}(r)dr \tag{16}$$

The stiffness and damping matrices are functions of the mass matrix, and the natural frequencies associated with every mode shape as follows;

$$\boldsymbol{K} = \begin{bmatrix} {\omega_{f1}}^2 GM_1 & 0 & 0 \\ 0 & {\omega_{e1}}^2 GM_2 & 0 \\ 0 & 0 & {\omega_{f2}}^2 GM_3 \end{bmatrix} \tag{17}$$

Where,

ω_{f1} is the first flap-wise,

ω_{e1} is the first edge-wise. And

ω_{f2} is the second flap-wise natural frequencies.

$$\boldsymbol{C} = \begin{bmatrix} \omega_{f1} GM_1 \dfrac{\delta_{f1}}{\pi} & 0 & 0 \\ 0 & \omega_{e1} GM_2 \dfrac{\delta_{e1}}{\pi} & 0 \\ 0 & 0 & \omega_{f2} GM_3 \dfrac{\delta_{f2}}{\pi} \end{bmatrix} \tag{18}$$

Where;

δ is the logarithmic decrement associated with every mode shape.

Finally, the generalized forces array F_g, can be calculated as follows;

$$\begin{bmatrix} F_{g,1} \\ F_{g,2} \\ F_{g,3} \end{bmatrix} = \begin{bmatrix} \int L_{x_B}(r) u_{x_B}^{f1}(r) dr + L_{y_B}(r) u_{y_B}^{f1}(r) dr \\ \int L_{x_B}(r) u_{x_B}^{e1}(r) dr + L_{y_B}(r) u_{y_B}^{e1}(r) dr \\ \int L_{x_B}(r) u_{x_B}^{f2}(r) dr + L_{y_B}(r) u_{y_B}^{f2}(r) dr \end{bmatrix} \tag{19}$$

The same model is used for the tower as well, except that the modes chosen in case of the tower are the first and second fore-aft, and the first side-side modes, denoted by u^{fa1}, u^{fa2}, and u^{ss1} respectively.

The model represents uncoupled differential equations that can be solved numerically. 4th order Runge-Kutta numerical technique [40] was used to solve these systems of equations, to result in the values of $\boldsymbol{x}$, $\dot{\boldsymbol{x}}$, and $\ddot{\boldsymbol{x}}$, in which the deformation of either the blade or the tower is assumed to be dependent on, as a linear combination of the three modes. For instance, in case of the blade, with a stiff tower, the deformation distribution along the blade section position (r), denoted by u_{xB} in the flap-wise direction and u_{yB} in the edge-wise direction, will be as follows;

$$u_{xB}(r) = x_1 u_{xB}^{f1}(r) + x_2 u_{xB}^{e1}(r) + x_3 u_{xB}^{f2}(r) \tag{20}$$

$$u_{yB}(r) = x_1 u_{yB}^{f1}(r) + x_2 u_{yB}^{e1}(r) + x_3 u_{yB}^{f2}(r) \tag{21}$$

Since the modes are constant, the velocities and accelerations along the blade are as follows;

$$\dot{u_{xB}}(r) = \dot{x_1} u_{xB}^{f1}(r) + \dot{x_2} u_{xB}^{e1}(r) + \dot{x_3} u_{xB}^{f2}(r) \quad (22)$$

$$\dot{u_{yB}}(r) = \dot{x_1} u_{yB}^{f1}(r) + \dot{x_2} u_{yB}^{e1}(r) + \dot{x_3} u_{yB}^{f2}(r) \quad (23)$$

and;

$$\ddot{u_{xB}}(r) = \ddot{x_1} u_{xB}^{f1}(r) + \ddot{x_2} u_{xB}^{e1}(r) + \ddot{x_3} u_{xB}^{f2}(r) \quad (24)$$

$$\ddot{u_{yB}}(r) = \ddot{x_1} u_{yB}^{f1}(r) + \ddot{x_2} u_{yB}^{e1}(r) + \ddot{x_3} u_{yB}^{f2}(r) \quad (25)$$

2.4. Aeroelastic Coupling

The deformation of the blade, together with the velocity and acceleration of its vibration, will result in a change in the loads and hence structure deformation in the next time-step. The relative wind velocity components on the blade sections can now be updated to include the blade vibrations, with the blade velocity distribution always opposing the wind direction. Equations 1 and 2 can be updated as follows;

$$V_{rel,xB} = V_{0,xB} + w_{xB} - \dot{u}_{xB} \quad (26)$$

$$V_{rel,yB} = V_{0,yB} - \omega r + w_{yB} - \dot{u}_{yB} \quad (27)$$

The loads on the blade sections are also updated, to include gravitational loads, and inertia loads due to the blade vibrations. The total load distribution along the blade sections in the normal and tangential directions to the plane of rotation will be as follows [41];

$$L_{xB}(r) = L_{xB,aero}(r) - m'(r)\ddot{u}_{xB}(r) + m'(r) g \, sin(\theta_t + sin\theta_c) \, cos \, \theta_A \quad (28)$$

$$L_{yB}(r) = L_{yB,aero}(r) - m'(r)\ddot{u}_{yB}(r) + m' \, sin \, \theta_A \quad (29)$$

Where;

θ_t is the rotor tilt angle,

θ_c is the cone angle, and

θ_A is the azimuth angle.

The updated relative wind velocity and loads are used for the next time step, guaranteeing that both the aerodynamics and structure models affect each other, to create an aeroelastic model.

It should be noted in the previous model that all the loads in the longitudinal direction of the blades were neglected, since it is insignificant compared to the other loads.

For the tower, it is modelled independently from the blades, the rotor loads are transmitted to the tower, including rotor thrust, weight, and torque, taking into consideration the aeroelastic behaviour of those loads. Also, the aerodynamic load on the tower itself is calculated, considering the tower vibrations in the relative wind speed to the tower, and the tower inertial loads.

2.5. NREL Aeroelastic Tools

In this thesis, NREL aeroelastic tools were used as pre-calculators for the current developed tool, and as an aeroelastic simulators to compare their results with the outcomes of the thesis. In this section, an introduction for each of these tools will be discussed.

2.5.1. Modes

Modes is a tool made by NREL, which was used in this work to generate mode shapes for both the tower and blades. In the input file to Modes, the blades can be rotating at a specified rate, or can be stationary. The tower and blades are considered as beams which are divided into rigid and flexible sections. Basic information on geometry, mass and stiffness distributions are defined in the input file to use Modes.

Modes was developed for obtaining an analytical solution for the vibration modes and natural frequencies of rotating beams. The governing differential equation of a rotating beam is derived using an extension of the classical Bernoulli-Euler beam theory. The beam is assumed to be prismatic and fabricated with a homogenous, isotropic, and linear elastic material. It is also assumed that the beam is stiff within the plane of rotation. Which means that the deflections and torsion are neglected.

2.5.2. TurbSim

TurbSim was used to generate a turbulent flow field to be used as an input to the developed tool. It is a stochastic inflow turbulence tool which provides a numerical simulation of a full-field flow containing coherent turbulence structures.

Different wind spectral models are included in TurbSim. Whether turbulence models associated with nocturnal boundary layer flows, or IEC Kaimal and von Karman normal turbulence models. It efficiently generates randomized coherent turbulent structures which are superimposed on the random turbulent field as produced by one of the spectral models.

Turbulence can be defined as the random and fast fluctuation of wind speeds around its mean value, in a small time-scale [42, 43]. These fluctuations occur in longitudinal, lateral, and vertical directions. The two main causes of turbulence are; friction with the ground caused by the

earth's topography, and thermal effects where air moves vertically as a result of temperature difference.

It is a complex process to represent the turbulence mathematically because it is a random process which cannot be simply described by deterministic equations. So, it is more useful to describe turbulence according to its statistical properties. Among the statistical properties which can describe the turbulence, is the turbulence intensity (TI). It measures the overall turbulence level, and can be defined as;

$$I = \frac{\sigma}{\overline{U}} \tag{30}$$

Where; I is the turbulence intensity, σ is the standard deviation of the wind speed, and $\overline{U}$ is the mean wind speed.

Both standard deviation and the mean value of wind speeds are calculated over a time scale longer than that of the turbulence, but shorter than the time scale of other types of changes (e.g., Diurnal variations).

The turbulence spectrum is a description of the frequency of variation of the wind speed. The spectrum follows an asymptotic boundary which is, at high frequencies, proportional to $n^{-5/3}$; where n is the frequency in Hz, according to Kolmogorov law [44].

Two spectral models are commonly used to express the spectrum of the longitudinal wind component, denoted by a subscript "u". Those models are the von Karman and Kaimal spectral models. They can be expressed as follows [42];

Kaimal Model:

$$\frac{nS_u(n)}{\sigma_u^2} = \frac{4nL_{1u}/\overline{U}}{(1 + 6nL_{1u}/\overline{U})^{5/3}} \tag{31}$$

von Karman Model:

$$\frac{nS_u(n)}{\sigma_u^2} = \frac{4nL_{2u}/\overline{U}}{(1 + 70.8(nL_{2u}/\overline{U})^2)^{5/6}} \tag{32}$$

Where; $S_u(n)$ is the wind's longitudinal component's spectral density function, σ_u is the longitudinal wind speed's standard deviation, L_{1u} and L_{2u} are length scales with values depending on the surface roughness z_0 and the above ground height z.

The von Karman spectral model can give a better description of turbulence occurring in wind tunnel tests, while the Kaimal model fits better to the atmospheric turbulence [45].

In this work, the Kaimal model was used to simulate a more realistic atmospheric turbulence field.

In the Kaimal model, an exponential coherence model can be used in conjunction. This is to correspond with the spatial correlation of the longitudinal component of the wind velocity. The coherence model can be described as follows [46];

$$Coh(r,f) = exp\left[-12\left(\left(f.\frac{r}{V_{hub}}\right)^2 + \left(0.12\frac{r}{L_c}\right)^2\right)^{0.5}\right] \quad (33)$$

Where;

Coh (r,f) is the coherence function,

r is the magnitude of the projection of the separation vector between two points on a plane normal to the wind direction,

f is the frequency, and

L_C is the coherence scale parameter.

In TurbSim, the turbulence intensity can be chosen manually, or use the standard IEC 61400 turbulence class A, B, or C [46]. According to the standard, the reference turbulence intensities (I_{ref}) at the average wind speed of 15 m/s are 16%, 14% and 12% for turbulence classes A, B, and C respectively. In order to know the turbulence intensity for different average wind speeds at the hub height, the following equation can be used;

$$\sigma = I_{ref}(0.75\overline{U} + 5.6) \quad (34)$$

Then the turbulence intensity can be calculated by knowing the standard deviation corresponding to the average wind velocity for each turbulence class.

2.5.3. FAST

FAST (Fatigue, Aerodynamics, Structures, and Turbulence) is an aeroelastic simulator which is capable of predicting extreme and fatigue loads of two and three-bladed wind turbines. It was used in this thesis as a verification method for the developed tool. The results of FAST were compared to those of the developed tool for the single-rotor configuration.

The FAST model employs a combined modal and multi-body dynamics (MBD) formulation. The model for two-bladed turbines relates nine rigid and four flexible bodies through 22 degrees of freedom (DOFs). It can also model a three-bladed HAWT with 24 DOFs. For both the two and three-bladed configurations, any combination of the available DOFs and features during the analysis can be enabled. The DOFs and features combination is dictated by the configuration of the wind turbine subject to analyse.

FAST joins a set of Computer-Aided Engineering (CAE) modules for Aerodynamics (AeroDyn), Hydrodynamics (HydroDyn), Control and electrical systems (ServoDyn), and Structure dynamics (ElastoDyn). Those modules are coupled providing a nonlinear aero-hydro-servo-elastic analysis in a time marching scheme [36].

The aerodynamic module AeroDyn uses data from the inflow wind, to solve for the rotor-wake including the dynamic stall and get the blade-element load. HydroDyn module simulates the incident waves and currents whether regular or irregular. It solves for the hydrostatic, and viscous loads on the offshore substructure.

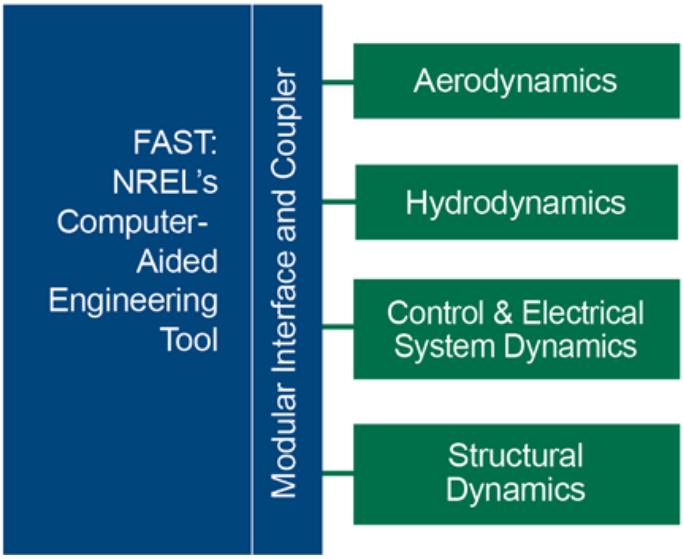

Figure 2.3. NREL's modular CAE tool, FAST [36]

ServoDyn includes both control and electrical system modules. The control system module simulates the blade-pitch's controller logic, as well as the sensors, and the actuators. It also simulates other control devices like the nacelle-yaw or the generator-torque. The electrical system module simulates the generator and the power-converting components. The structure dynamics module, ElastoDyn, applies the aero and hydrodynamic loads, in addition to the gravitational loads, the control reaction loads over the structure, and simulates the elasticity of all the turbine components and structure elements. Finally, the modular interface and the coupler enable the interaction between all modules and results in a time-marching aeroelastic simulation [36].

This page is intentionally left blank.

Chapter 3

Verification with a Single-Rotor Model

Contents

3.1. Chapter Overview 35

3.2. Model Outline 36

3.3. Rotor Aerodynamics 38

3.4. Modal Analysis 40

3.4.1. Blades 40

3.4.2. Tower 42

3.5. Aeroelastic Analysis 43

3.5.1. Blades 44

3.5.2. Tower 46

3.6. Chapter Summary 47

3.1. Chapter Overview

The approach for validation of the present tool, is by comparing the results of the present tool's simulation over a single-rotor configuration, to

the well-established FAST aeroelastic tool's results. The wind turbine under study in this chapter is the NREL 5MW turbine [46]. First, the model outline will be shown, then verification for the aeroelastic tool step by step. Starting from the steady-state responses of the turbine, through the modal analysis, and finally the aeroelastic coupling between the aerodynamics and structural behaviour of both the blades and the tower [47].

3.2. Model Outline

The geometric and material properties of the turbine blades and tower are fully defined in the NREL definition report. General rotor specifications are shown below;

- Rating: 5 MW.
- Rotor orientation, configuration: Upwind, 3 Blades.
- Rotor Diameter: 126 m.
- Hub Height: 90 m.
- Cut-in, Cut-out Wind Speed: 3 m/s, 25 m/s.
- Rated Wind Speed: 11.4 m/s.
- Rotor Mass: 110,000 kg.
- Nacelle Mass: 240,000 kg.
- Tower Mass: 347,460 kg.

Figure 3.1 shows a CAD model for the turbine blade.

Figure 3.1. NREL 5MW wind turbine blade [48]

Chapter 3. Verification with a Single-Rotor Model

The blade and tower structural specifications are fully defined in the definition report. Figures 3.2-3.5 show the distribution of these properties along normalized lengths.

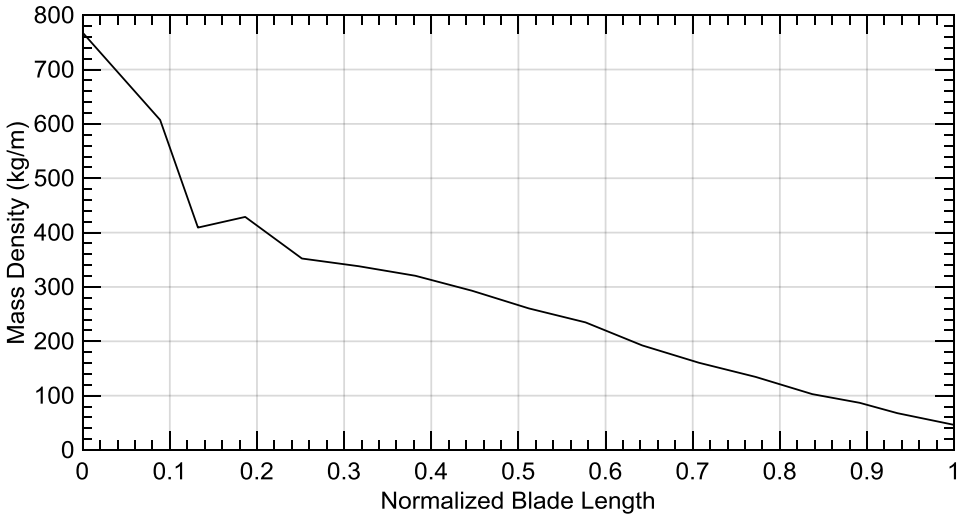

Figure 3.2. Blade mass density distribution

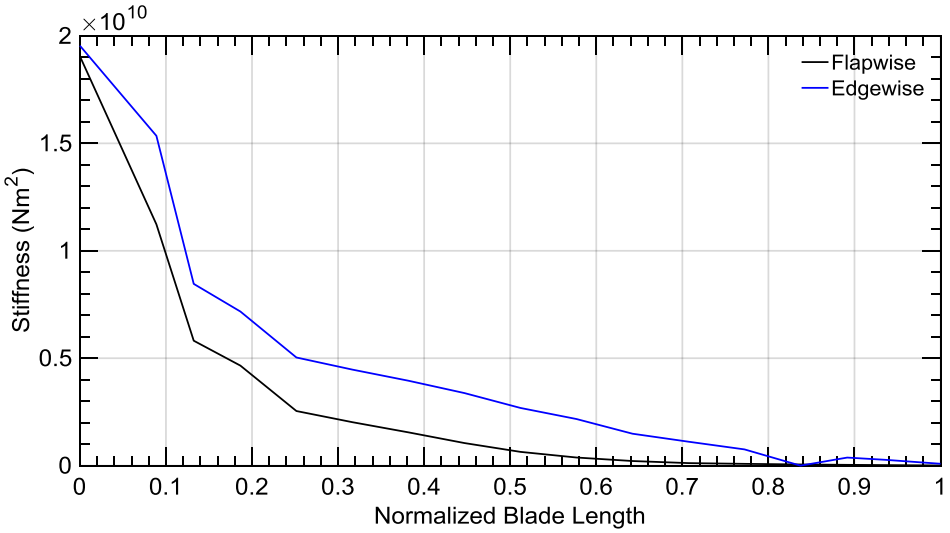

Figure 3.3. Blade stiffness distribution

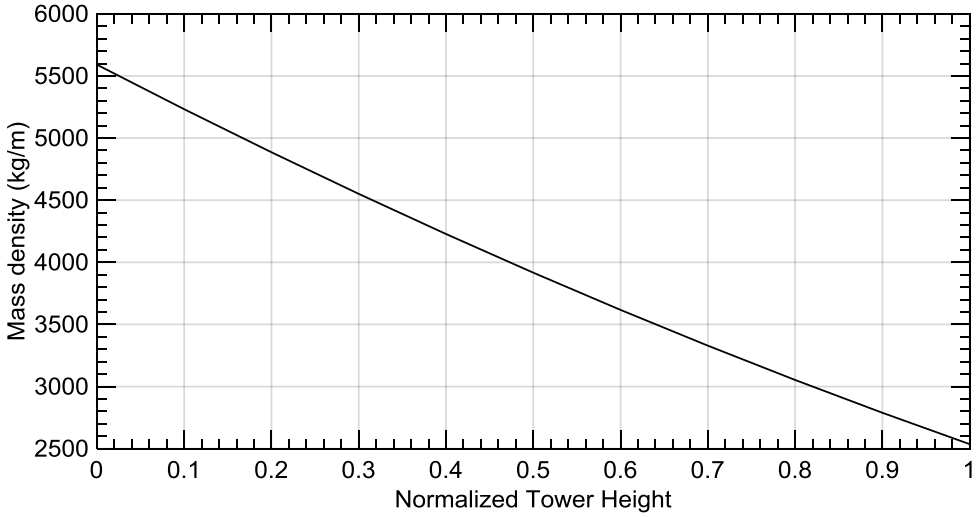

Figure 3.4. Tower mass density distribution

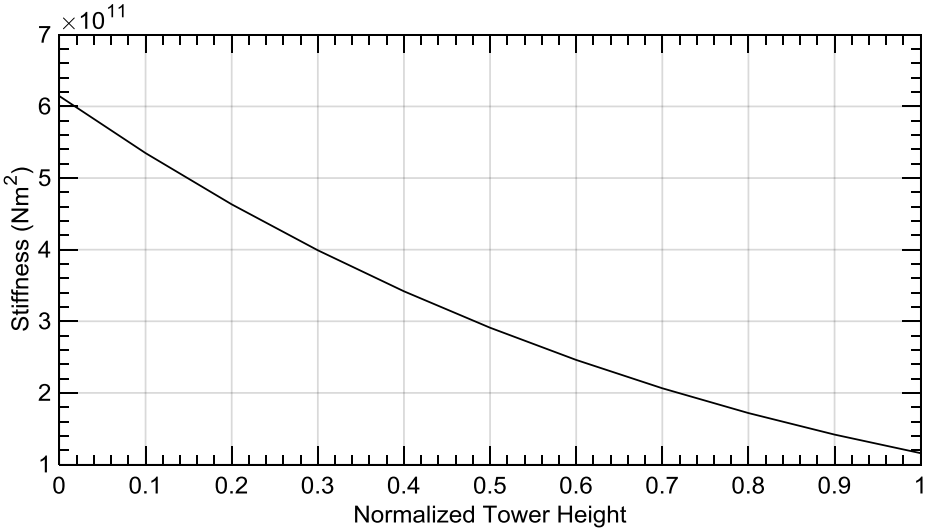

Figure 3.5. Tower stiffness distribution

3.3. Rotor Aerodynamics

The NREL 5MW wind turbine is a pitch-controlled turbine. Over the rated wind speed of 11.4 m/s, the pitch control is applied to maintain the rated power output and loads. Figure 3.6 shows the steady state

responses of the wind turbine over all ranges of wind speed, from cut-in to cut-out wind speed.

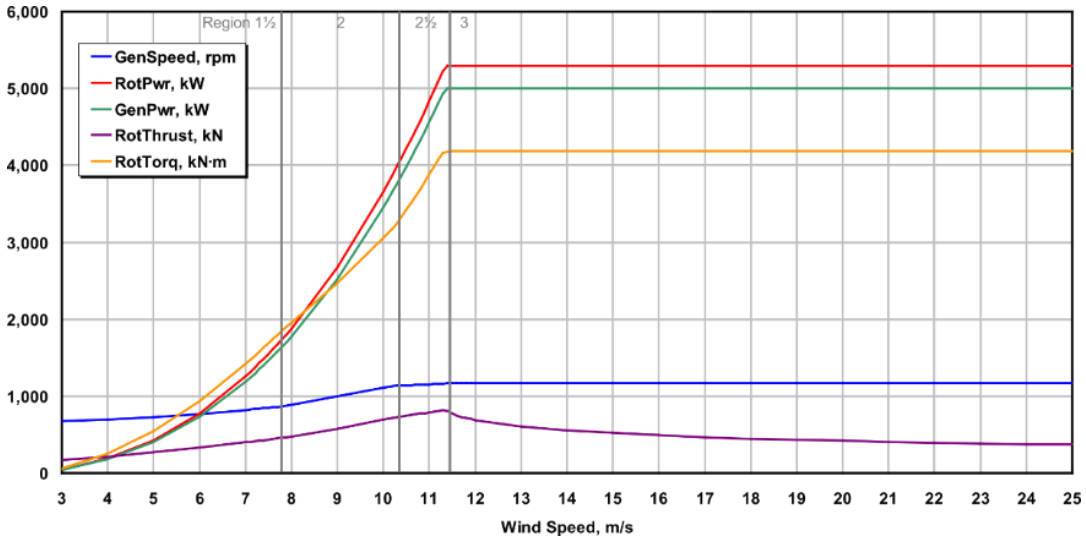

Figure 3.6. Steady state responses for different wind speeds [46]

The BEM in the developed tool is run for wind speeds starting from the cut-in speed of 3 m/s, to the rated speed of 11.4 m/s. The rotor power, thrust, and torque are compared. The results are shown in Figure 3.7.

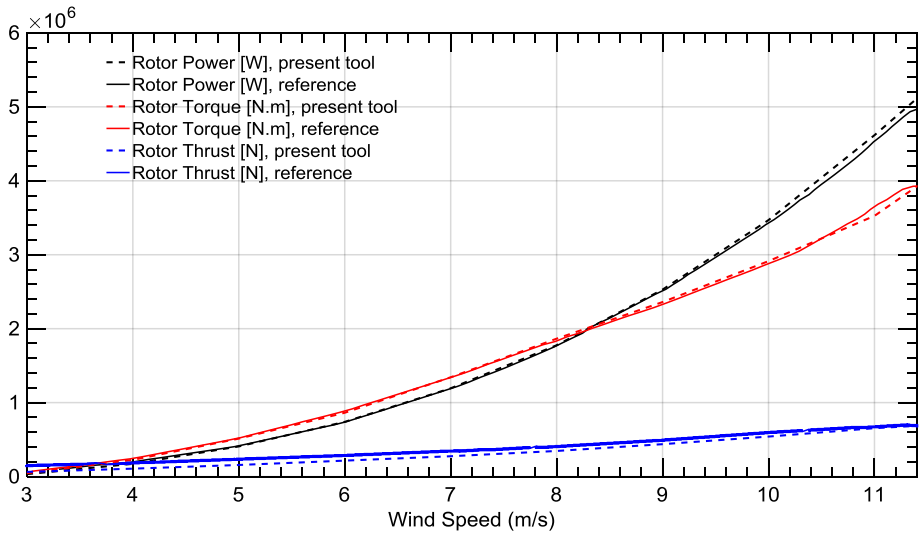

Figure 3.7. Steady state responses - Comparison between results of the developed tool to NREL reference file

Figure 3.7 shows good agreement between the calculated steady state values of the power, torque, and thrust of the developed tool, compared to the turbine definition document's results. This agreement proves that the first part of the tool concerning calculating the aerodynamic responses, without considering the aeroelastic behaviour of the blades, is reliable, and the next step would be the dynamic responses of the blades and tower.

3.4. Modal Analysis

In this section, the free vibration modes of the blades and tower is investigated. The structural model is based on the uncoupled modes of vibrations, and it is important that the mode shapes and natural frequencies will be correct, before proceeding to the aeroelastic coupling between the aerodynamics and structural behaviour of both the blade and the tower.

The NREL tool Modes [49] was used to calculate the uncoupled mode shapes and natural frequencies of the blades and the tower. Mass, and stiffness distribution along the blade and tower are available in the NREL 5MW definition document and were used as input to Modes. The mode shapes and natural frequencies are also available in the definition document and are shown for comparison with the results of simulation.

3.4.1. Blades

The mode shapes used in the structural model are the first and second flap-wise modes, and the first edge-wise mode. Natural frequencies and mode shape comparison are shown in Table 3.1.

The results of the natural frequencies from Modes simulation agree with the reference values.

Table 3.1. Natural frequencies of the blade

Mode	Calculated (Hz)	Reference (Hz)	Deviation (%)
First flap-wise	0.71	0.70	1.4
Second flap-wise	2.02	2.02	0.0
First edge-wise	1.08	1.08	0.0

In Figures 3.8 and 3.9, the mode shapes calculated by Modes are compared to the mode shapes in the NREL 5MW definition file. The results are almost identical for both the flap-wise and edge-wise modes.

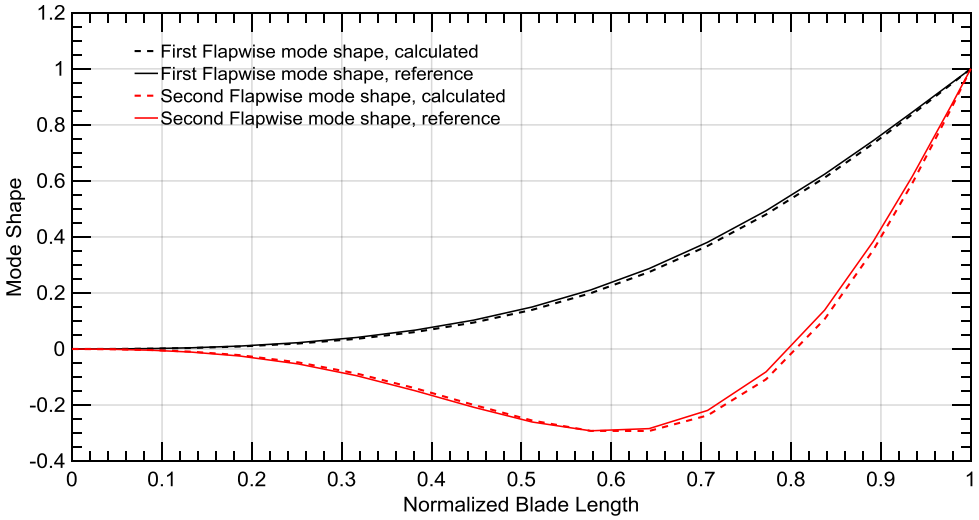

Figure 3.8. Blade flap-wise mode shapes

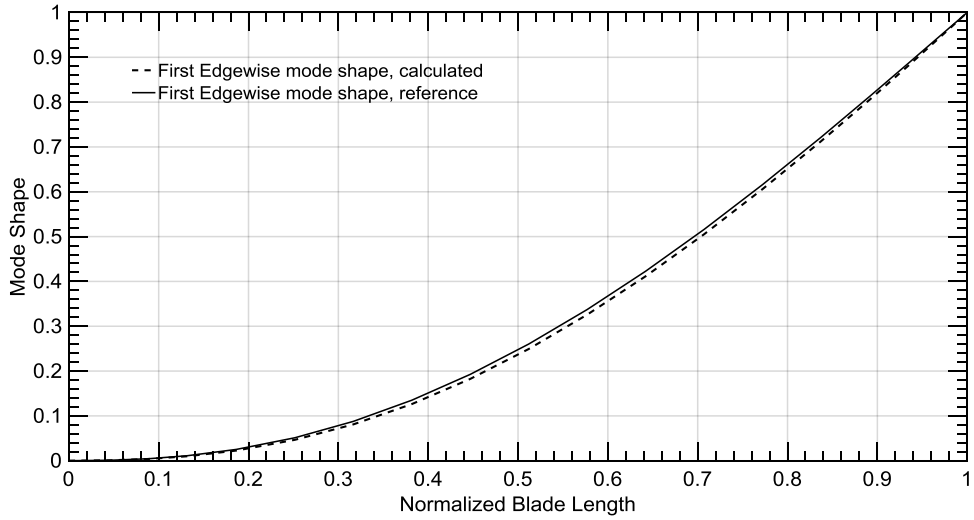

Figure 3.9. Blade edge-wise mode shape

3.4.2. Tower

Similarly, the free vibrations of the tower are compared. The modes considered in the aeroelastic tool are the first and second fore-aft modes, and the first side-side mode. Natural frequencies and mode shapes are shown below.

Natural frequencies as well as mode shapes of the tower show agreement between the results of Modes compared to the reference.

With the aerodynamic steady state response and the structure dynamic response verified separately, the next step is validation of the aeroelastic tool, where both aerodynamics and structure of the turbine are coupled.

Table 3.2. Natural frequencies for the tower - Single rotor configuration

Mode	Calculated (Hz)	Reference (Hz)	Deviation (%)
First fore-aft	0.32	0.32	0.0
Second fore-aft	3.06	2.90	5.2
First side-side	0.32	0.31	3.1

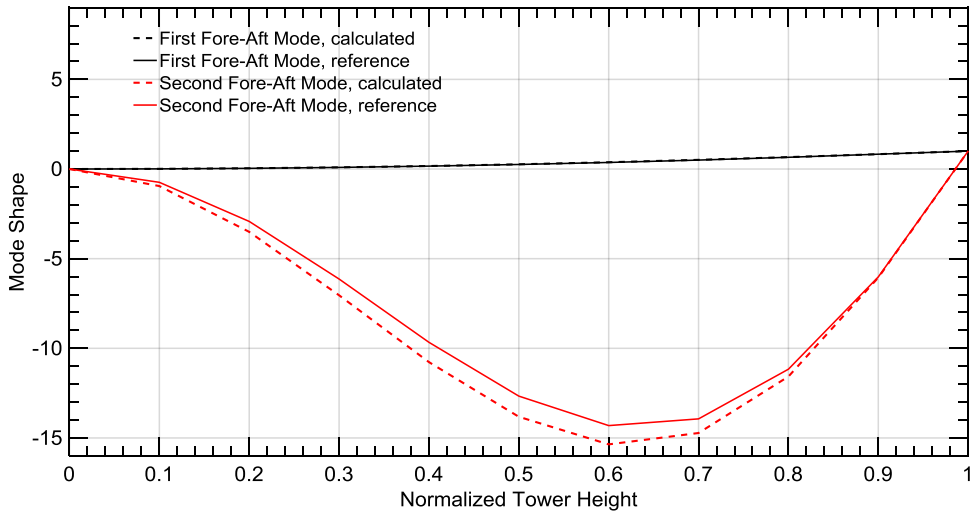

Figure 3.10. Tower fore-aft mode shapes - Single rotor configuration

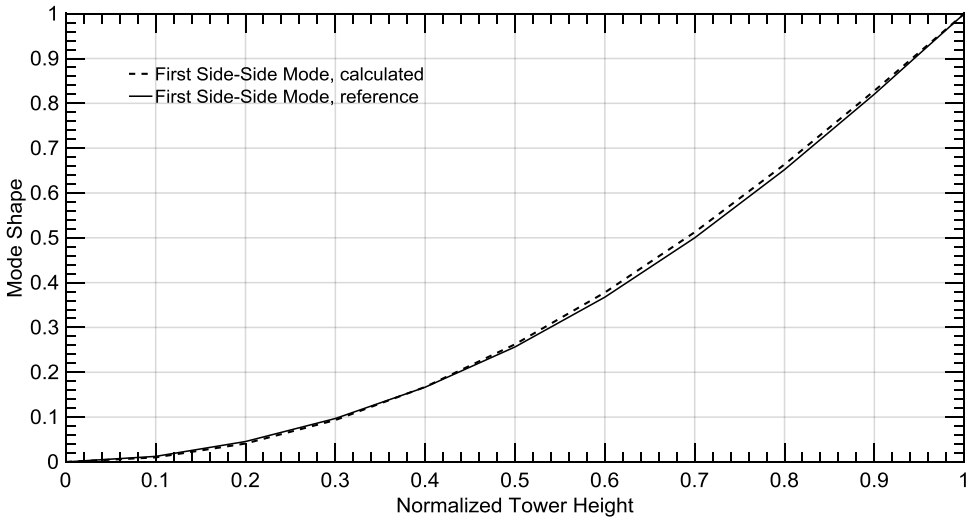

Figure 3.11. Tower side-side mode shape - Single rotor configuration

3.5. Aeroelastic Analysis

In this subsection, the coupling between the aerodynamic loads and the structural behaviour is introduced. The aerodynamic loads affecting the blades causes deformation, and hence the relative velocities on the blade sections are changed. Inertial loads generated from the blade vibration also affect the structural behaviour. The effects of blade vibrations are considered every time step in the simulation to catch the aeroelastic behaviour for both the blades and the tower.

For validation of the results, a FAST simulation is made for the NREL 5MW wind turbine blades and tower, using the same simulation conditions as in the in-house tool. The blades are subject to a constant wind speed and are rotating at a constant angular speed. Simulation parameters are as follows;

- Wind speed: 11.4 m/s (Rated wind speed)
- Rotational velocity: 12.1 rpm (Constant)

- Pitch angle: 0^o
- Time step: 0.01 s
- Simulation time: 50 s

3.5.1. Blades

For the simulation of the blades, the tower is considered as stiff body. The dynamics are generated by the rotation of the blades in azimuth direction, and the vibrations in the flap-wise and edge-wise directions. The tower is considered as a stiff body in the FAST simulation as well to create a similar simulation environment for comparison. In Figures 3.12 and 3.11, bending moments at the blade root in the flap-wise and edge-wise directions are shown with the azimuth position of the blade.

The periodic behaviour of the dynamic response of the blade is due to the effect of gravity and inertia on the blades while in different azimuth positions [50], as well as the shear layer of the flow. As the blade rotates, considering the rotor tilt angle, the mass centers along the blade length moves such that the blade moves towards or away from the plane of rotation.

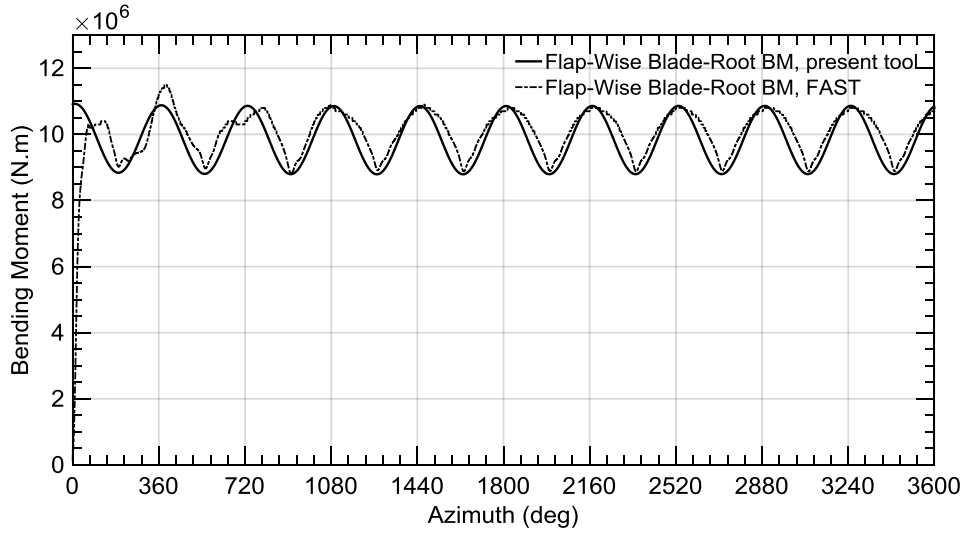

Figure 3.12. Blade-root, flap-wise bending moment

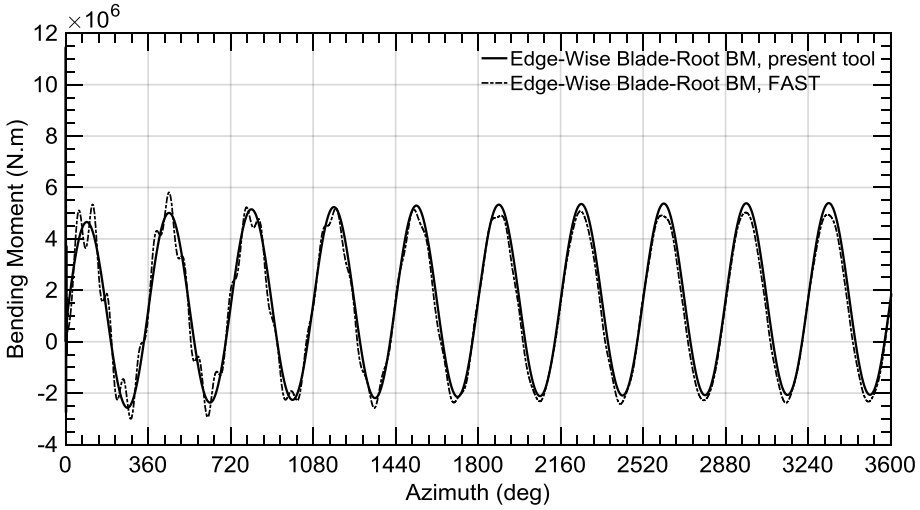

Figure 3.13. Blade-root, edge-wise bending moment

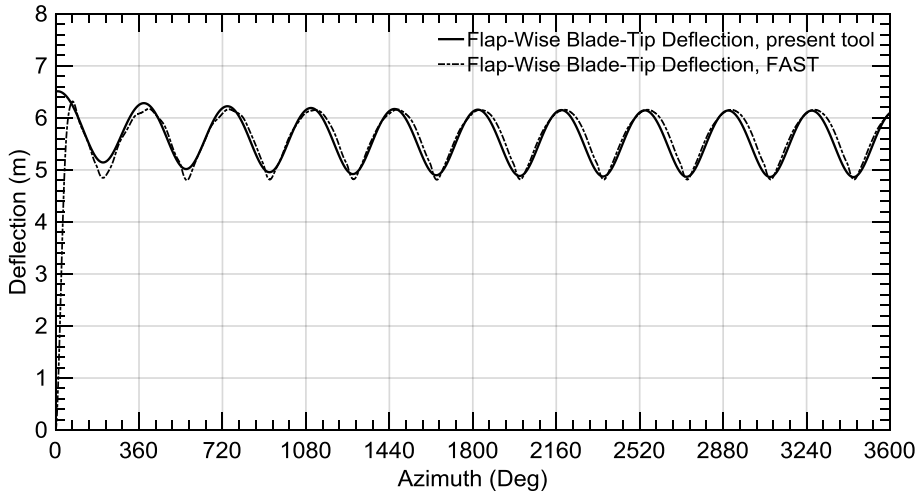

Figure 3.14. Blade-tip, flap-wise deflection

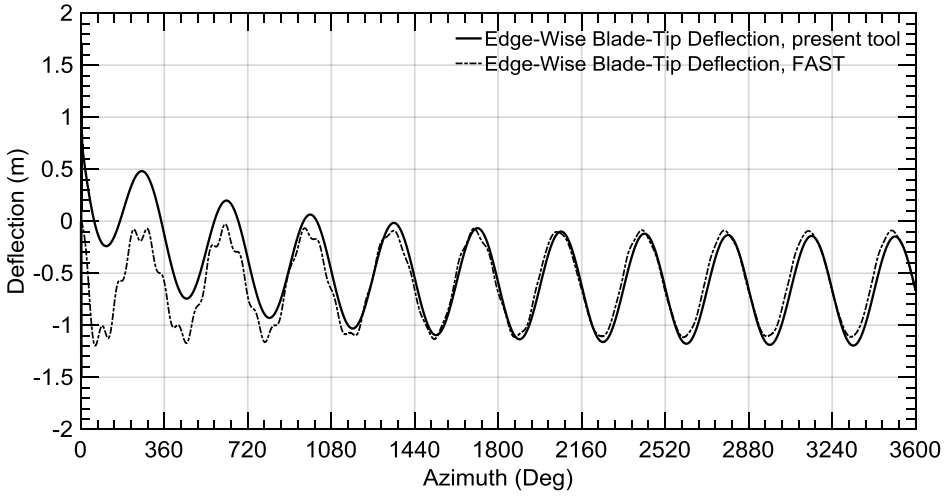

Figure 3.15. Blade-tip, edge-wise deflection

Other than the initial condition, there is a very good agreement between the results of the present tool and FAST results in terms of the ranges of values, mean values, and frequencies of each time series. Consequently, the proposed tool has proved its sufficiency of describing the blade dynamics, and then the tower can be modelled.

3.5.2. Tower

The tower is now considered for study. Similarly, the same conditions of simulation were set for both the proposed tool and FAST. The loads were transmitted from the rotor to the tower, considering the dynamic behaviour of the rotor loads. The elasticity of the tower together with the aerodynamic and gravitational loads of the tower itself was also considered. As observed from the dynamic responses of the blade, the out-of-plane quantities are more significant than the in-plane ones, and hence, the out-of-plane properties for the tower are shown for comparison.

It is observed in Figures 3.16 and 3.17 that there is a very good agreement between the results of the present tool compared to FAST.

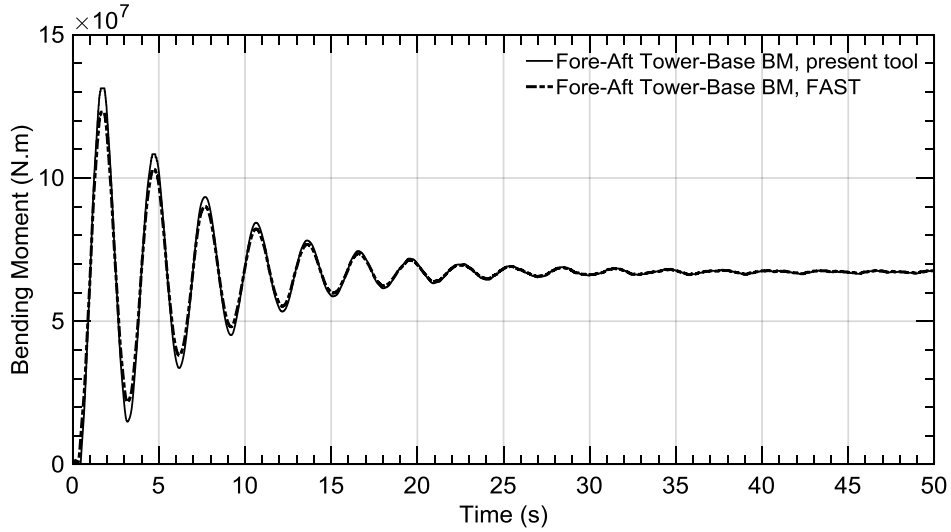

Figure 3.16. Tower-base, fore-aft bending moment

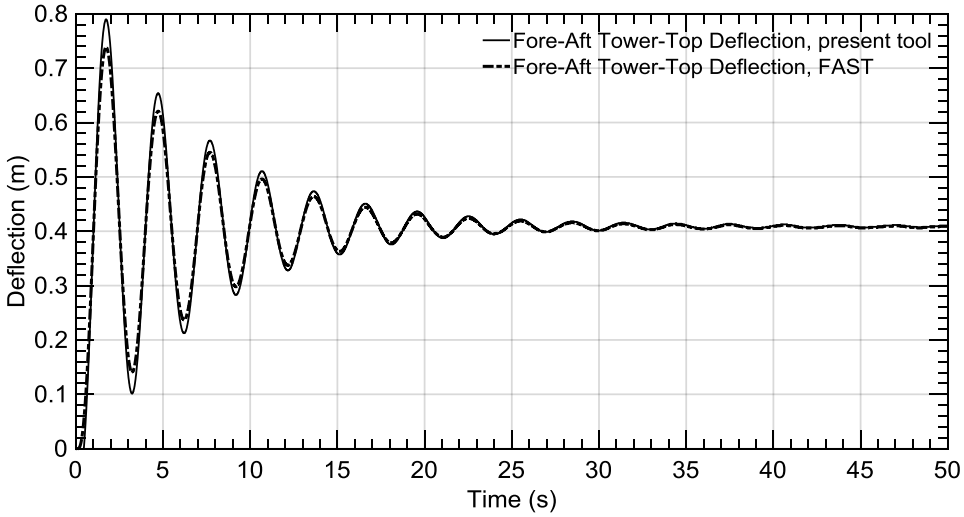

Figure 3.17. Tower-top, fore-aft deflection

For both the blade and tower dynamic responses, the results of the proposed tool have shown the credibility in modeling the aeroelastic behavior of a wind turbine.

3.6. Chapter Summary

In this chapter, simulations over a single-rotor configuration has been made for verification of the present tool. Results of both the present tool and FAST simulation agree well. The tool is valid to generate loads and deflections' time series of the turbine parts in case of steady wind so far. In the next section, another rotor is added on the same tower, and the tower dynamics are studied.

This page is intentionally left blank.

Chapter 4

Simulation of Twin-Rotor Model

Contents

4.1. Chapter Overview 49

4.2. Twin-Rotor Wind Turbine Model 50

4.3. Tower Analysis 53

4.3.1. Steady Flow Condition 53

4.3.2. Turbulent Flow Condition 58

4.4. Side-Boom Analysis 65

4.5. Chapter Summary 72

4.1. Chapter Overview

In the chapter, a twin-rotor turbine with two NREL 5MW rotors is modeled. The same manner of simulation of the single-rotor configuration is followed in the twin-rotor configuration case. Aerodynamic interaction between the two rotors is neglected, so the main concern in this chapter is the supporting structure. First, the main tower is studied to calculate the tower loads and deflections. Then, the side booms supporting the rotors. The twin-rotor configuration parameters are introduced, then results of the simulation for different wind conditions.

4.2. Twin-Rotor Wind Turbine Model

The support structure is assumed to be a T-shaped structure, with the main tower and two side booms connecting the rotors. The side booms are assumed to be a scaled-down structure of the NREL 5MW main tower, each of 63.5 m length from the main tower center point, such that the two rotors are distanced at 127 meters from hub to hub. This boom length was chosen such that the tips of each of the 126m diameter rotors are 1m apart to reduce the total weight over the main tower. It is also assumed that there is no aerodynamic interaction between the two rotors. If the aerodynamic interaction is considered, the optimum distance between the rotors will be determined for the best performance of the turbine, and hence the optimum side boom length.

A pitch misalignment of 0.20deg and -0.20deg were added to each rotor's second and third blades respectively, which is common to generate the aerodynamic imbalance. Figure 4.1 shows a sketch of the proposed twin-rotor configuration.

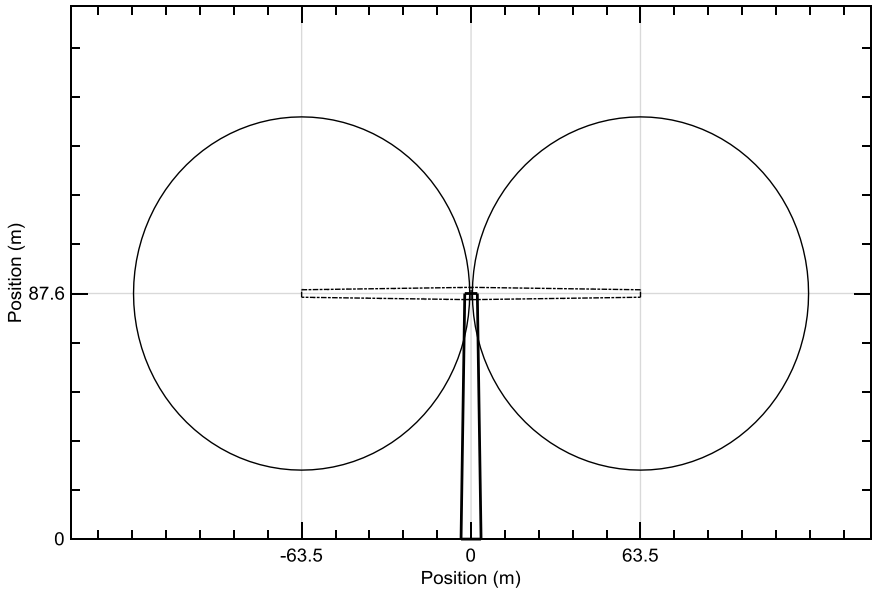

Figure 4.1. Sketch of the twin-rotor configuration

Chapter 4. Simulation of Twin-Rotor Model

As was explained in chapter 2, the natural frequencies and mode shapes are crucial factors in the structural model. The mathematical model of the structure is totally based on the free vibrations. Hence, for comparison of the tower structural behavior between single and twin rotor configurations, the main tower geometry and structural properties are changed such that the natural frequency of the first fore-aft mode is the same for both towers. The outer diameter of the tower is changed while the thickness is kept constant. It was found that an outer diameter 1.25 times the diameter of the single-rotor configuration turbine will cause the first fore-aft natural frequency of both configurations' towers to be equal. Table 4.1 shows the differences in the geometry between both configurations.

Table 4.1. Tower geometry – Single-rotor compared to twin-rotor configuration

Property (m)	Single rotor	Twin rotor
Tower base diameter	6.000	7.500
Tower base thickness	0.027	0.027
Tower top diameter	3.870	4.840
Tower top thickness	0.019	0.019
Tower height	87.600	87.600

Figures 4.2 and 4.3 show the difference in the mass and stiffness distributions between the single rotor and twin rotor configurations' towers.

The mass distribution and the total mass of the tower has increased compared to the single-rotor configuration, due to the change in the tower geometry. On the other hand, the stiffness has also significantly increased so that it will be able to support the extra loads added from the extra rotor.

The natural frequencies are then calculated for the twin-rotor configuration and compared to the single-rotor configuration in Table 4.2.

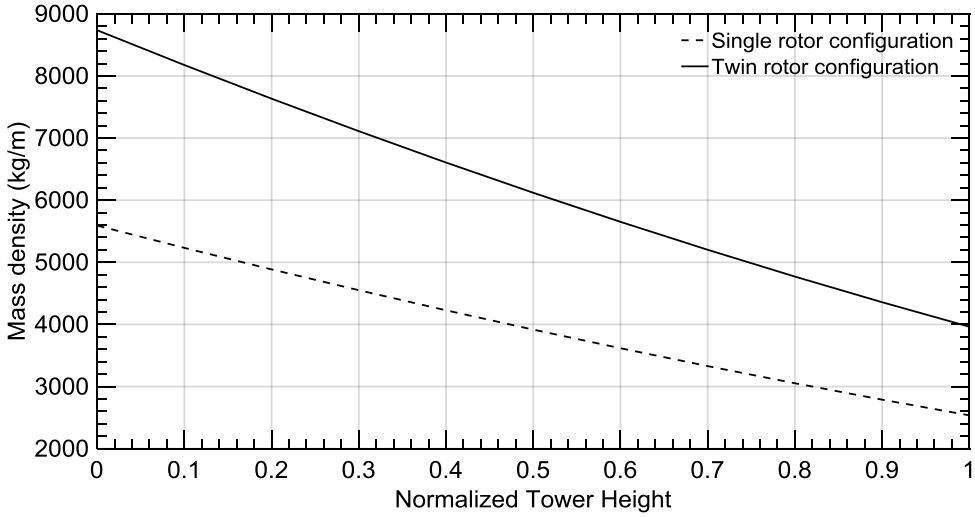

Figure 4.2. Tower mass density distribution – Single-rotor vs. Twin-rotor

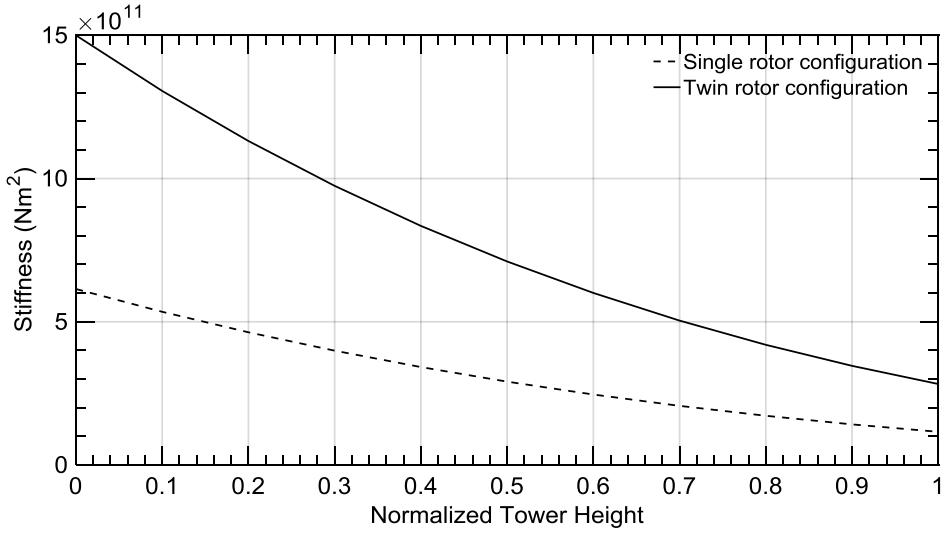

Figure 4.3. Tower stiffness distribution – Single-rotor vs. Twin-rotor

Table 4.2. Natural frequencies of the tower – Single vs. Twin rotor configuration

Mode	Single-rotor (Hz)	Twin rotor (Hz)	Deviation (%)
First fore-aft	0.32	0.32	0.0
Second fore-aft	3.06	3.20	4.4
First side-side	0.32	0.25	-21.8

The natural frequencies other than the first fore-aft mode are changed, compared to the single rotor configuration. The change is mainly due to the inertia added at the top of the tower. This means that the tower

stiffness and structural damping matrices in the mathematical model in the case of the twin rotor are different. Moreover, the loads are increased significantly due to the addition of another rotor, and hence the deformations are expected to change in a non-straightforward way.

4.3. Tower Analysis

Two load cases were investigated for the twin rotor configuration; one is in a steady wind condition, and the other is in turbulent wind conditions.

In steady wind case, the rotors are subject to the same conditions as in the case of single rotor; steady wind velocity of 11.4 m/s, rotating the rotors at 12.1 rpm. This case studies the aeroelastic properties when the two rotors are rotating simultaneously such that the rotor loads are superimposed in all loads' value ranges, and then investigates when the rotors have a 60^{o} phase change in the blades' azimuth positions.

In the turbulent wind condition case, the rotors are subject to a turbulent wind field created by NREL's tool TurbSim [51]. The rotors are subject to different turbulence classes according to IEC 61400-1 standards [52] at an average wind speed at the hub height of 8 m/s and turbulence intensities of class A (high turbulence), B (moderate turbulence), and C (low turbulence) respectively. A variable speed control algorithm is used in the turbulent case.

In all cases, the out-of-plane dynamic responses -deflection and bending moment- of the tower are shown.

4.3.1. Steady Flow Condition

In this case, the two rotors' loads superimpose in the whole range of values; in the peak values at the beginning of the rotation and until it

settles for the nominal value of the load, while the blades of both rotors are in the same azimuth position.

First, the tower was modeled as a stiff tower, the bending moment at the tower base is calculated. Then it's compared to an elastic tower model to see the differences in results. The results of this simulation are shown in Figure 4.4.

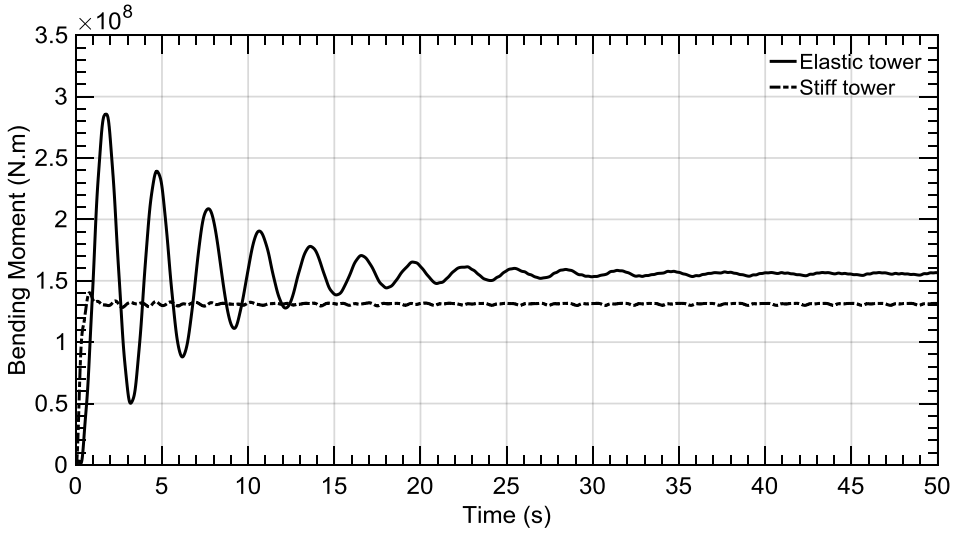

Figure 4.4. Tower-base fore-aft bending moment - Stiff vs. Elastic Tower

The stiff tower model doesn't show the dynamic behavior of the load, as well as the values are less than those in the elastic tower model. The gravity effects due to the vibration of the tower are eliminated in the case of stiff tower, and hence the loads are far from the real values. This proves that it is not proper to consider the tower to be stiff for load calculations and it is important to model it as an elastic tower.

Dynamic responses of the elastic tower model were then calculated, Figures 4.5 and 4.6 show the tower-base bending moment and tower-top deflection in the fore-aft direction respectively.

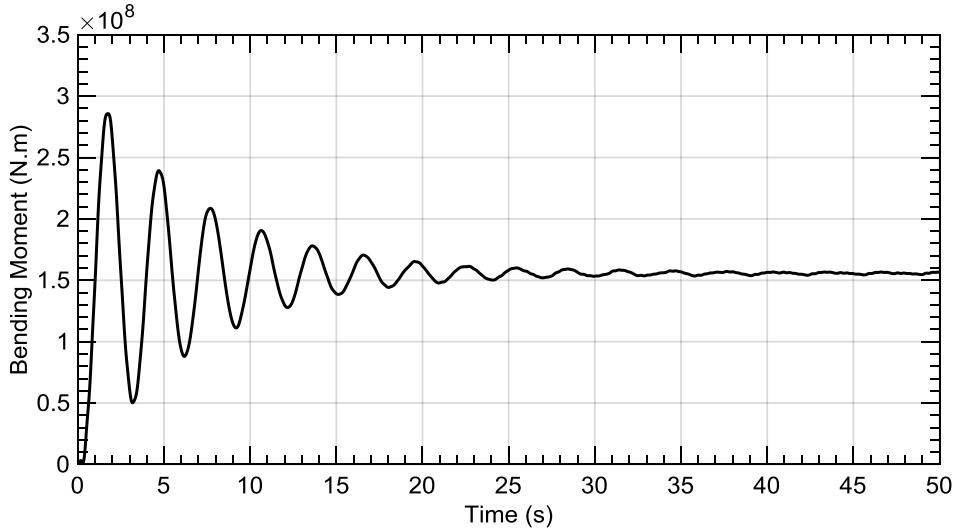

Figure 4.5. Tower-base, fore-aft bending moment

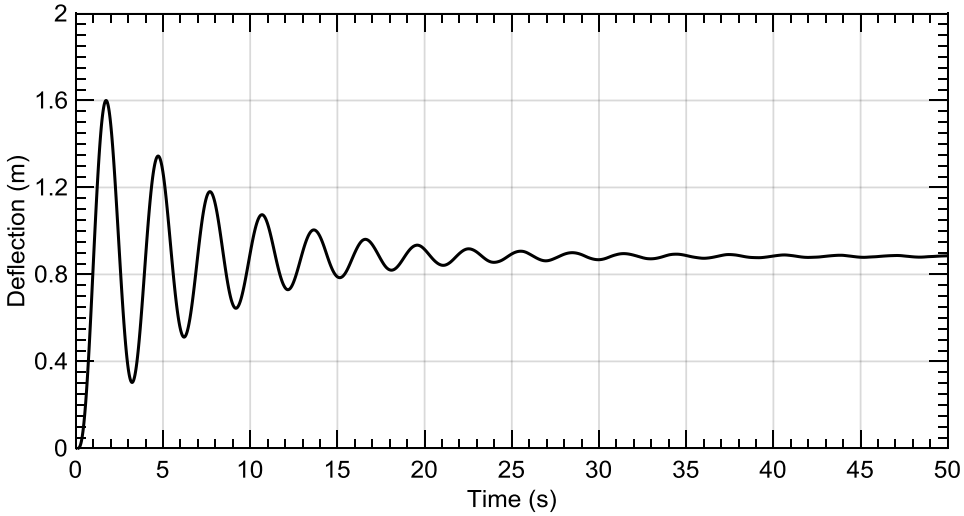

Figure 4.6. Tower-top, fore-aft deflection

As was expected, the deflection of the tower top and bending moment of the tower base change is not linear with the addition of an extra rotor. The change is affected by both the added load, and the change in the natural frequencies of the new tower geometrical properties and hence the stiffness and damping matrices in the mathematical model. The difference is elaborated clearly in Figures 4.7 and 4.8, where the results of the single-rotor and the twin-rotor are shown together.

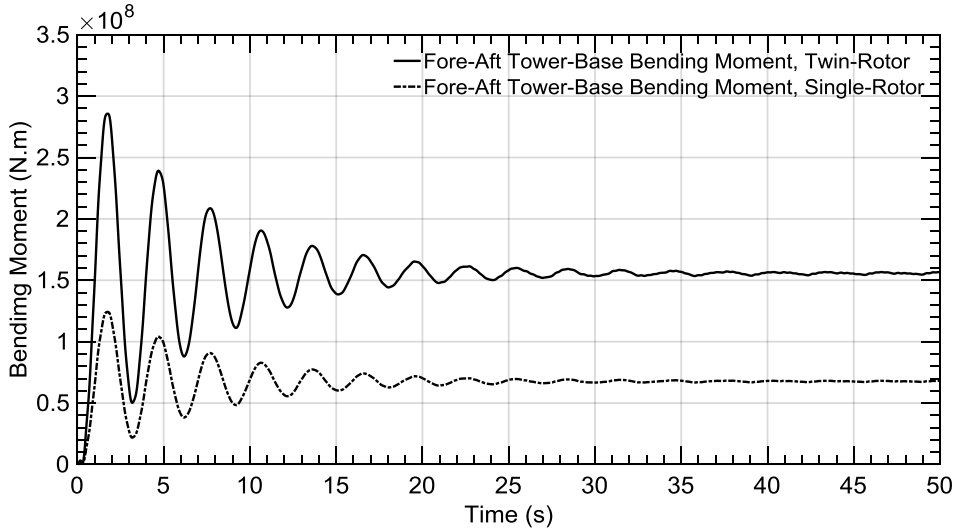

Figure 4.7. Tower-base, fore-aft bending moment - Single-rotor vs. Twin-rotor

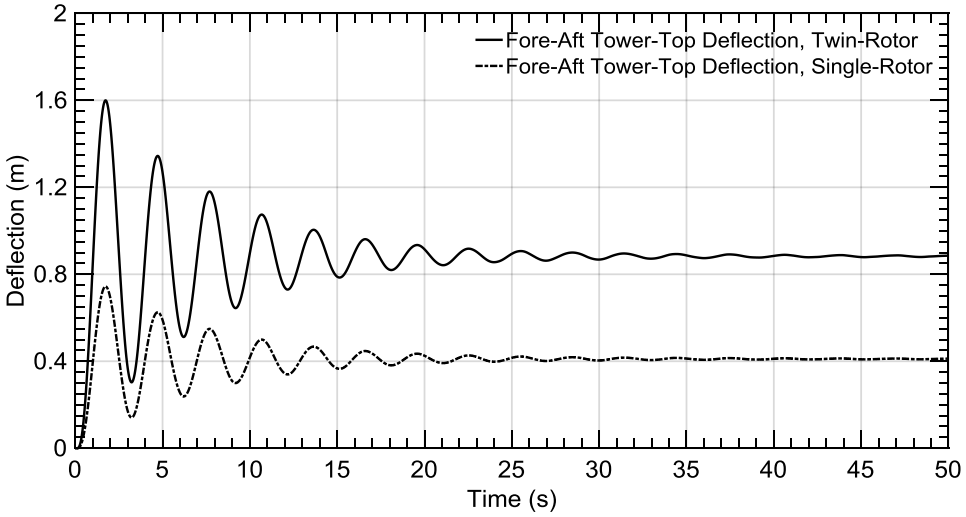

Figure 4.8. Tower-top, fore-aft deflection - Single-rotor vs. Twin-rotor

For a tower with the same first fore-aft natural frequency as the single-rotor configuration, the effect of adding one more rotor on the dynamic responses is not straightforward. Two simultaneously rotating rotors on the same tower increase the tower loads and deflections more than doubled. This is due to the change in the structure mathematical model and the added weight and rotor inertias on the top of the tower, which change the natural frequencies in the second fore-aft and first side-side directions.

Then, a phase difference in the initial azimuth position of the first blade of each rotor of 60° is investigated for comparison. The dynamic responses of the tower are shown in Figures 4.9 and 4.10.

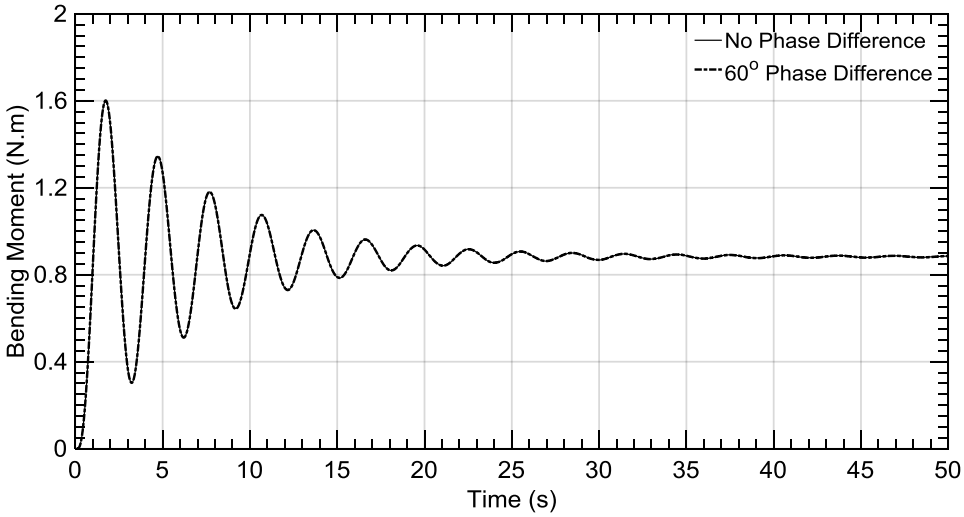

Figure 4.9. Tower-base, fore-aft bending moment

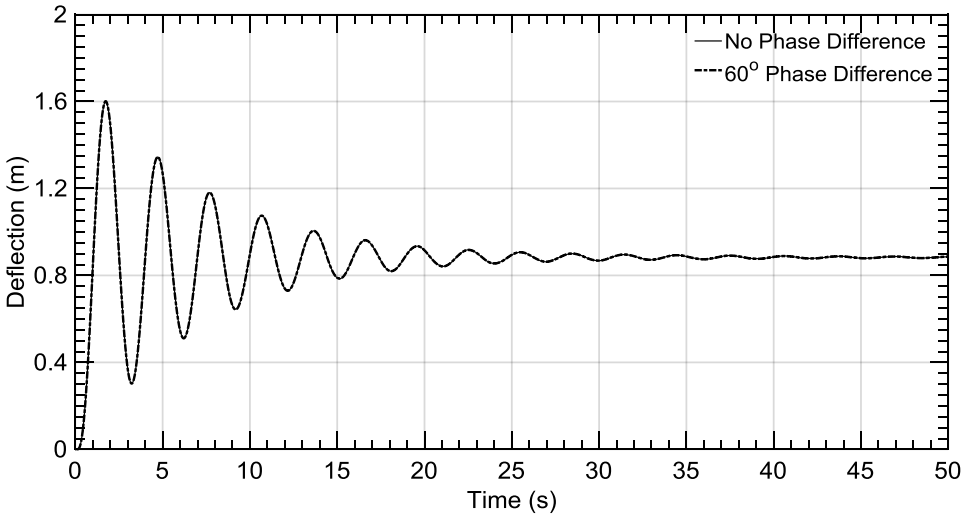

Figure 4.10. Tower-top, fore-aft deflection

Here, the dynamic responses of the tower are almost identical with the no-phase-difference case, there is a very slight difference which can only be seen only by zooming into the graph. However, with the phase change between the azimuth position of the rotor blades, there is a slight phase

change in the rotor loads and hence a twisting moment is generated on the tower causing a yawing deflection which should be studied to anticipate its effect. The yawing deflection of the tower-top is shown in Figure 4.11.

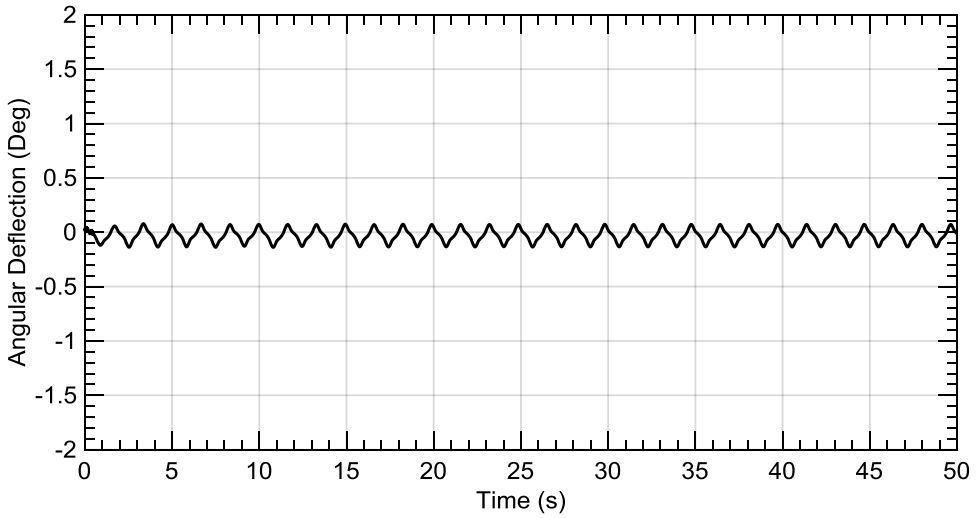

Figure 4.11. Tower top yawing deflection – 60^0 phase difference

When the two rotors were rotating simultaneously and under the same aerodynamic conditions, there was no twisting moment for the tower and hence no deflection. When only a phase change between the rotors occurred, a twisting moment was generated causing angular deflection. For different wind conditions the effect of twist can be severe and cause torsional fatigue and hence failure. So, for a twin-rotor configuration, torsional stiffness should be carefully considered in the tower design.

4.3.2. Turbulent Flow Condition

In this case, the rotors are subject to a turbulent flow field of IEC 61400 classes A, B, and C created by TurbSim, with an average wind speed of 8 m/s. The turbulent grid width was doubled to be able to cover both rotors. Variable speed control (VSC) is applied to control the rotating speed of the rotors. The generator specifications are available in the NREL 5MW definition report [46].

The variable speed control parameters are as follows;

- Gear ratio: 97:1,
- Generator efficiency: 94.4%, and
- Optimal constant of proportionality: 0.0255764 N.m/rpm2.

The simulation is run for 10 minutes, and the tower dynamic responses are calculated. Figure 4.12 shows the wind speed at the hub height for all the turbulent cases.

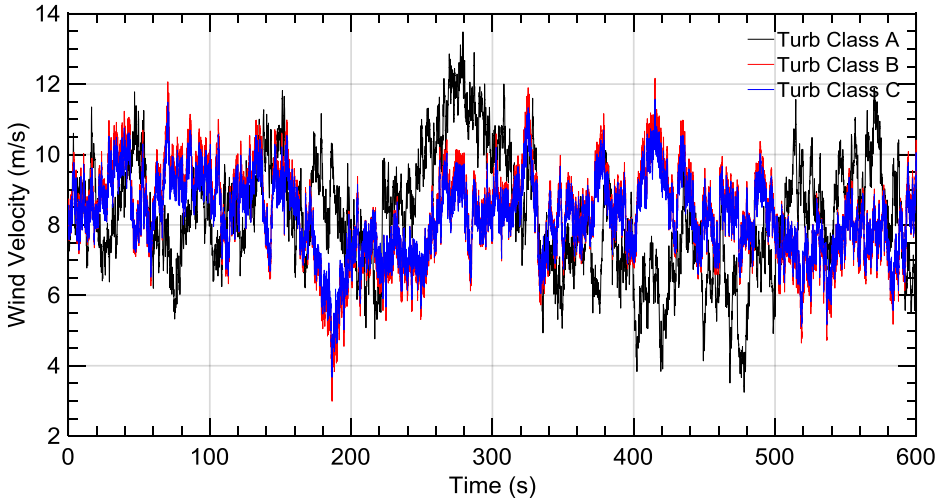

Figure 4.12. Average wind speed at hub height

Figures 4.13 and 4.14 show the dynamic responses for turbulence class A.

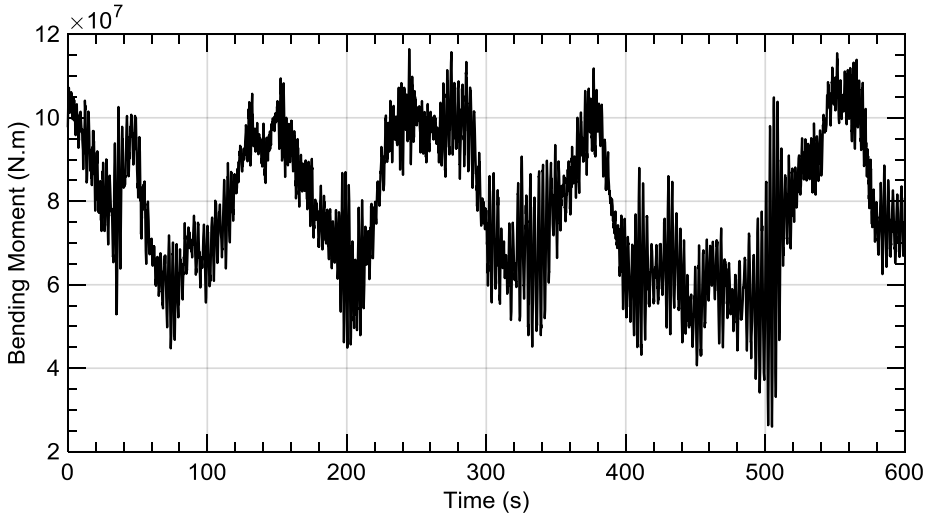

Figure 4.13. Tower-base fore-aft bending moment – Turb. Class A

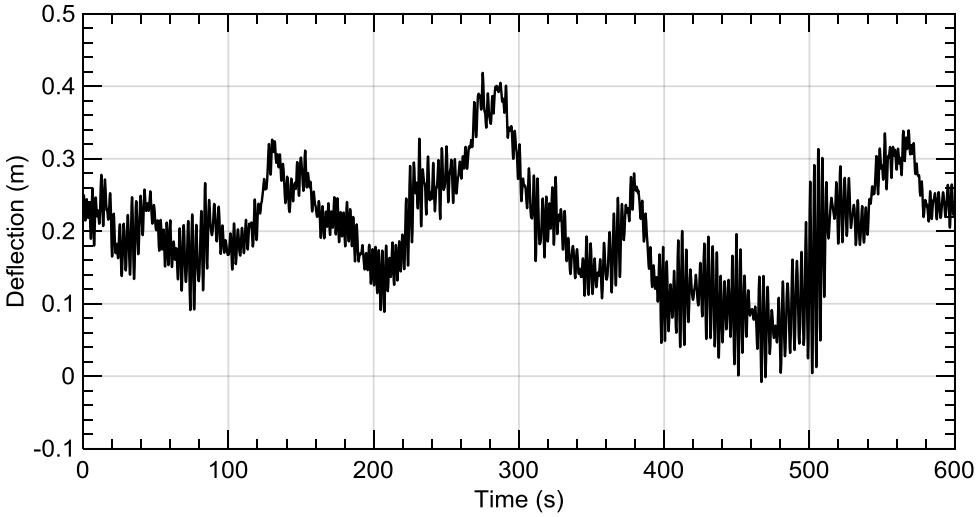

Figure 4.14. Tower-top fore-aft deflection – Turb. Class A

In the same manner as there was a phase change between the two rotors, now the rotors are subject to a turbulent field, where the loads are different on each of the two rotors. Accordingly, the yawing deflection problem will be effective. In order to see the effect of the load change between the rotors, Figure 4.15 shows the yawing deflection for the case where the flow is turbulent of class A.

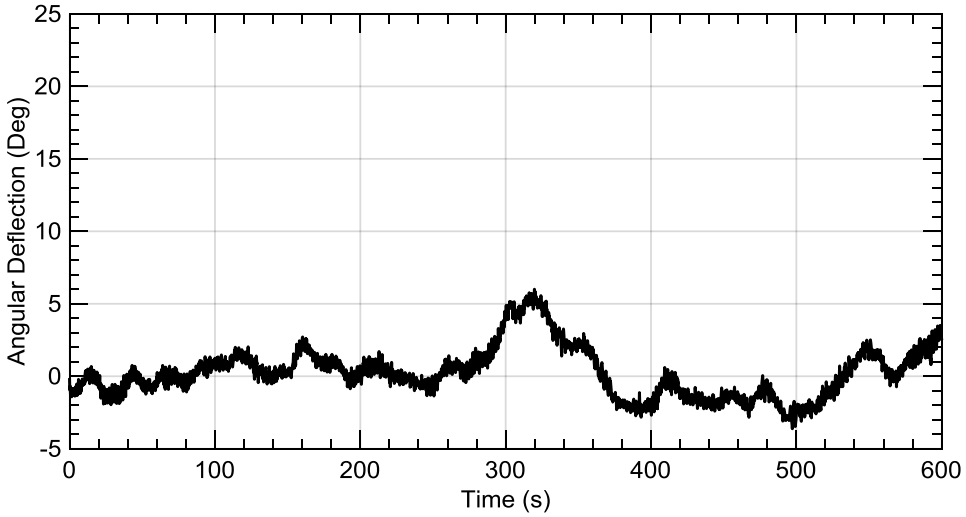

Figure 4.15. Tower-top yawing deflection – Turb. Class A

Similarly, dynamic responses of turbulence classes B and Care shown in Figures 4.16 to 4.21

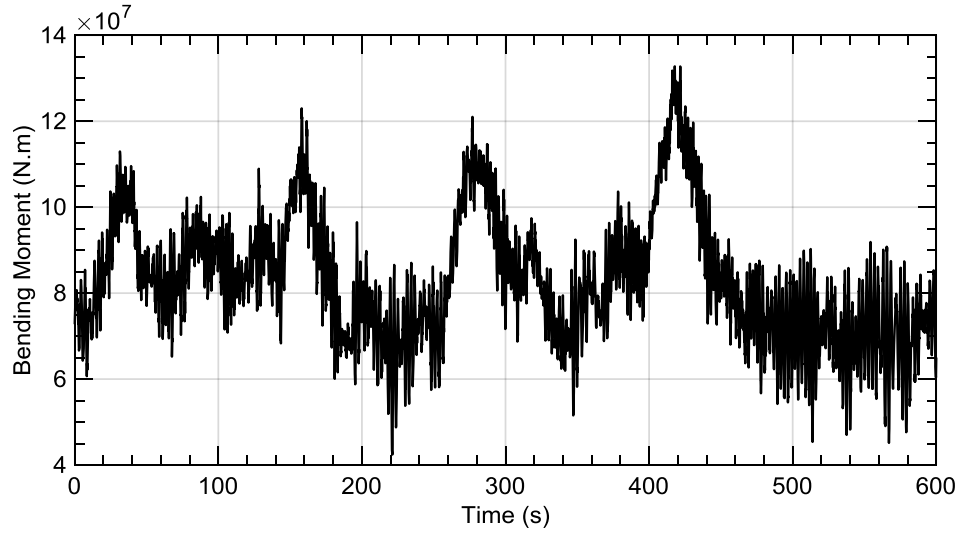

Figure 4.16. Tower-base fore-aft bending moment – Turb. Class B

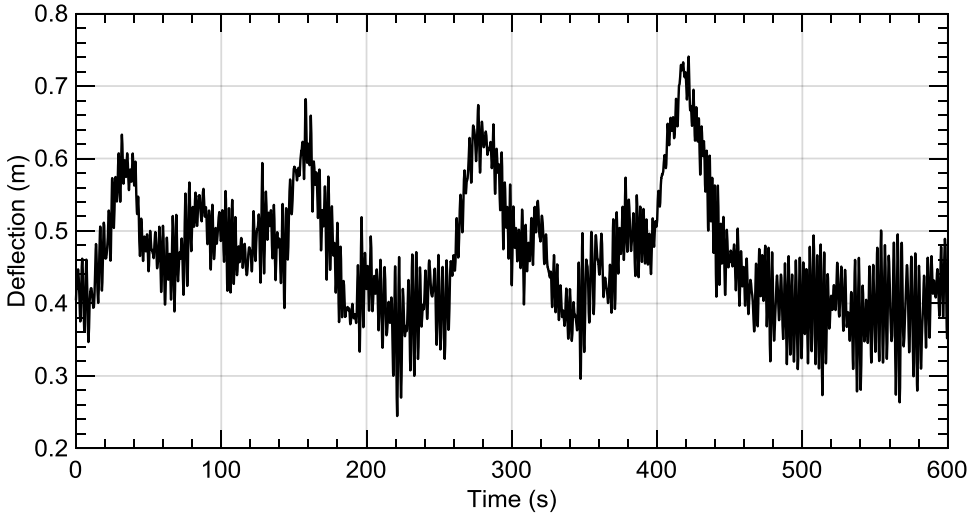

Figure 4.17. Tower-top fore-aft deflection – Turb. Class B

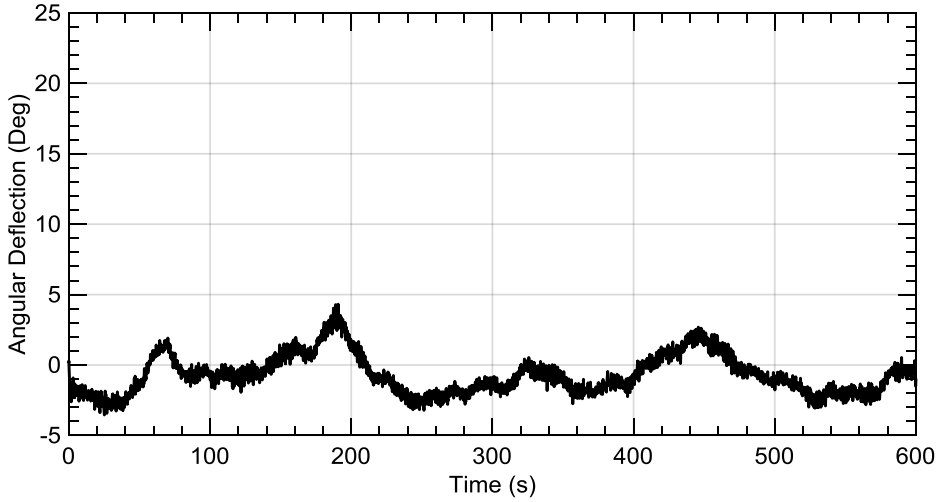

Figure 4.18. Tower-top yawing deflection – Turb. Class B

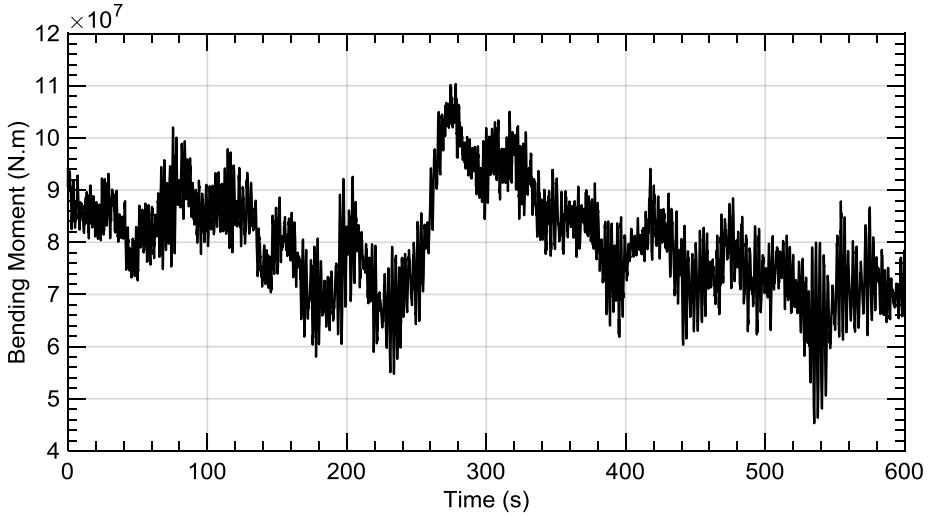

Figure 4.19. Tower-base fore-aft bending moment – Turb. Class C

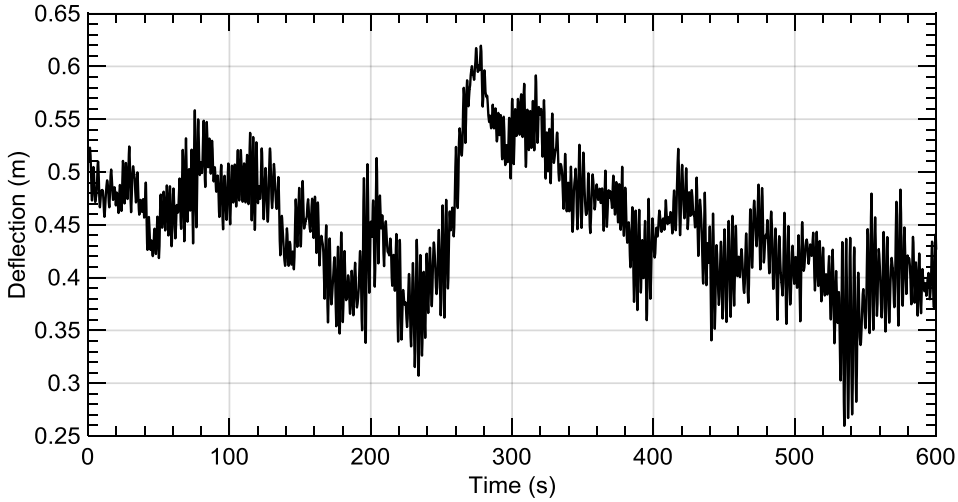

Figure 4.20. Tower-top fore-aft deflection – Turb. Class C

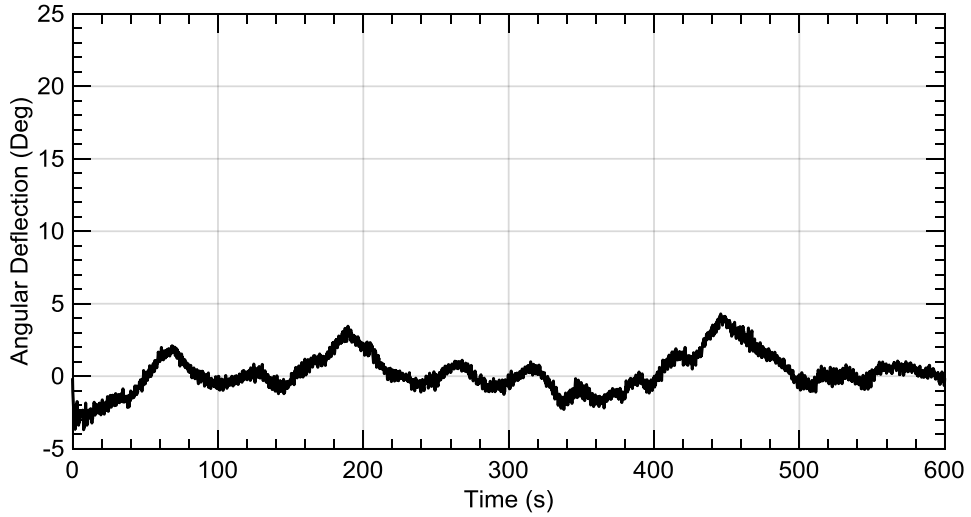

Figure 4.21. Tower-top yawing deflection – Turb. Class C

It is also important in the case of turbulence to study the responses in the frequency domain, to understand the dominant frequencies over the domain, and consider them in the design process to avoid resonance. A Fast Fourier Transform (FFT) was performed to show the frequency domain of the tower-base bending moment for each turbulence case. Figures 4.22 to 4.24 show the results.

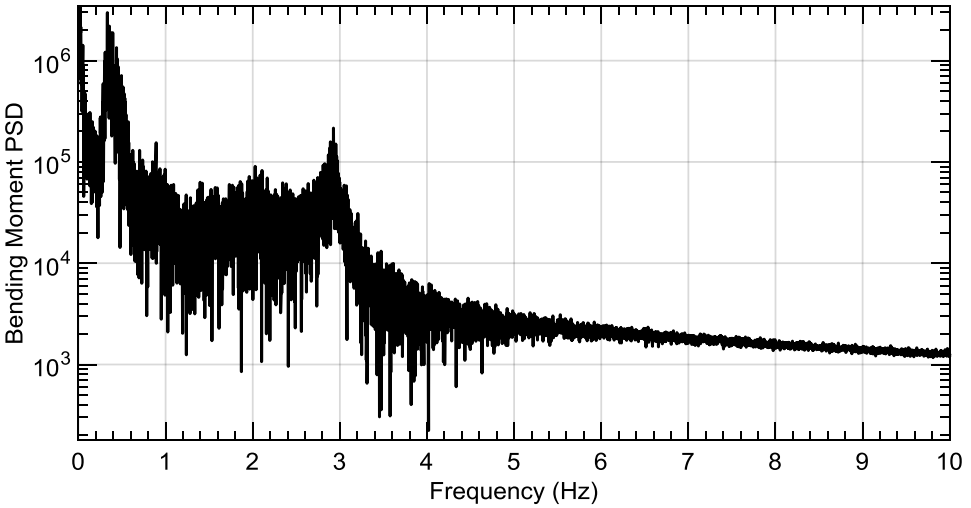

Figure 4.22. Frequency analysis, tower-base bending moment - Turb. Class A

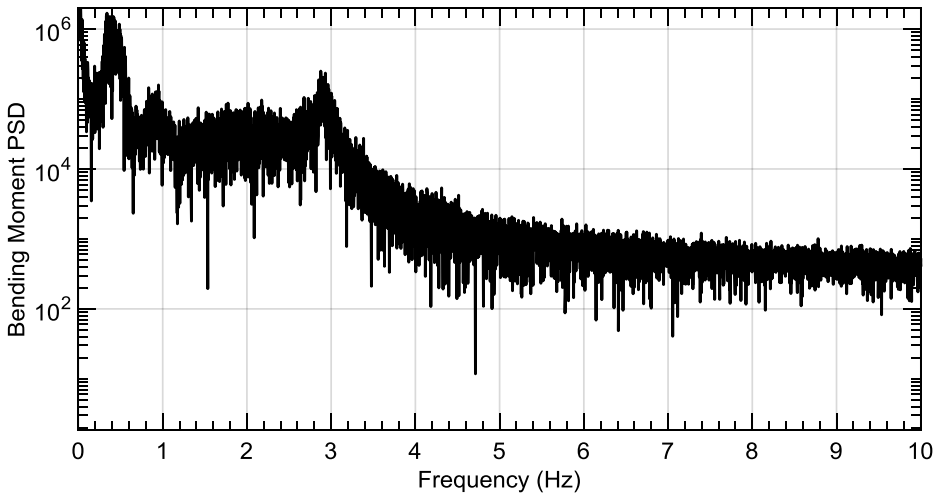

Figure 4.23. Frequency analysis, tower-base bending moment - Turb. Class B

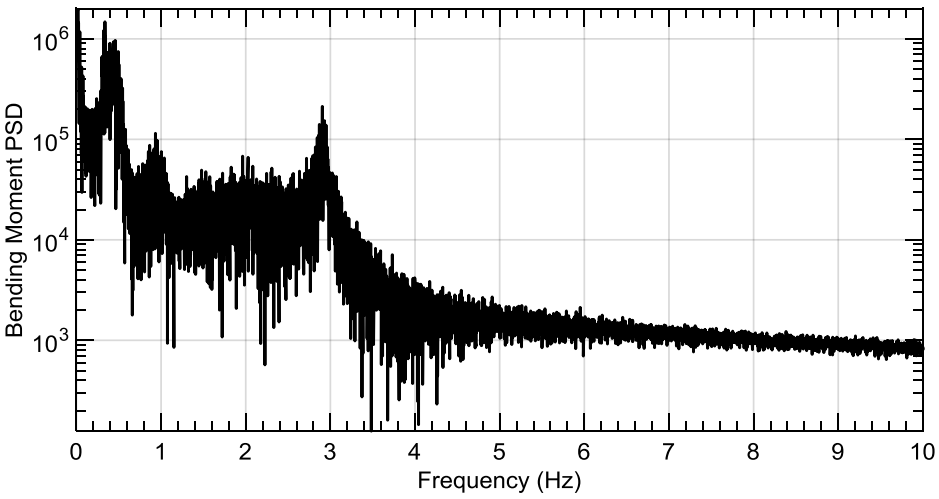

Figure 4.24. Frequency analysis, tower-base bending moment - Turb. Class C

Frequency analyses in all turbulent cases show that the dominant frequencies are at 0.32 Hz and 3 Hz, which are the same as the free vibration natural frequencies of the tower.

Comparison between the dynamic response of the tower-base bending moment for the turbulent flow load cases are shown in Table 4.3.

Table 4.3. Statistical analysis for tower-base bending moment in turbulent cases

Turbulence Class	Mean Value	Standard Deviation	Dominant Frequencies
A	8.00e+07	1.79e+07	0.32 Hz and 3.0 Hz
B	8.25e+07	1.53e+07	0.32 Hz and 3.0 Hz
C	8.06e+07	1.14e+07	0.32 Hz and 3.0 Hz

Statistical analysis in Table 4.3 has shown that the tower natural frequencies are dominant over the flow condition. For the high turbulence intensity, the mean value of the load is less than the other intensities, however a higher standard deviation occurs which indicates severe oscillation of the loads.

4.4. Side-Boom Analysis

In this section, the side-booms holding the rotors are studied. Initially, the side-booms model was chosen as a scaled-down version of the main tower of the NREL 5MW turbine. However, the side-booms' size is a function of many parameters. Length of the side-boom depends on the optimum spacing between the rotors in order to improve the whole turbine performance. The cross-section size and distribution depend on the stiffness accompanied with that size, to sustain the loads. This section is concerned with the cross-section size and distribution, and its effect on the deflections and loads of the side-booms.

Simulations have been made for three configurations for the side-boom in the turbulent load conditions. The first configuration is the original scaled-down version of the main tower. The second and third configurations have the same length and thickness, while the diameters are 1.25 and 1.5 times the original diameter. Comparison between the three configurations are shown in Table 4.4.

Table 4.4. Side-boom configurations

Property (m)	Side-boom 1	Side-boom 2	Side-boom 3
Root diameter	4.500	5.625	6.750
Root thickness	0.027	0.027	0.027
Tip diameter	2.900	3.625	4.350
Tip thickness	0.019	0.019	0.019
Length	63.500	63.500	63.500

Figures 4.25 and 4.26 show the mass and stiffness distributions along the side-boom length for three configurations.

Although the mass of the side booms has increased for the larger diameter side-booms, the stiffness has also increased which indicates more strength and ability to withstand higher loads.

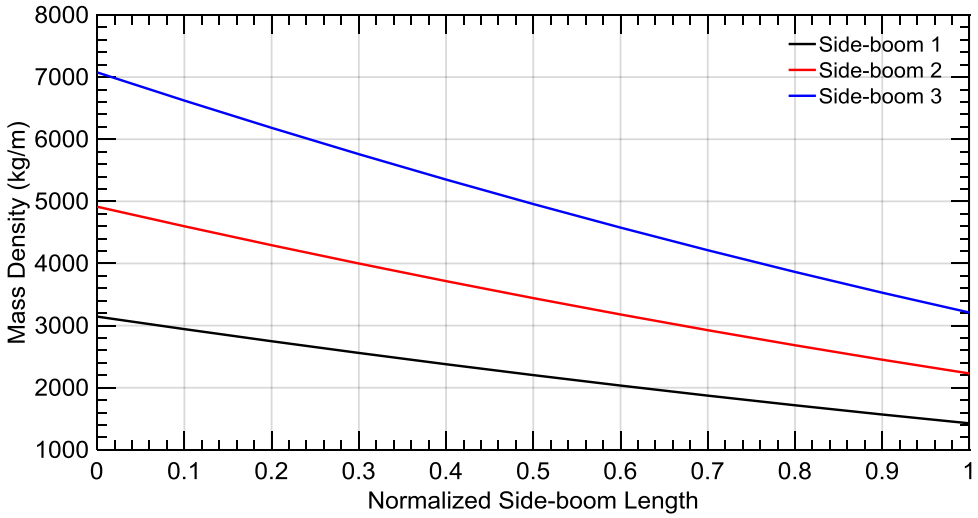

Figure 4.25 Side-boom mass density distribution

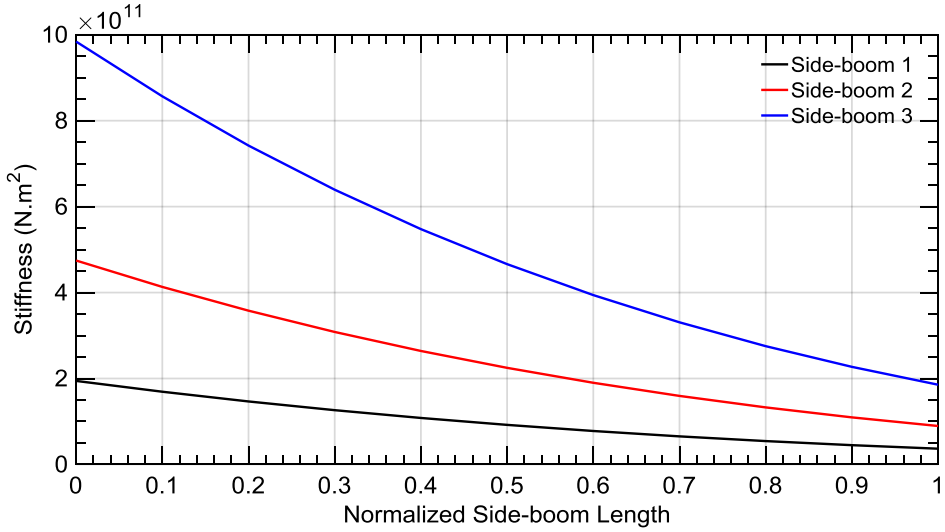

Figure 4.26. Side-boom stiffness distribution

To compare between the performance of different booms, the boom deflections for the different turbulent cases have been studied. Deflections in the fore-aft (out of rotor plane) and side-side (in rotor plane) were calculated. Figures 4.27 to 4.32 show the deflections of the first configuration side-boom tip for turbulence classes A, B, and C

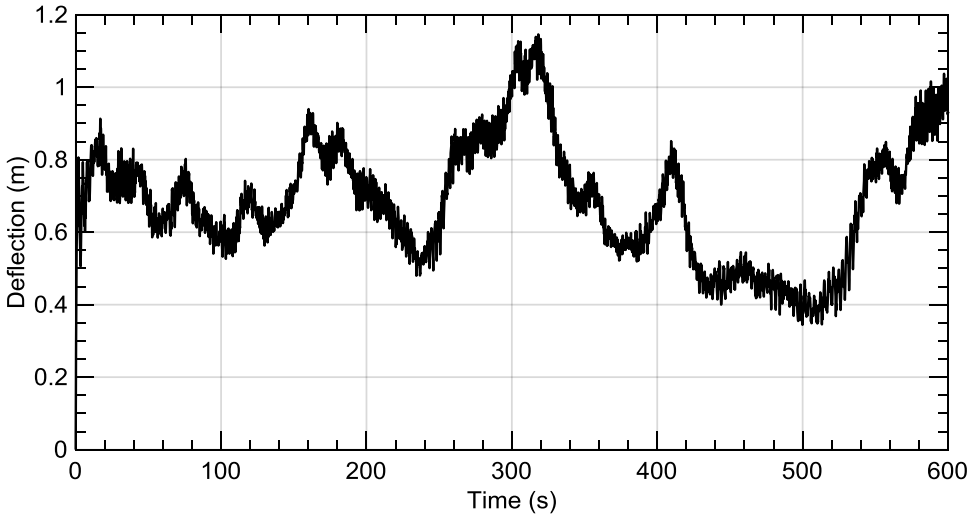

Figure 4.27. Fore-aft tip deflection - Side-boom 1 - Turb. Class A

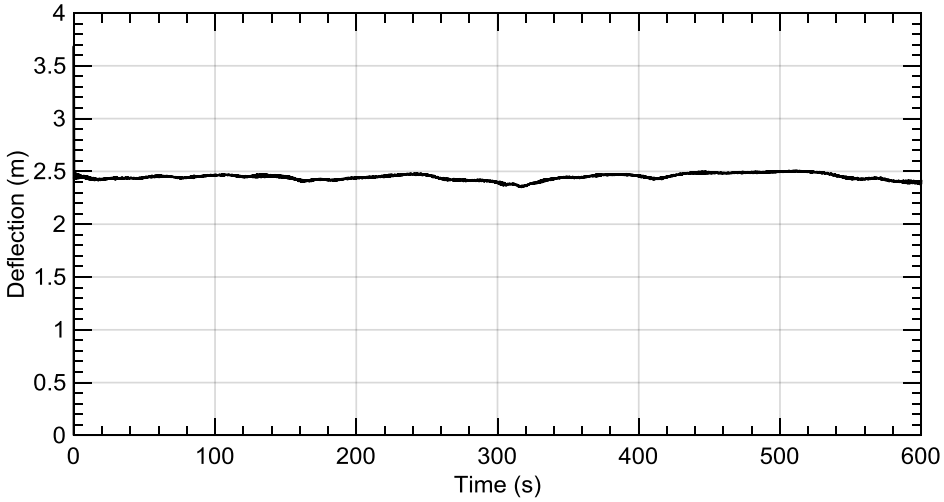

Figure 4.28. Side-side tip deflection - Side-boom 1 - Turb. Class A

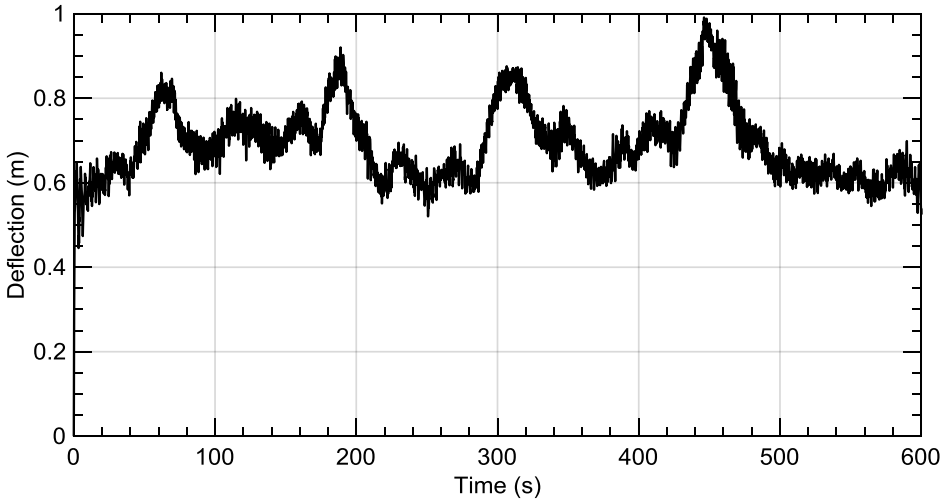

Figure 4.29. Fore-aft tip deflection - Side-boom 1 - Turb. Class B

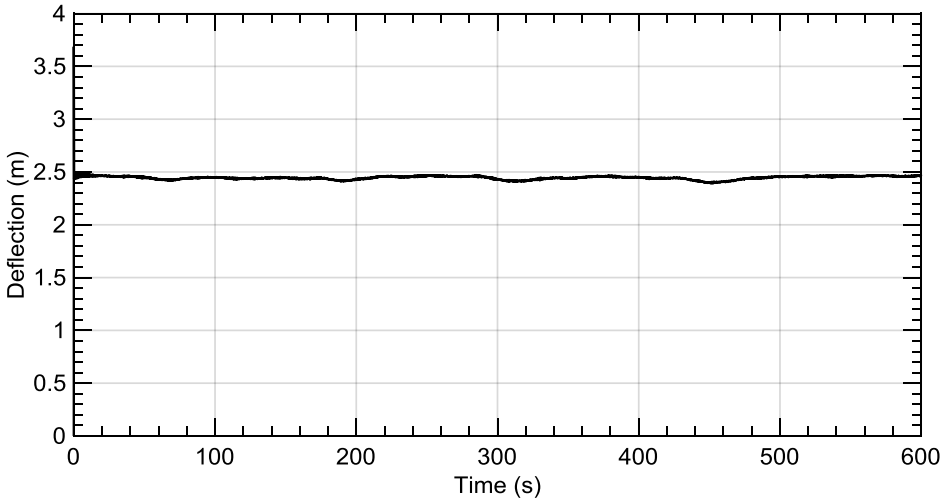

Figure 4.30. Side-side tip deflection - Side-boom 1 - Turb. Class B

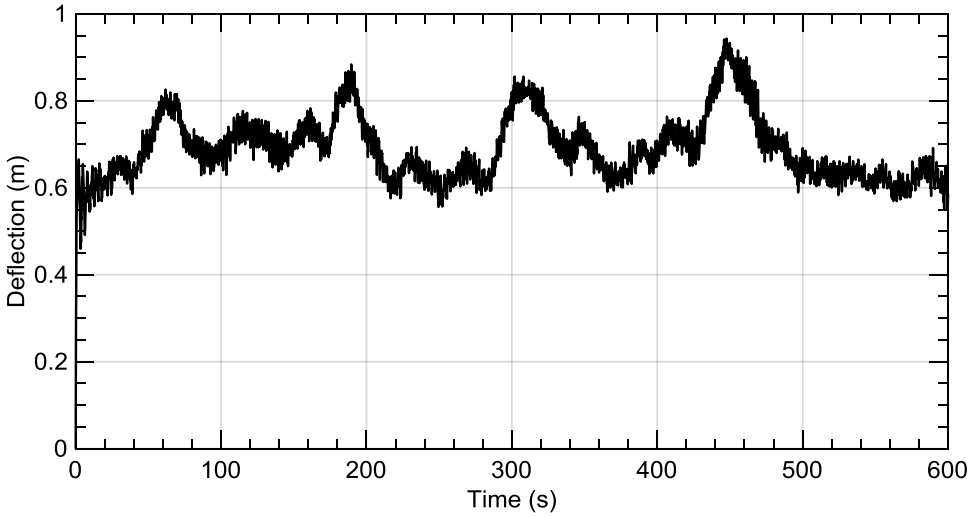

Figure 4.31. Fore-aft tip deflection - Side-boom 1 - Turb. Class C

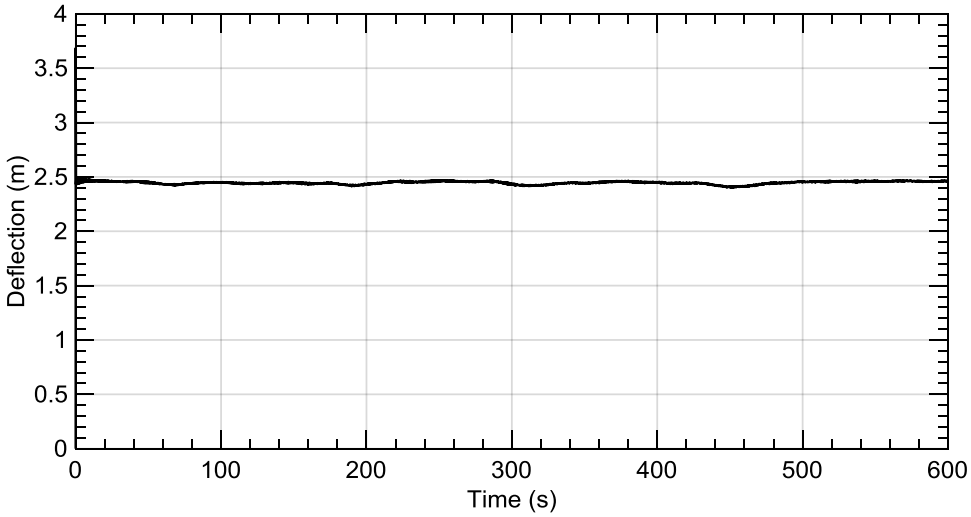

Figure 4.32. Side-side tip deflection - Side-boom 1 - Turb. Class C

It can be noted that the random behavior of the turbulence doesn't take place in the side-side deflections. This may be due to the dominance of the rotor weight load over the fluctuating aeroelastic loads on the side-boom. It is also noted that for all turbulence classes, the mean value of the deflection is almost the same, so for the other two configurations, results for turbulence class A only will be shown.

Figures 4.33 to 4.36 show the deflections of side-booms second and third configuration, for turbulence class A.

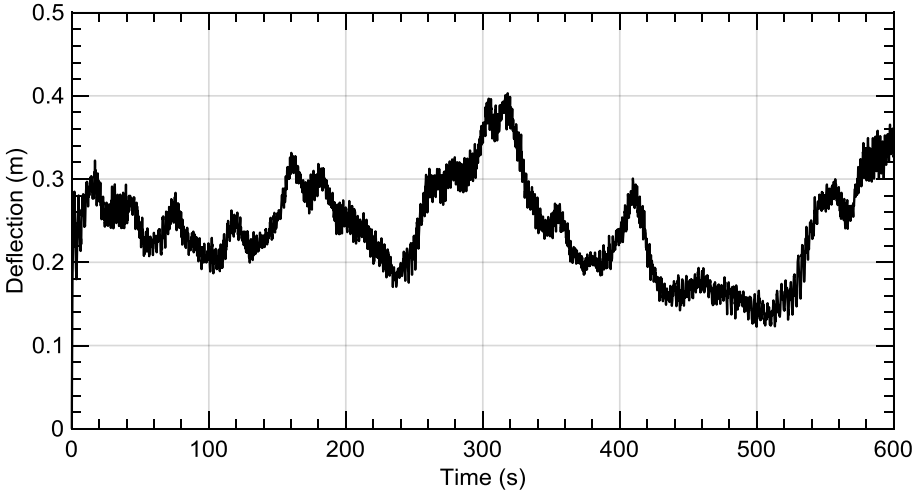

Figure 4.33. Fore-aft tip deflection - Side-boom 2 - Turb. Class A

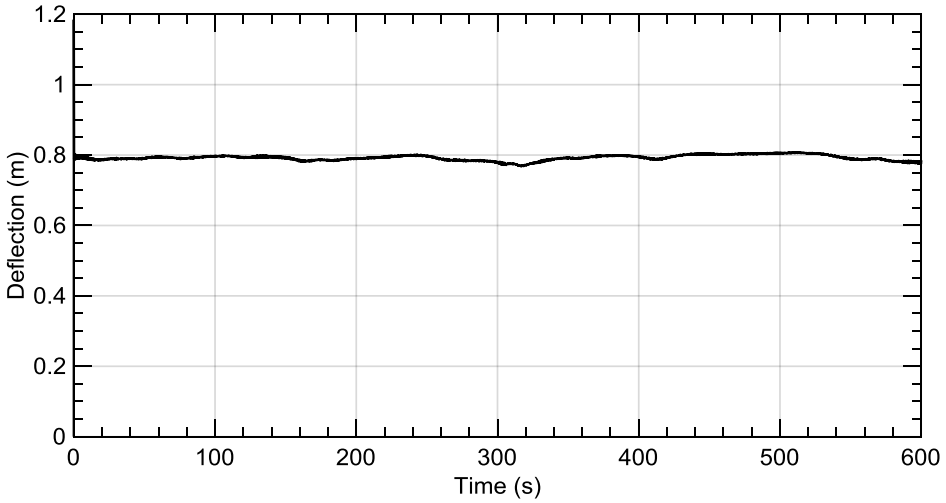

Figure 4.34. Side-side tip deflection - Side-boom 2 - Turb. Class A

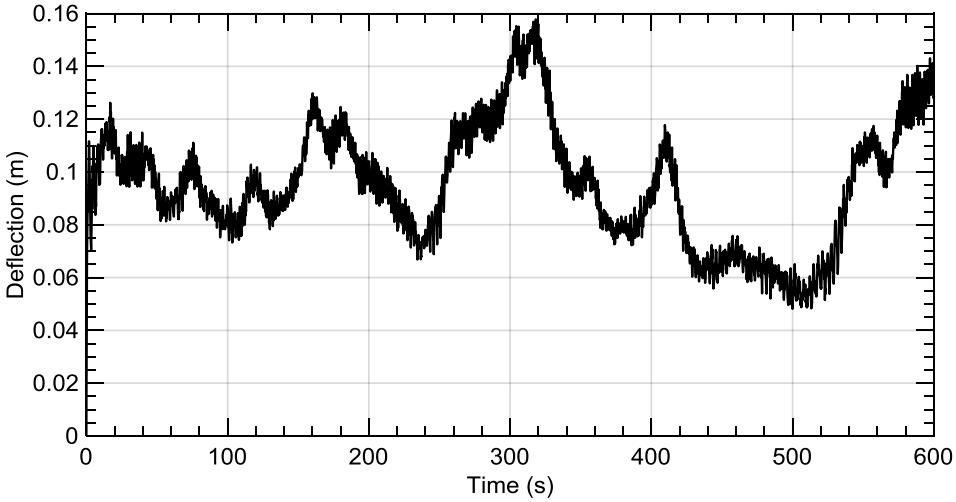

Figure 4.35. Fore-aft tip deflection - Side-boom 3 - Turb. Class A

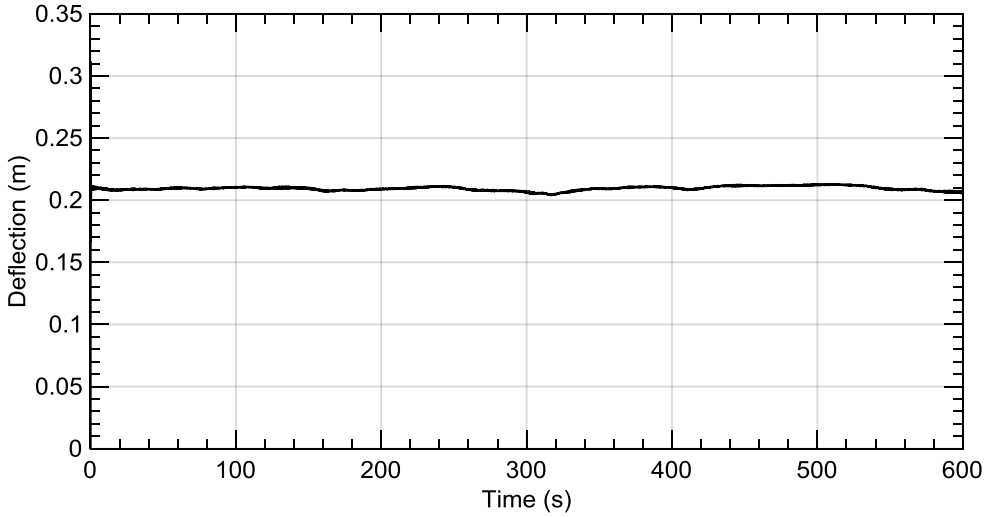

Figure 4.36. Side-side tip deflection - Side-boom 3 - Turb. Class A

The increased diameter of the side-booms significantly affects the stiffness of the structure and hence decreases the unfavorable deformations. The third side-boom configuration has the least deformation, yet the highest weight. Weight to strength ratio should be compromised for the optimum performance of the whole turbine.

Figure 4.37 shows the mean stiffness of each side-boom configuration plotted against the mean deflection in the fore-aft direction for turbulence class A.

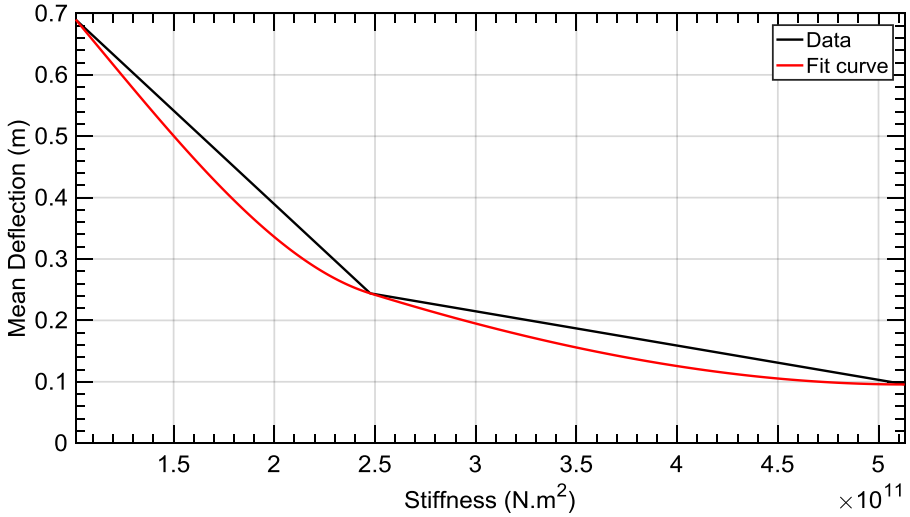

Figure 4.37. Side-boom stiffness vs. mean deflection

From the curve fitting in Figure 4.37, the relation between the stiffness of the side boom and the mean deflection value seems to be of the second order.

4.5. Chapter Summary

In this chapter, the present tool is tested by simulating a twin-rotor configuration. Dynamic response of the main tower and the side booms were studied. It is found that for a twin-rotor, not only the linear deflections are important, but also the yawing deflections since there is a lateral difference between the loads of the two rotors. Also, the side-booms side is a function of the aerodynamic interaction between the rotors and the added weight on the top tower; comptonization between both factors should be considered to get the optimum design.

Chapter 5

Simulation of Multi-Rotor Configurations

Contents

5.1. Chapter Overview 73

5.2. Three-Rotor Configuration 73

5.2.1. Three-Rotor Tower Analysis 76

5.3. Four-Rotor Configuration 81

5.2.2. Four-Rotor Tower Analysis 84

5.4. Chapter Summary 89

5.1. Chapter Overview

In this chapter, the simulation is extended to include more configurations of the multi-rotor wind turbines. Three -rotor and four-rotor configurations have been modelled. Tower dynamics are studied for steady and turbulent wind conditions to see the effect of adding extra rotors on the structural behavior of the main tower.

5.2. Three-Rotor Configuration

The main tower is extended vertically to include one more rotor on the top, in addition to the two lower rotors in the same manner as the twin-

rotor configuration. All rotors are the same as previous, NREL 5MW rotors, with a total capacity of the turbine of 15MW. Similarly, for comparison purposes, the dominant frequency of the 1st fore-aft frequency is assumed to be the same as the single-rotor and the twin-rotor configurations.

Adjustments to the main tower geometry have been made accordingly. The tower base diameter has increased to be 2.85 times the original, single-rotor tower, while keeping the thickness the same as before and increasing the height to be 197.6 m. This height of the tower keeps the distance between one rotor and the other to be 1 m, to decrease the total weight of the support structure. Figure 5.1 shows a sketch of the three-rotor configuration.

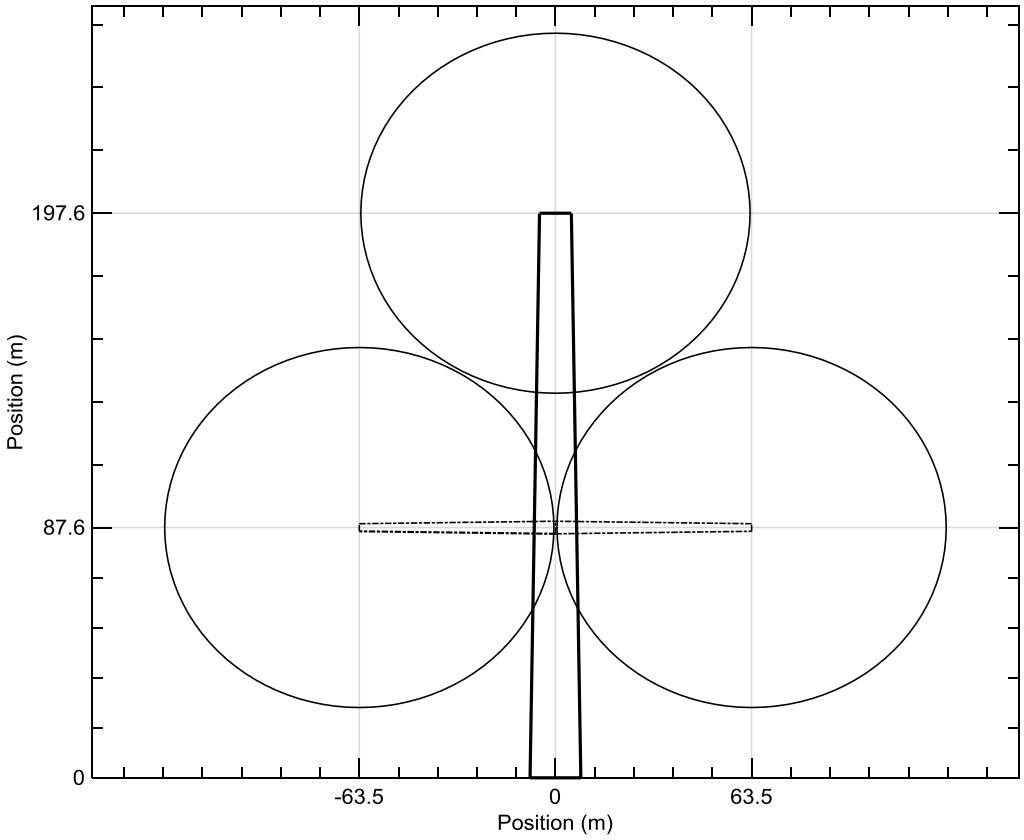

Figure 5.1 Three-rotor configuration sketch

Chapter 5. Simulation of Multi-Rotor Configurations

Table 5.1 shows the geometrical dimensions of the three-rotor configuration tower, compared to the single-rotor configuration.

Table 5.1. Tower geometry – Single-rotor compared to three-rotor configuration

Property (m)	Single rotor	Three-rotor
Tower base diameter	6.000	16.440
Tower base thickness	0.027	0.027
Tower top diameter	3.870	10.300
Tower top thickness	0.019	0.019
Tower height	87.600	197.600

It can be shown that the tower diameter has significantly increased. This is to stand for the added weight of one more rotor and the extra portion of the tower itself. Figures 5.2 and 5.3, show the mass and stiffness distributions along the tower height.

Although the mass distribution has increased to nearly 6 times compared to the single-rotor configuration, the stiffness distribution has increased drastically. That stiffness is needed to stand for the added loads.

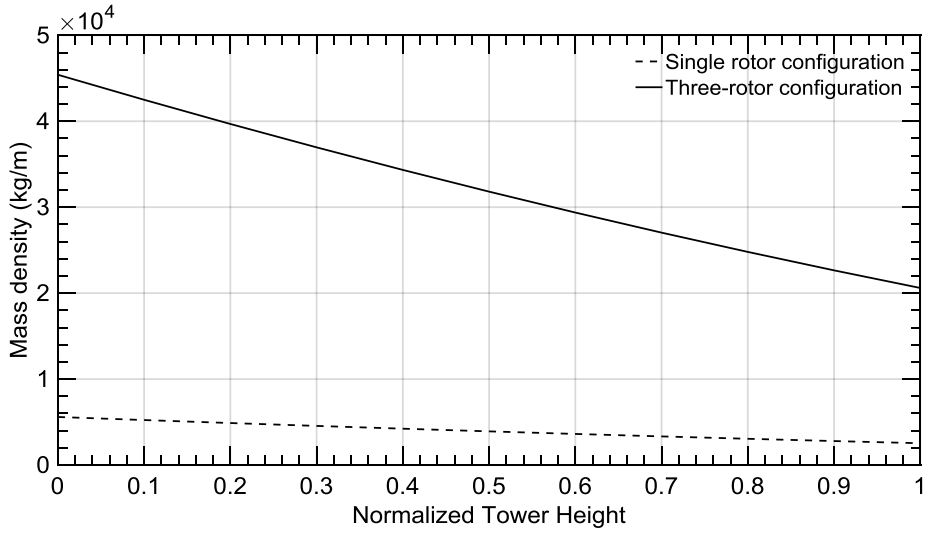

Figure 5.2. Tower mass density distribution – Single-rotor vs. Three-rotor

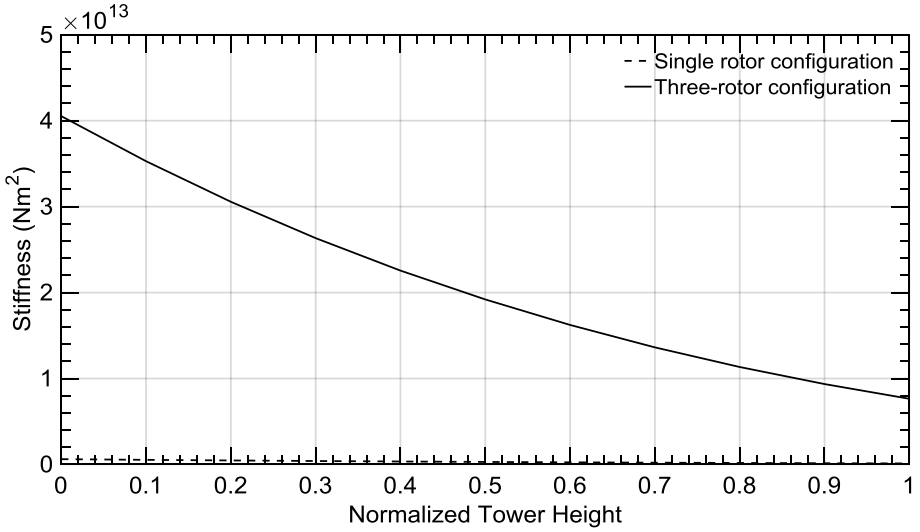

Figure 5.3. Tower stiffness distribution – Single-rotor vs. Three-rotor

The natural frequencies are then calculated for the three-rotor configuration and compared to the single-rotor configuration in Table 5.2.

Table 5.2. Natural frequencies of the tower – Single vs. Three-rotor configuration

Mode	Single-rotor (Hz)	Three-rotor (Hz)	Deviation (%)
First fore-aft	0.32	0.32	0.0
Second fore-aft	3.06	2.24	-26.8
First side-side	0.32	0.29	-9.4

Frequencies in the 2nd fore-aft and 1st side-side directions are decreased due to the difference in the tower geometry and the extra weight added. As has been shown in chapter 4, the natural frequencies are dominant regarding the tower dynamics. With the difference between the natural frequencies of the three-rotor configuration compared to the single-rotor, the dynamics are expected to be different.

5.2.1. Three-Rotor Tower Analysis

Simulation over the three-rotor configuration has been made in turbulent wind condition. Similar to the twin-rotor case, IEC turbulence classes A, B, and C are used for the simulation. The turbulence window has

been enlarged to include all the three rotors and then the tower dynamics have been calculated. Figures 5.4 and 5.5 show the tower top deflection and the corresponding frequency analysis for turbulence class A.

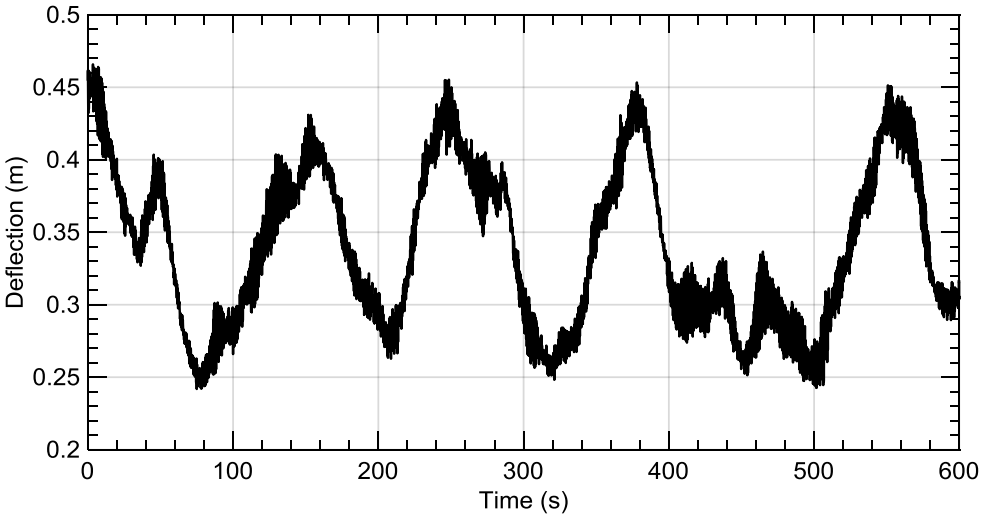

Figure 5.4. 3R Tower-top fore-aft deflection – Turb. Class A

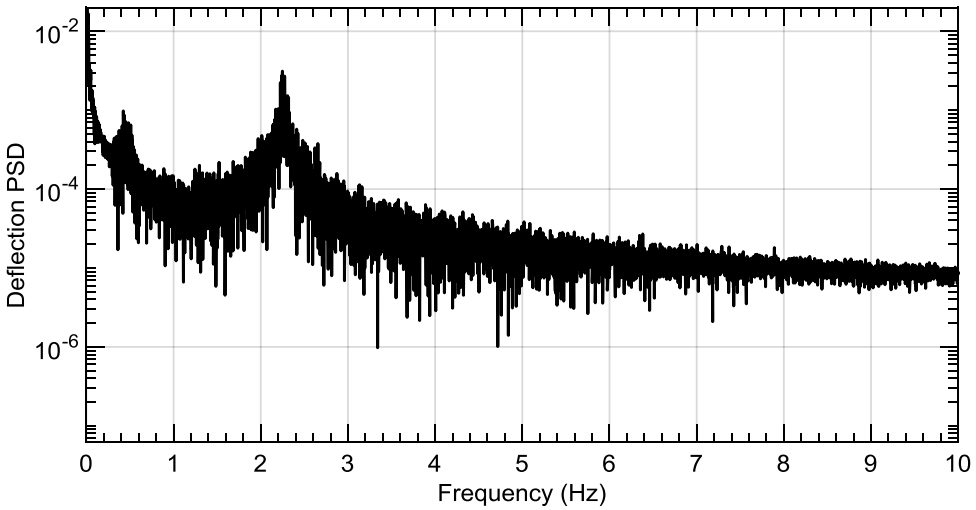

Figure 5.5. 3R Frequency analysis, tower-top deflection – Turb. Class A

Compared to the twin-rotor configuration which had an average tower-top deflection with a mean value around 0.2 m, the three-rotor configuration has a mean value around 0.35 m. The change is not linear with the number of rotors, which is a result of the big difference in the higher

order natural frequencies, as well as the increased tower height and the extra weight added at the tip, which increases the effect of inertial loads on the tower vibrations.

Tower yawing deflection is studied as well. The yawing moment results from the variation between the loads on the side rotors. Figure 5.6 shows the yawing deflection of the tower top.

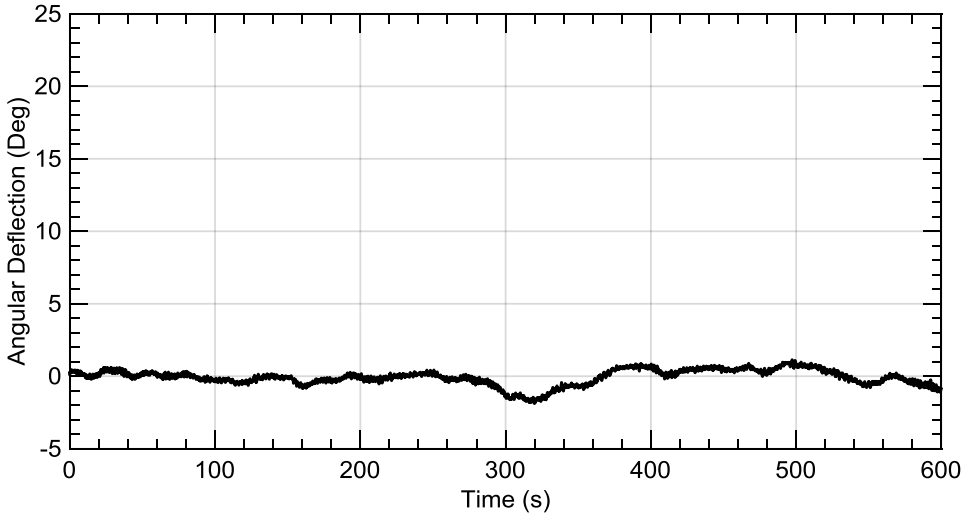

Figure 5.6. 3R Tower-top yawing deflection – Turb. Class A

The yawing deflection of the tower top is decreased significantly compared to the twin-rotor configuration. The cause of yawing moment is the difference between the loads on the side rotors, the same as the twin-rotor. However, the main tower is stiffer and has a larger diameter, which makes it more endurable to similar value of loads.

Figures 5.7 and 5.8 show the tower dynamics for the turbulence class B.

The results of the turbulence field of class B show a similar behavior of the tower dynamics, as well as the dominant frequencies and the reduced yawing deflections.

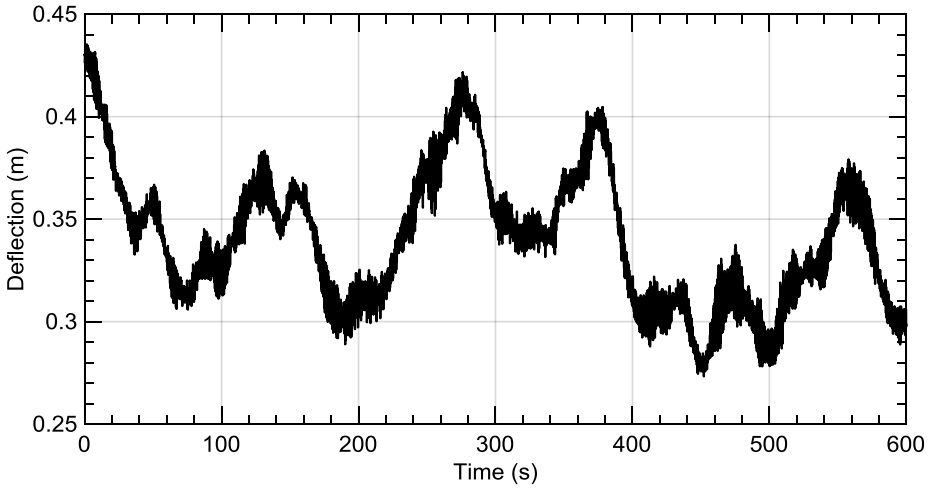

Figure 5.7. 3R Tower-top fore-aft deflection – Turb. Class B

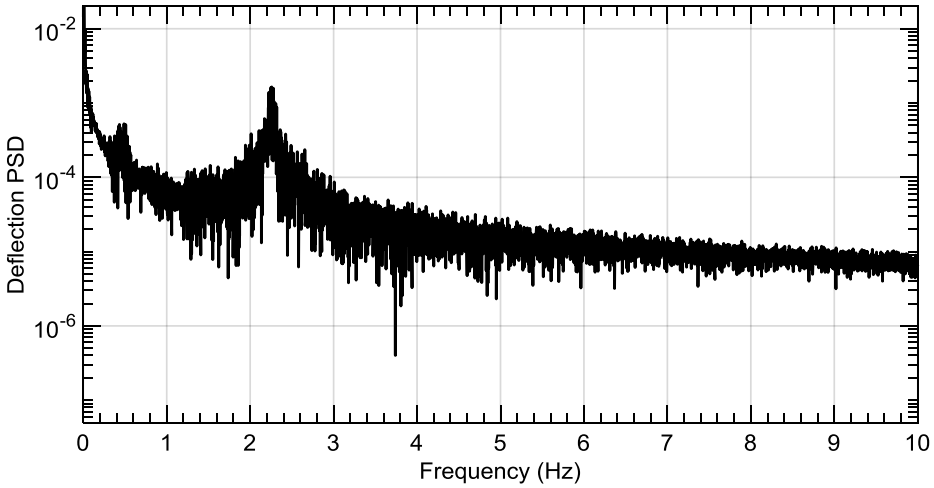

Figure 5.8. 3R Frequency analysis, tower-top deflection – Turb. Class B

Figure 5.9 shows the yawing deflection at the tower top.

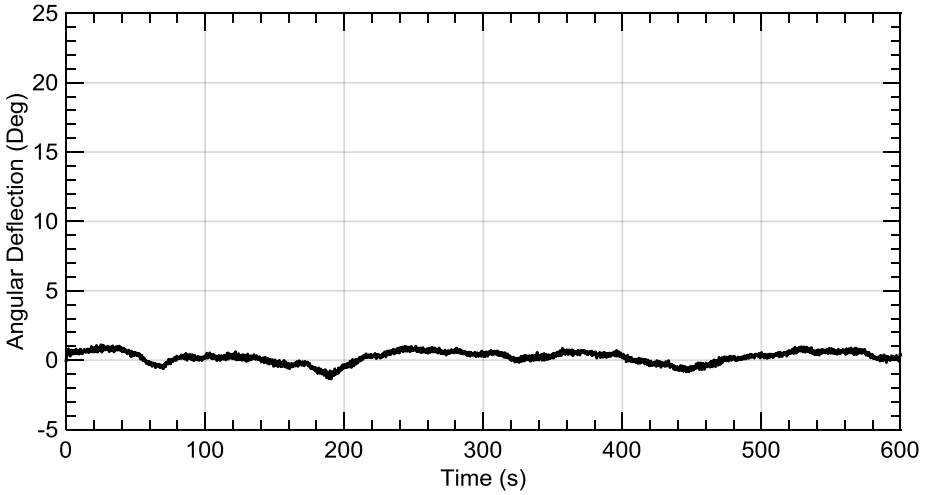

Figure 5.9. 3R Tower-top yawing deflection – Turb. Class B

Turbulence class C results are shown in Figures 5.10 to 5.12.

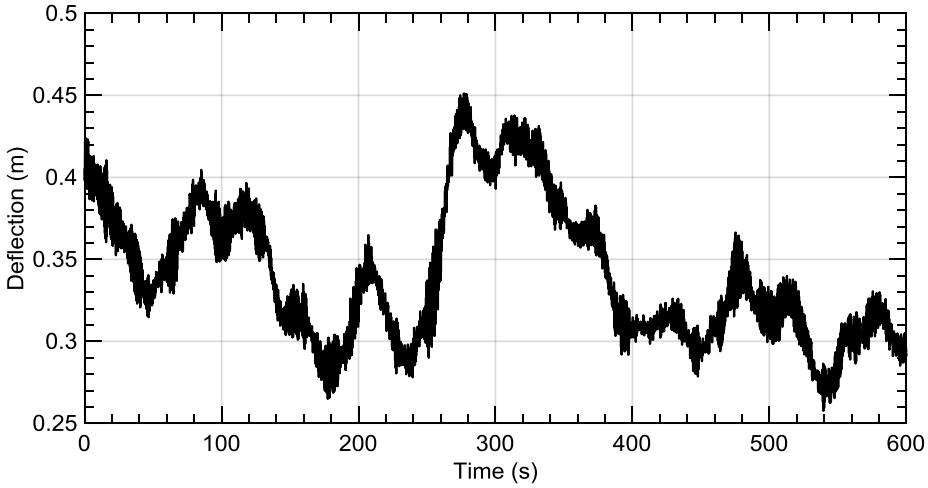

Figure 5. 10. 3R Tower-top fore-aft deflection – Turb. Class C

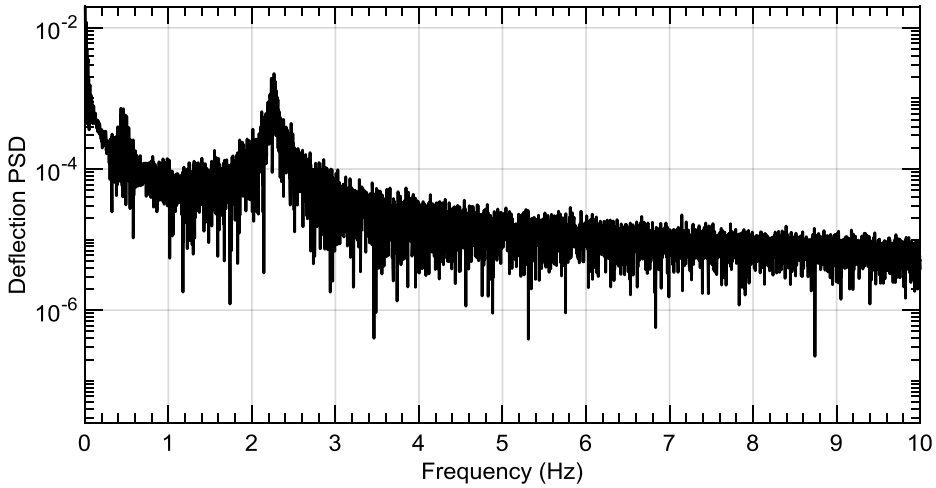

Figure 5.11. 3R Frequency analysis, tower-top deflection – Turb. Class C

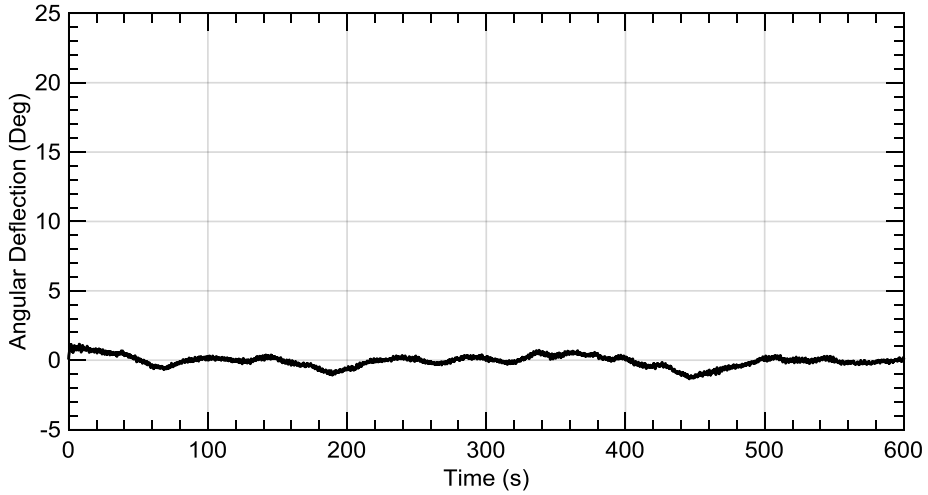

Figure 5. 12. 3R Tower-top yawing deflection – Turb. Class C

Summary of the tower-top deflection results are shown in Table 5.3.

Table 5.3. Statistical analysis for tower-top deflection in turbulent cases – 3R

Turbulence Class	Mean Value	Standard Deviation	Dominant Frequencies
A	0.343	0.057	0.32 Hz and 2.24 Hz
B	0.343	0.044	0.32 Hz and 2.24 Hz
C	0.344	0.036	0.32 Hz and 2.24 Hz

In the same manner as the twin-rotor results, results of the three-rotor configuration show that the turbulence class does not affect the mean tower dynamics value highly, however, the standard deviation is highly affected. Also, the natural frequencies are dominant over the wind conditions. Excitations in the frequency domain occur at the same exact values of the natural frequencies.

5.3. Four-Rotor Configuration

In the same manner, the main tower geometry is changed to suite the added loads. The diameter is further increased to be 3.3 times the single rotor configuration, while the height is increased to be 214.6 m. The total capacity of this configuration is 20 MW. Figure 5.13 shows a sketch of the four-rotor configuration.

Table 5.4 shows the geometric model of the four-rotor configuration.

Table 5.4. Tower geometry – Single-rotor compared to four-rotor configuration

Property (m)	Single rotor	Three-rotor
Tower base diameter	6.000	19.000
Tower base thickness	0.027	0.027
Tower top diameter	3.870	11.800

Property (m)	Single rotor	Three-rotor
Tower top thickness	0.019	0.019
Tower height	87.600	214.600

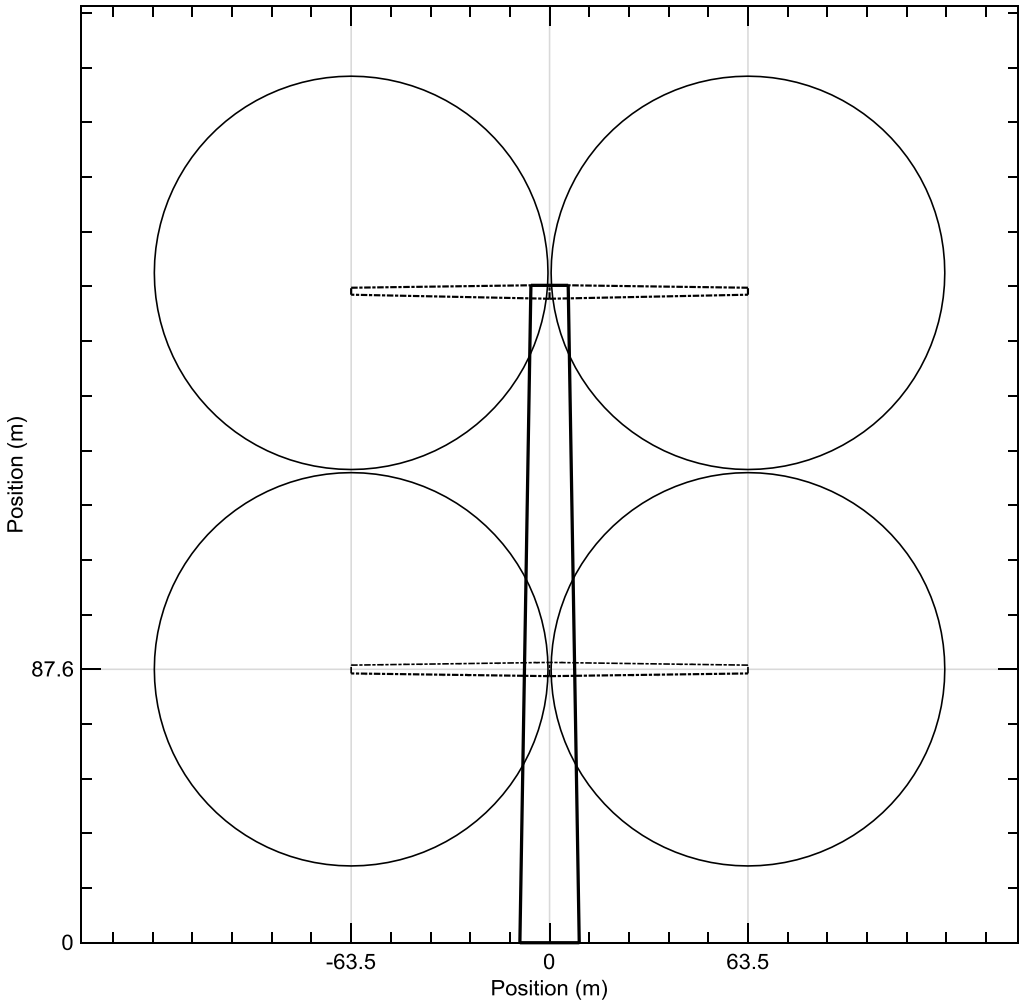

Figure 5.13. Four-rotor configuration sketch

Figures 5.14 and 5.15 show the mass and stiffness distributions of the four-rotor configuration main tower.

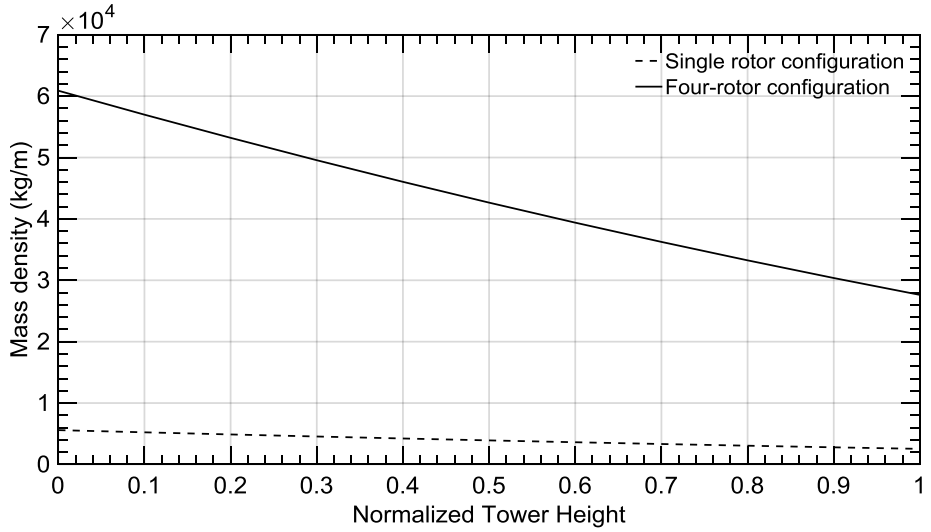

Figure 5.14. Tower mass density distribution – Single-rotor vs. Four-rotor

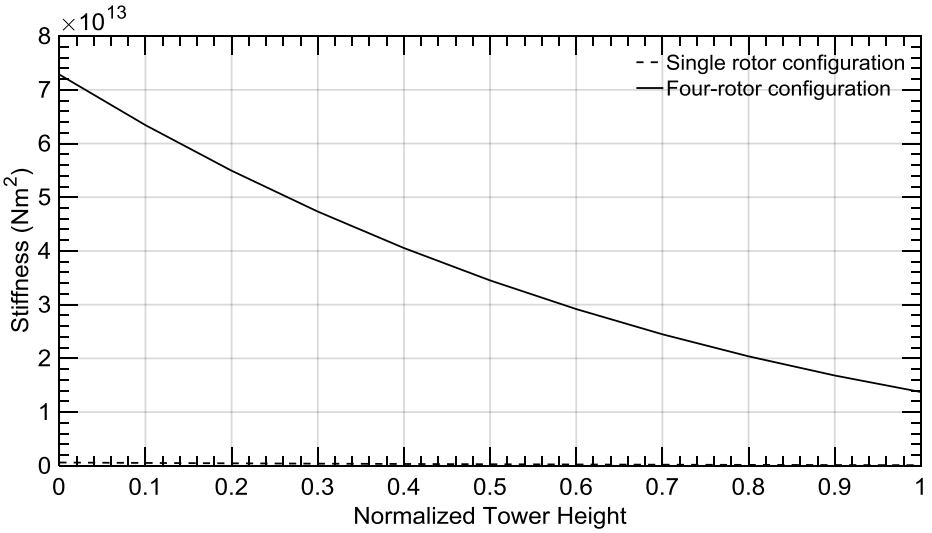

Figure 5.15. Tower stiffness distribution – Single-rotor vs. Four-rotor

The values of mass density and stiffness are still significantly larger than those of the single-rotor tower, however, it's not much higher than the three-rotor configuration.

Natural frequencies of the four-rotor configuration are very close to the values of those of the three-rotor. This is due to the close values of the tower geometry parameters between the two configurations. Consequently,

the dynamic behavior of the main tower of four-rotor and three-rotor configurations is expected to be comparable.

The natural frequencies are calculated and shown in Table 5.5.

Table 5.5. Natural frequencies of the tower – Single vs. Four-rotor configuration

Mode	Single-rotor (Hz)	Three-rotor (Hz)	Deviation (%)
First fore-aft	0.32	0.32	0.0
Second fore-aft	3.06	2.22	-27.4
First side-side	0.32	0.28	-12.5

5.2.2. Four-Rotor Tower Analysis

Simulation is extended to the four-rotor configuration. The same simulation conditions are applied over the four-rotor wind turbine, with the turbulent flow window extended further to cover all the four rotors. Figures 5.16 and 5.17 show the tower dynamics for the turbulence intensity class A, and the corresponding frequency analysis respectively.

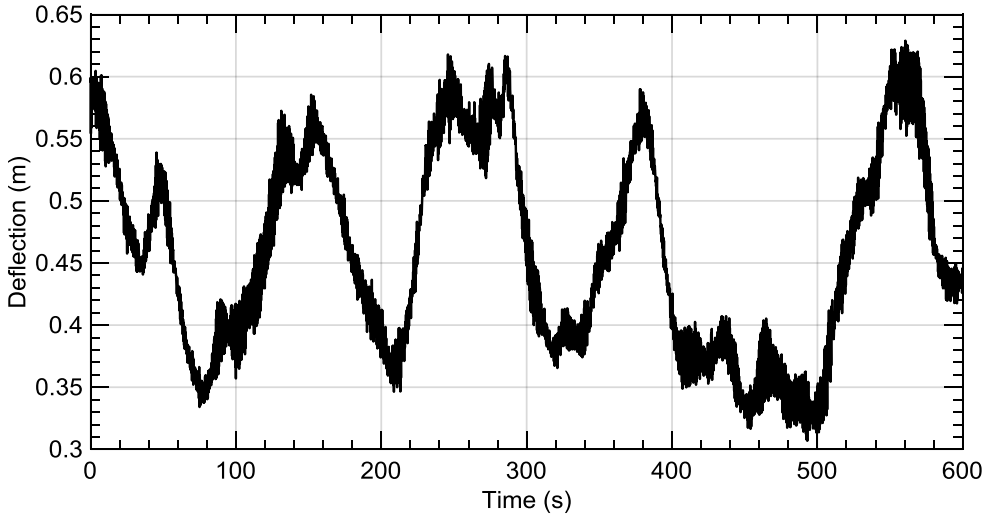

Figure 5.16. 4R Tower-top fore-aft deflection – Turb. Class A

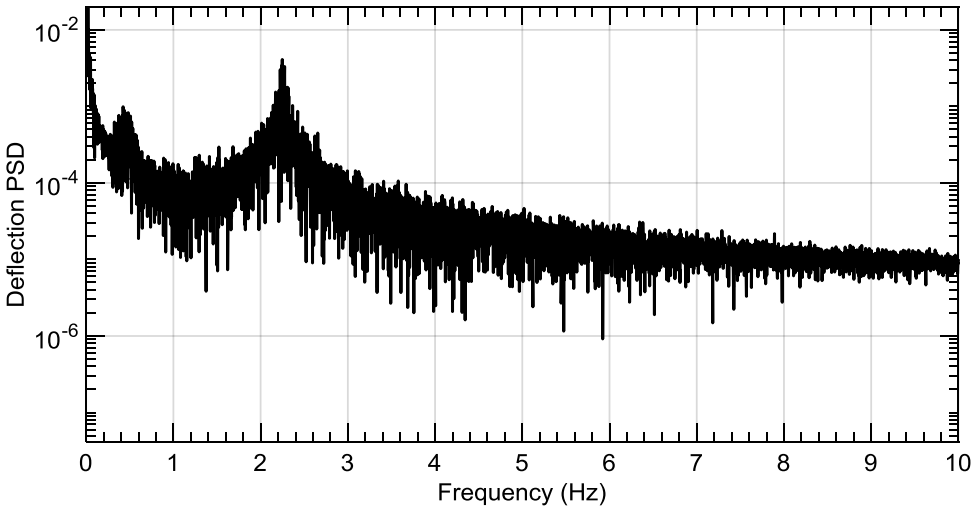

Figure 5.17. 4R Frequency analysis, tower-top deflection – Turb. Class A

As was expected, the values of deformation at the tower-top are comparable to their corresponding values in the three-rotor configuration. Also, the dominant frequencies are the natural frequencies of the tower, which have very close values to those of the three-rotor model.

Figure 5.18 shows the yawing deflection in case of the four-rotor configuration.

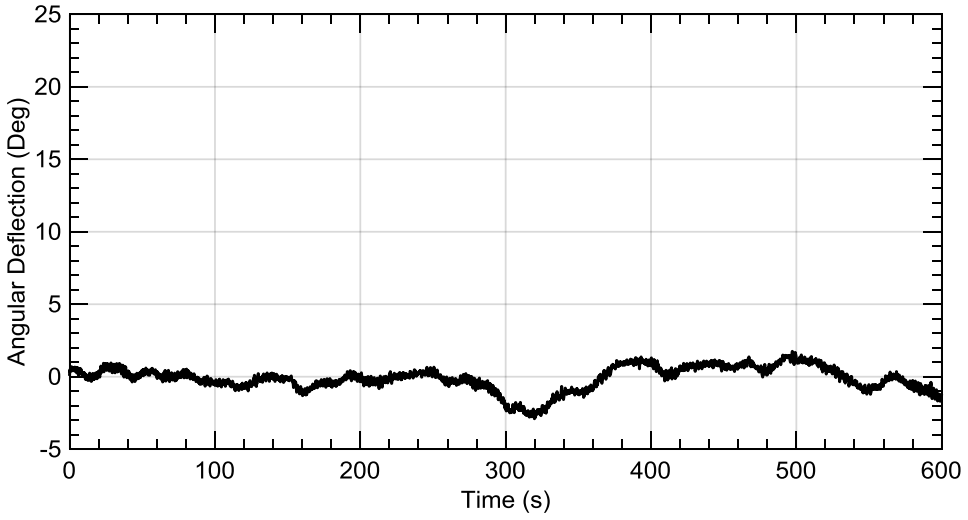

Figure 5.18. 4R Tower-top yawing deflection – Turb. Class A

Yawing deflection at the tower-top is slightly higher than the values of the three-rotor configuration, however, they are small compared to the twin-rotor results. The random behavior of wind loads over the four rotors can be opposed in some intervals of time and overlapping during other intervals. With the higher stiffness of the tower, the extra loads of the rotors are accounted for and the deflections are reduced.

Figures 5.19 to 5.24 show the results of the turbulence classes B and C simulation.

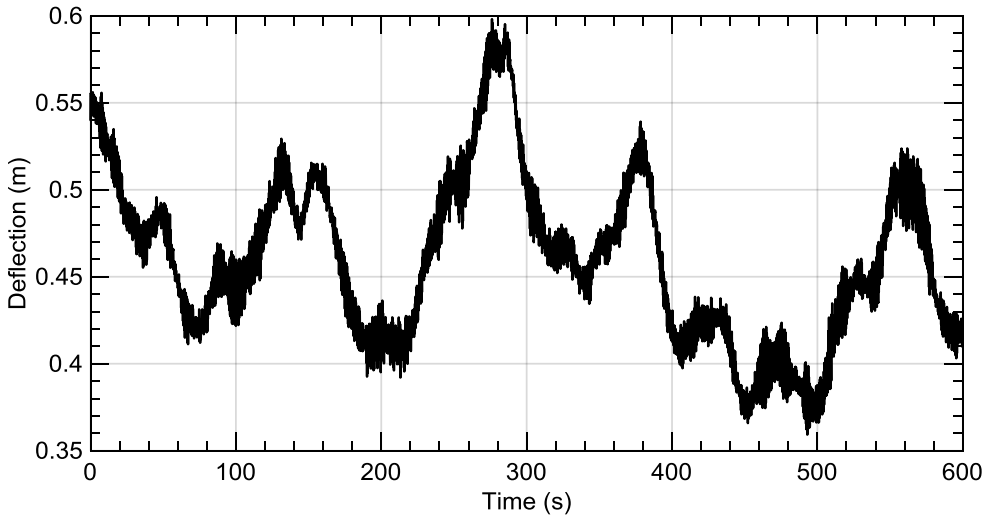

Figure 5.19. 4R Tower-top fore-aft deflection – Turb. Class B

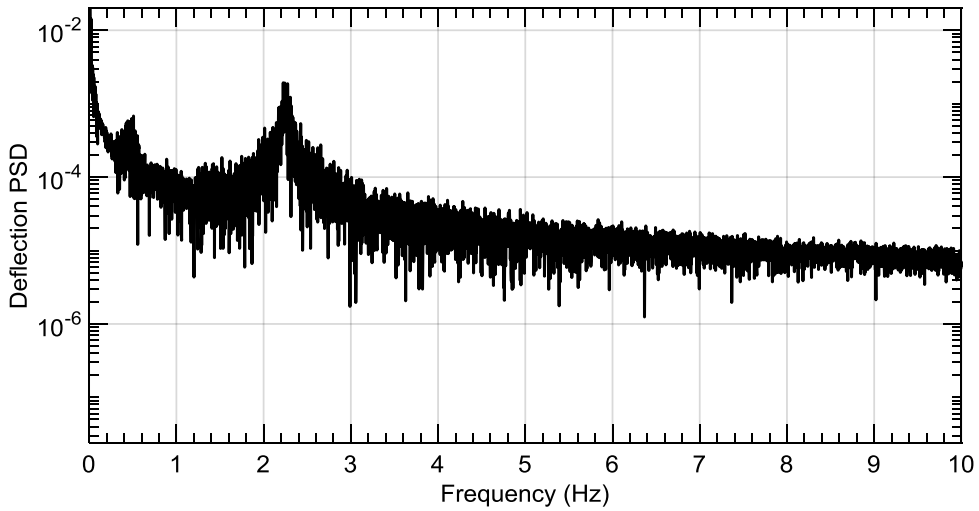

Figure 5.20. 4R Frequency analysis, tower-top deflection – Turb. Class B

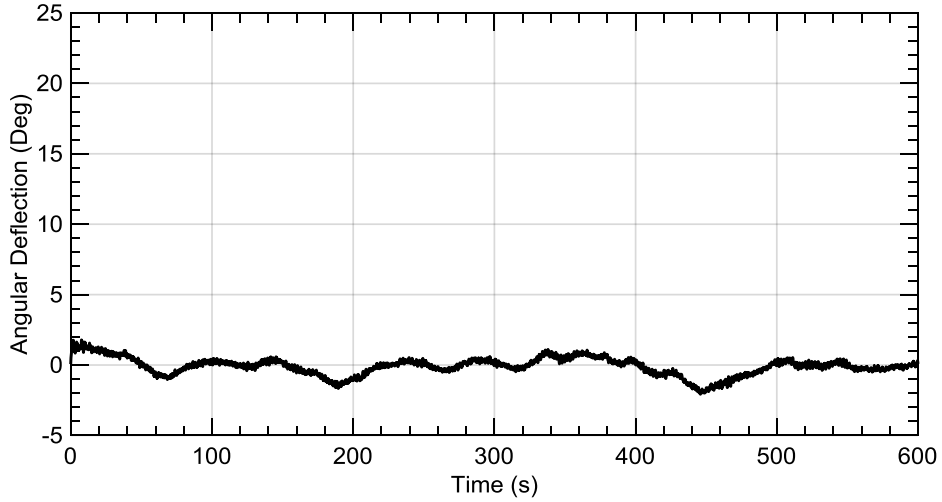

Figure 5.21. 4R Tower-top yawing deflection – Turb. Class B

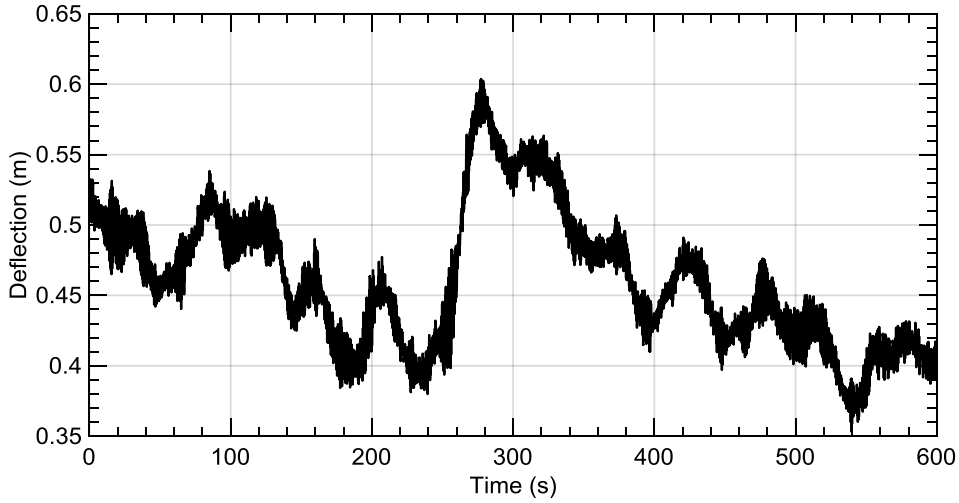

Figure 5.22. 4R Tower-top fore-aft deflection – Turb. Class C

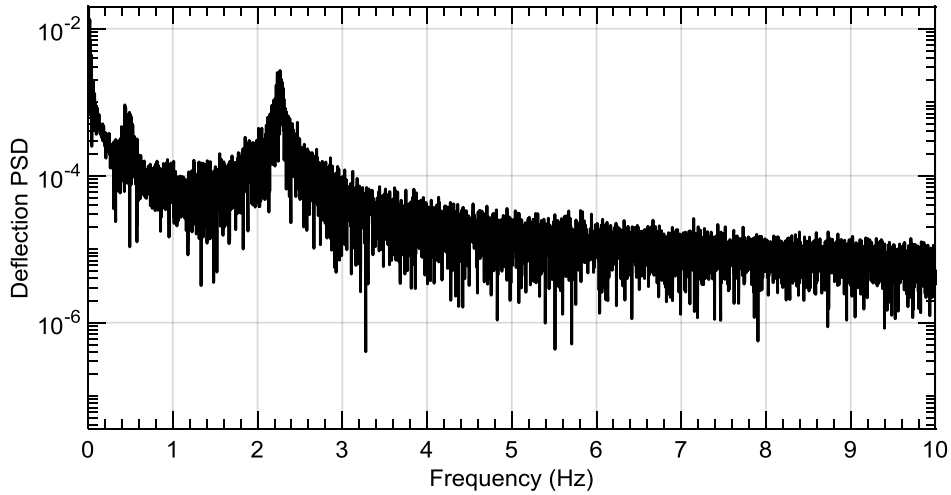

Figure 5.23. 4R Frequency analysis, tower-top deflection – Turb. Class C

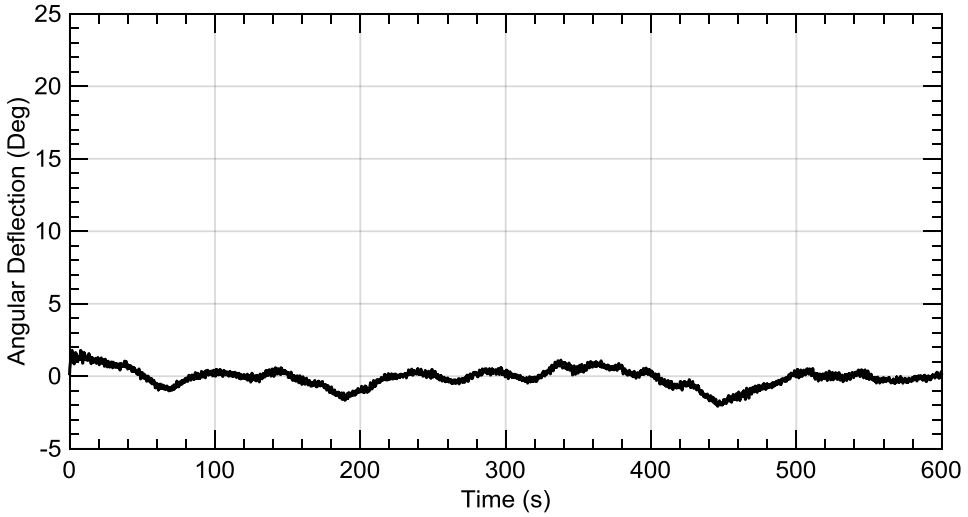

Figure 5.24. 4R Tower-top yawing deflection – Turb. Class C

The results of simulations for the four-rotor configuration can be summarized as shown in Table 5.6.

Table 5.6. Statistical analysis for tower-top deflection in turbulent cases – 4R

Turbulence Class	Mean Value	Standard Deviation	Dominant Frequencies
A	0.463	0.082	0.32 Hz and 2.22 Hz
B	0.462	0.056	0.32 Hz and 2.22 Hz
C	0.463	0.049	0.32 Hz and 2.22 Hz

The simulation results of the four-rotor configuration strengthen the findings of the work. For all configurations, natural frequencies have been found to be dominant.

The dynamic responses of the four-rotor configuration compared to the three-rotor configuration, show that the four-rotor configuration is advantageous. With the comparable deflections at the tower top, whether in the fore-aft direction or the yawing deflection, the four-rotor configuration will be more technically feasible. More power is produced

with very comparable dynamic responses should be the main point of comparison between three-rotor and four-rotor configurations.

5.4. Chapter Summary

In this chapter, the simulation extended to the three-rotor and four-rotor configurations. The dynamic response of the main tower was studied in the same manner as in the twin-rotor case. It was found that the four-rotor configuration is more technically feasible compared to the three-rotor configuration, since the produced power is increased, however the dynamics are comparable.

This page is intentionally left blank

Chapter 6

Conclusions

Contents

6.1. Main Findings 91

6.2. Future Work 94

6.1. Main Findings

This thesis is concerned with the study of the structure dynamics of a Multi-Rotor System (MRS) wind turbine. One of the major challenges in an MRS is the complexity of the support structure. In order to anticipate the dynamic structure behaviour of the support structure, an aeroelastic tool has been developed to provide an aeroelastic model for wind turbine blades and tower. This tool was built based on deterministic models. The Blade Element Momentum theory was used for the aerodynamics loads calculations, Newton's second law using Virtual Work Method with a modal approach was used for the structural calculations, and then

aeroelastic coupling between the two theory was made for the aeroelastic simulation.

This tool was the first approach to make an aeroelastic simulation for a multi-rotor wind turbine configuration. Since there is no available data in the literature, or a benchmark model for validating the results of the developed tool, the approach for verification of the tool was by verifying the results for a Single Rotor System (SRS) wind turbine. The tool was verified by comparing its results for an SRS with a similar analysis under the same simulation conditions using the well-established aeroelastic tool FAST. This comparison showed very good agreement and the tool was trusted to proceed with modelling multi-rotor configurations.

The tool was later extended to model a coplanar twin-rotor configuration. The tower was assumed to be a T-shaped tower with two rotors on top connected by side-booms. The main tower geometry was updated to confirm that the first fore-aft natural frequency is the same as in the single-rotor configuration since it is the dominant factor in the tower structure dynamics.

Two main cases were studied for the twin-rotor configuration. A steady wind case and turbulent wind case. The tower was first modelled as a stiff body, however, compared to an elastic model, the stiff tower model results didn't count for the vibration and hence the inertial loads of the tower causing misleading results. Which means that tower elasticity should be considered while studying the tower dynamics.

Chapter 6. Conclusions

For the steady wind case, it was found that for a tower with the same first fore-aft natural frequency, if one more rotor is added; it does not only increase the loads, but also changes the natural frequencies of the rotor and hence the stiffness and structural damping. Accordingly, the change in the tower deflections and loads is not straightforward with the number of rotors. It was also found that tower torsion is very crucial in case of twin-rotor configuration. The normal case is that the two rotors are not rotating simultaneously, and the results of this work have shown yawing deflections of the tower in case there is a slight phase change in the rotor loads' time series. So, for realistic wind conditions when there is a larger difference between the two rotors' loads, the yawing deflection will become severer and my cause failure due to torsional shear stress.

Simulation of the twin-rotor configuration under turbulent flow conditions has shown that the tower natural frequencies are dominant over the flow conditions for the tower loads and deflections. For three different turbulence intensities, A, B, and C classes according to the IEC 61400 standards, although the flow conditions were different and accordingly the loads and deformations, but the results have shown that the dominant frequencies were still the same; the natural frequencies of the tower.

The side-booms carrying the rotors were also analysed in the same manner. Three different configurations of the side-booms with different diameters were considered for study in the turbulent flow condition. It was found that the larger the diameter of the side-boom, the stiffer it is, and it can significantly improve the dynamic response. However, the increase in the weight was also significant which affect the dynamics of the main tower.

Compromise between the dynamics of the main tower and the side-booms' size should be carefully considered in the design phase.

More configurations were considered in the analysis. Three and Four-rotor configurations were modelled. Simulations on three-rotor and four-rotor configurations have strengthened the importance of the tower natural frequencies, being dominant over the wind conditions.

It was also found that the four-rotor configuration is more technically feasible than three-rotor configuration. The four-rotor configuration produces more power; however, the dynamic responses were comparable to those of the three-rotor configuration.

6.2. Future Work

In order to improve the current tool, two main aspects can be considered. First, pitch control can be added to that high-power regions can be simulated. And second, Aerodynamic interaction between the rotors can be considered for more realistic results.

Bibliography

[1] Martin Pasqualetti, Robert Righter, and Paul Gibe, "Encyclopedia of Energy," vol. 6, Arizona, Elsevier, 2004, pp. 419-433.

[2] [Online]. Available: https://www.dkfindout.com/us/history/ancient-egypt/ancient-egyptian-boats/. [Accessed 2019].

[3] Lucas, Adam, "Wind, Water, Work: Ancient and Medieval Milling Technology," Boston, Brill, 2006.

[4] Price, Trevor J., "James Blyth - Britain's First Modern Wind Power Engineer," *Wind Engineering,* vol. 29, no. 3, pp. 191-200, 2005.

[5] Shackelton Jonathan, "World First for Scotland Gives Engineering Student a History Lesson," The Robert Gordon University, 2008.

[6] Shabhu Ratan Awasthi, Wind Power: Practical Aspects, New Delhi: TERI Press, 2018.

[7] Prasad D. Chougule and Soren R.K. Nielsen, "Modal Parameter Identification of New Design of Vertical Axis Wind Turbine," in *31st IMAC, A conference on Structural Dynamics*, USA, 2013.

[8] Noble Environmental Power, LLC, The Return of Windpower to Grandpa's Knob and Rutland County, 2007.

Bibliography

[9] Abou Taleb, Sayed Matewalli, Badr Azzam, and Basman El-Hadidi, "Optimum Design of Horizontal Axis Wind Turbine Composite Blades Structure; PhD thesis," Cairo University, Cairo, 2012.

[10] Global Wind Energy Council (GWEC), "Global Wind Report," 2018.

[11] Vestas, "Offshore V164-8.0," [Online]. Available: http://www.vestas.com/en/wind-power-plants/procurement/turbineoverview/. [Accessed 2019].

[12] GE, "Haliade X," [Online]. Available: https://www.ge.com/renewableenergy/wind-energy/turbines/haliade-x-offshore-turbine. [Accessed 2019].

[13] "Vox," [Online]. Available: https://www.vox.com/energy-and-environment/2018/3/8/17084158/wind-turbine-power-energy-blades. [Accessed 2019].

[14] Hofmann M, and Sperstad I.B., "Will 10 MW wind turbines bring down the operation and maintenance cost of offshore wind farms?," *Energy Procedia,* vol. 53, pp. 231-238, 2014.

[15] Jameison, Peter, Innovation in wind turbine design, Chichester, UK: Wiley-Blackwell, 2011.

[16] Goltenbott Uli, Ohya Yuji, Yoshida Shigeo, and Jameison Peter, "Aerodynamic interaction of diffuser augmented wind turbines in multi-rotor systems," *Renewable Energy,* vol. 112, pp. 25-34, 2017.

Bibliography

[17] Chasapogiannis P, Prospathopoulos J.M., Voutsinas S.G., and Chaviaropoulos T.K., "Analysis of the aerodynamic performance of the multi-rotor concept," *Journal of Physics, Conference Series,* vol. 524, 2014.

[18] "Coherence Effects on the Power and Tower Loads of a 7 x 2 MWMulti-RotorWind Turbine System," *Energies,* vol. 9, 2016.

[19] Ghaisas N.S., Ghate A.S., and Lele S.K., "Large-eddy simulation study of multi-rotor wind turbines," *Journal of Physics, Conference Series,* vol. 1037, 2018.

[20] Maarten Paul van der Laan, Søren Juhl Andersen, Néstor Ramos García, Nikolas Angelou, Georg Raimund Pirrung, Søren Ott, Mikael Sjöholm, Kim Hylling Sørensen, Julio Xavier Vianna Neto, Mark Kelly, Torben Krogh Mikkelsen, and Gunner Christian Larsen, "Power curve and wake analyses of the Vestas multi-rotor demonstrator," *Wind Energy Science (WES),* vol. 44, 2019.

[21] P., Verma, "Multi Rotor Wind Turbine Design and Cost Scaling, MSc. Thesis," University of Massachusetts Amherst, Amherst, USA, 2013.

[22] G.M., Mate, "Development of A Support Structure for Multi-Rotor Wind Turbines, MSc. Thesis," University of Massachusetts Amherst, Amherst, USA, 2014.

[23] M H Hansen, "Aeroelastic Stability Analysis of Wind Turbines Using an Eigenvalue Approach," *Wind Energy,* vol. 7, pp. 133-143, 2004.

Bibliography

[24] M H Hansen, "Aeroelastic Instability Problems for Wind Turbines," *Wind Energy,* vol. 10, pp. 551-577, 2007.

[25] Donghoon Lee, Dewey H. Hodges, and Mayuresh J. Patil, "Multi-flexible-body Dynamic Analysis of Horizontal Axis Wind Turbines," *Wind Energy,* vol. 5, pp. 281-300, 2002.

[26] Jason Jonkman, and Paul Sclavounos, "Development of Fully Coupled Aeroelastic and Hydrodynamic Models for Offshore Wind Turbines," in *AIAA*, Nevada, 2006.

[27] Gunjit Bir and Jason Jonkman, "Aeroelastic Instabilities of Large Offshore and Onshore Wind Turbines," *Journal of Physics: Conference Series,* vol. 75, no. 75, p. 012069, 2007.

[28] Musial W, Butterfield S, and Ram B, "Energy From Offshore Wind," in *Offshore Technology Conference*, Houston, TX, 2006.

[29] Watson Greg, "A Framework for Offshore Wind Energy Development in the United States," 2005. [Online]. Available: http://www.mtpc.org/offshore/final_09_20.pdf. [Accessed 2019].

[30] Bazilevs Y., Yan J., Deng X., and Korobenko A, "Computer Modeling of Wind Turbines: 2. Free-Surface FSI and Fatigue-Damage," *Archives of Computational Methods in Engineering,* 2018.

[31] Halawa A., Sessarego M., Shen W.Z., and Yoshida S., "Numerical Fluid-Structure Interaction Study on the NREL 5MW HAWT," *Journal of Physics, Conference Series,* vol. 1037, no. 2, p. 022026, 2018.

Bibliography

[32] M Carrion, R Steijl, M. Woodgate, G N Barakos, X Munduate, and S Gomez-Iradi, "Aeroelastic Analysis of Wind Turbines Using a Tightly-Coupled CFD-CSD Method," *Journal of Dluids and Structures,* vol. 50, pp. 392-415, 2014.

[33] Bazilevs Y, Hsu M., Kiendel J, Wunchner R, and Bletzinger K U, "3D simulation of Wind Turbine Rotors at Full Scale. Part II: Fluid-Structure Interaction Modelling with Composite Blades," *International Journal for Numerical Methods in Fluids,* vol. 65, pp. 236-253, 2011.

[34] S Streiner, E Kramer, A Eulitz, and P Armbruster, "Aeroelastic Analysis of Wind Turbines Applying 3D CFD Computational Results," *Journal of Physics: Conference Series,* vol. 75, no. 75, 2007.

[35] MOL Hansen, J N Sorennsen, S Voutsinas, N Sorensen, and H A Madsen, "State of the Art in Wind Turbine Aerodynamics and Aeroelasticity," *Progress in Aerospace Sciences,* vol. 42, no. 4, pp. 285-330, 2006.

[36] Jason Jonkman, "The New Modularization Framework for the FAST Wind Turbine CAE Tool," 51st AIAA Aerospace Sciences Meeting, Texas, USA, 2013.

[37] Hansen, Martin O.L, "Unsteady BEM Model," in *Aerodynamics of Wind Turbines*, 2nd ed., London, UK, Earthscan, 2008, pp. 85-102.

Bibliography

[38] Vorpahl F. and Popko W., "Description of the load cases and output sensors to be simulated in the OC4 project," IEA Wind Annex 30, IWES, Fraunhofer, 2016.

[39] Hansen, Martin O.L., "Dynamic Structural Model of a Wind turbine," in *Aerodynamics of Wind Turbines*, 2nd ed., London, UK, Earthscan, 2008, pp. 125-138.

[40] Gear, C.W., "Numerical Initial Value Problems in Ordinary Differential Equations," Englewood Cliffs, N.J., Prentice-Hall, 1971.

[41] M. o. Hansen, "Beam Theory for the Wind turbine Blade," in *Aerodynamics of Wind Turbines*, London, UK, Earthscan, 2008, pp. 107-124.

[42] Tony Burton, Nick Jenkins, David Sharpe, and Ervin Bossanyi, Wind Energy Handbook, UK: John Wiley & Sons, 2011.

[43] Amr Ismaiel and Shigeo Yoshida, "Study of Turbulence Intensity Effect on The Fatigue Lifetime of Wind Turbines," *Evergreen,* vol. 05, no. 01, pp. 25-32, 2018.

[44] Meneveau, C.; and Sreenivasan, K.R., "The Multifractal Nature of Turbulent Energy Dissipation," *Journal of Fluid Mechanics,* vol. 224, 1991.

[45] Petersen, E.L., Mortensen, N.G., Landberg, L., Højstrup, J., and Frank, H.P.,, "Wind power meteorology, Part I: Climate and turbulence," *Wind Energy,* 1998.

Bibliography

[46] Jonkman J., Butterfield S., Musial W., and Scott G., "Definition of a 5-MW Reference Wind Turbine for Offshore System Developmen," National Renewable Energy Labortory (NREL), Colorado, USA, 2009.

[47] Amr Ismaiel and Shigeo Yoshida, "Aeroelastic Analysis of a Coplanar Twin-Rotor Wind Turbine," *Energies,* vol. 12, no. 10, 2019.

[48] Bazilevs Y., Hsu M.C., Akkerman I. Wright S., Tazikawa K, Henicke B., Spielman T., and Tezduyar T.E., "3D Simulation of Wind Turbine Rotors at Full Scale. Part I: Geometry Modeling and Aerodynamics," *International Journal for Numerical Methods in Fluids,* vol. 65, pp. 207-235, 2011.

[49] "National Wind technology Center (NWTC) Information Portal, Modes," [Online]. Available: https://nwtc.nrel.gov/Modes. [Accessed 2019].

[50] Riziotis V.A., Voutsinas S.G., Dimitris I.M., Evangelos S.P., and Chaviaropoulos P.K., "Aeroelastic Analysis of Pre-Curved Rotor Blades," in *EWEA*, Warsaw, Poland, 2010.

[51] Jonkman B.J., and Kilcher L., "TurbSim's user guide: Version 1.06.00," National Renewable Energy Laboratory (NREL), Colorado, USA, 2012.

[52] "19.22. Wind Turbines—Part 1: Design RequirementsIEC-61400-1," International Electrotechnical Commision (IEC), Geneva, Switzerland, 2005.

Bibliography

[53] J. Jonkman, "The new modularization framework for the FAST wind turbine CAE tool," in *51st AIAA Aerospace Sciences Meeting*, Texas, 2013.

Appendix A: FAST Input Files

A.1 FAST Primary Input File

```
------- FAST v8.16.* INPUT FILE ------------------------------------------------
FAST Certification Test #18: NREL 5.0 MW Baseline Wind Turbine (Onshore)
---------------------- SIMULATION CONTROL --------------------------------------
false        Echo           - Echo input data to <RootName>.ech (flag)
"FATAL"      AbortLevel     - Error level when simulation should abort (string) {"WARNING", "SEVERE", "FATAL"}
       60    TMax           - Total run time (s)
     0.01    DT             - Recommended module time step (s)
        1    InterpOrder    - Interpolation order for input/output time history (-) {1=linear, 2=quadratic}
        0    NumCrctn       - Number of correction iterations (-) {0=explicit calculation, i.e., no corrections}
    99999    DT_UJac        - Time between calls to get Jacobians (s)
    1E+06    UJacSclFact    - Scaling factor used in Jacobians (-)
---------------------- FEATURE SWITCHES AND FLAGS ------------------------------
        1    CompElast      - Compute structural dynamics (switch) {1=ElastoDyn; 2=ElastoDyn + BeamDyn for blades}
        1    CompInflow     - Compute inflow wind velocities (switch) {0=still air; 1=InflowWind; 2=external from OpenFOAM}
        2    CompAero       - Compute aerodynamic loads (switch) {0=None; 1=AeroDyn v14; 2=AeroDyn v15}
        0    CompServo      - Compute control and electrical-drive dynamics (switch) {0=None; 1=ServoDyn}
        0    CompHydro      - Compute hydrodynamic loads (switch) {0=None; 1=HydroDyn}
        0    CompSub        - Compute sub-structural dynamics (switch) {0=None; 1=SubDyn}
        0    CompMooring    - Compute mooring system (switch) {0=None; 1=MAP++; 2=FEAMooring; 3=MoorDyn; 4=OrcaFlex}
        0    CompIce        - Compute ice loads (switch) {0=None; 1=IceFloe; 2=IceDyn}
---------------------- INPUT FILES ---------------------------------------------
"5MW_Baseline/NRELOffshrBsline5MW_Onshore_ElastoDyn.dat"  EDFile      - Name of file containing ElastoDyn input parameters (quoted string)
"5MW_Baseline/NRELOffshrBsline5MW_BeamDyn.dat"  BDBldFile(1)  - Name of file containing BeamDyn input parameters for blade 1 (quoted string)
"5MW_Baseline/NRELOffshrBsline5MW_BeamDyn.dat"  BDBldFile(2)  - Name of file containing BeamDyn input parameters for blade 2 (quoted string)
"5MW_Baseline/NRELOffshrBsline5MW_BeamDyn.dat"  BDBldFile(3)  - Name of file containing BeamDyn input parameters for blade 3 (quoted string)
```

Appendix A: FAST Input Files

"5MW_Baseline/NRELOffshrBsline5MW_InflowWind_12mps.dat" InflowFile - Name of file containing inflow wind input parameters (quoted string)
"5MW_Baseline/NRELOffshrBsline5MW_Onshore_AeroDyn15.dat" AeroFile - Name of file containing aerodynamic input parameters (quoted string)
"5MW_Baseline/NRELOffshrBsline5MW_Onshore_ServoDyn.dat" ServoFile - Name of file containing control and electrical-drive input parameters (quoted string)
"unused" HydroFile - Name of file containing hydrodynamic input parameters (quoted string)
"unused" SubFile - Name of file containing sub-structural input parameters (quoted string)
"unused" MooringFile - Name of file containing mooring system input parameters (quoted string)
"unused" IceFile - Name of file containing ice input parameters (quoted string)
---------- OUTPUT ----------
True SumPrint - Print summary data to "<RootName>.sum" (flag)
5 SttsTime - Amount of time between screen status messages (s)
99999 ChkptTime - Amount of time between creating checkpoint files for potential restart (s)
"default" DT_Out - Time step for tabular output (s) (or "default")
0 TStart - Time to begin tabular output (s)
1 OutFileFmt - Format for tabular (time-marching) output file (switch) {1: text file [<RootName>.out], 2: binary file [<RootName>.outb], 3: both}
True TabDelim - Use tab delimiters in text tabular output file? (flag) {uses spaces if false}
"ES10.3E2" OutFmt - Format used for text tabular output, excluding the time channel. Resulting field should be 10 characters. (quoted string)
---------- LINEARIZATION ----------
False Linearize - Linearization analysis (flag)
2 NLinTimes - Number of times to linearize (-) [>=1] [unused if Linearize=False]
30, 60 LinTimes - List of times at which to linearize (s) [1 to NLinTimes] [unused if Linearize=False]
1 LinInputs - Inputs included in linearization (switch) {0=none; 1=standard; 2=all module inputs (debug)} [unused if Linearize=False]
1 LinOutputs - Outputs included in linearization (switch) {0=none; 1=from OutList(s); 2=all module outputs (debug)} [unused if Linearize=False]
False LinOutJac - Include full Jacobians in linearization output (for debug) (flag) [unused if Linearize=False; used only if LinInputs=LinOutputs=2]
False LinOutMod - Write module-level linearization output files in addition to output for full system? (flag) [unused if Linearize=False]
---------- VISUALIZATION ----------
0 WrVTK - VTK visualization data output: (switch) {0=none; 1=initialization data only; 2=animation}

Appendix A: FAST Input Files

```
       1   VTK_type         - Type of VTK visualization data: (switch) {1=surfaces;
2=basic meshes (lines/points); 3=all meshes (debug)} [unused if WrVTK=0]
true         VTK_fields      - Write mesh fields to VTK data files? (flag) {true/false}
[unused if WrVTK=0]
      15   VTK_fps         - Frame rate for VTK output (frames per second){will use
closest integer multiple of DT} [used only if WrVTK=2]
```

A.2 Elastodyn Input File

```
------- ELASTODYN v1.03.* INPUT FILE -------------------------------------------
NREL 5.0 MW Baseline Wind Turbine for Use in Offshore Analysis. Properties
from Dutch Offshore Wind Energy Converter (DOWEC) 6MW Pre-Design
(10046_009.pdf) and REpower 5M 5MW (5m_uk.pdf)
---------------------- SIMULATION CONTROL --------------------------------------
False        Echo        - Echo input data to "<RootName>.ech" (flag)
       1   Method      - Integration method: {1: RK4, 2: AB4, or 3: ABM4} (-)
"DEFAULT"     DT          - Integration time step (s)
---------------------- ENVIRONMENTAL CONDITION ---------------------------------
   9.80665   Gravity     - Gravitational acceleration (m/s^2)
---------------------- DEGREES OF FREEDOM --------------------------------------
True         FlapDOF1    - First flapwise blade mode DOF (flag)
True         FlapDOF2    - Second flapwise blade mode DOF (flag)
True         EdgeDOF     - First edgewise blade mode DOF (flag)
False        TeetDOF     - Rotor-teeter DOF (flag) [unused for 3 blades]
False        DrTrDOF     - Drivetrain rotational-flexibility DOF (flag)
False        GenDOF      - (false)Generator DOF (flag)
False        YawDOF      - Yaw DOF (flag)
True         TwFADOF1    - First fore-aft tower bending-mode DOF (flag)
True         TwFADOF2    - Second fore-aft tower bending-mode DOF (flag)
True         TwSSDOF1    - First side-to-side tower bending-mode DOF (flag)
False        TwSSDOF2    - Second side-to-side tower bending-mode DOF (flag)
False        PtfmSgDOF   - Platform horizontal surge translation DOF (flag)
False        PtfmSwDOF   - Platform horizontal sway translation DOF (flag)
False        PtfmHvDOF   - Platform vertical heave translation DOF (flag)
False        PtfmRDOF    - Platform roll tilt rotation DOF (flag)
False        PtfmPDOF    - Platform pitch tilt rotation DOF (flag)
False        PtfmYDOF    - Platform yaw rotation DOF (flag)
---------------------- INITIAL CONDITIONS --------------------------------------
       0   OoPDefl     - Initial out-of-plane blade-tip displacement (meters)
       0   IPDefl      - Initial in-plane blade-tip deflection (meters)
       0   BlPitch(1)  - Blade 1 initial pitch (degrees)
       0   BlPitch(2)  - Blade 2 initial pitch (degrees)
       0   BlPitch(3)  - Blade 3 initial pitch (degrees) [unused for 2 blades]
```

Appendix A: FAST Input Files

```
        0   TeetDefl    - Initial or fixed teeter angle (degrees) [unused for 3 blades]
        0   Azimuth     - Initial azimuth angle for blade 1 (degrees)
       12.1  RotSpeed    - Initial or fixed rotor speed (rpm)
        0   NacYaw      - Initial or fixed nacelle-yaw angle (degrees)
        0   TTDspFA     - Initial fore-aft tower-top displacement (meters)
        0   TTDspSS     - Initial side-to-side tower-top displacement (meters)
        0   PtfmSurge   - Initial or fixed horizontal surge translational displacement
of platform (meters)
        0   PtfmSway    - Initial or fixed horizontal sway translational displacement
of platform (meters)
        0   PtfmHeave   - Initial or fixed vertical heave translational displacement
of platform (meters)
        0   PtfmRoll    - Initial or fixed roll tilt rotational displacement of platform
(degrees)
        0   PtfmPitch   - Initial or fixed pitch tilt rotational displacement of platform
(degrees)
        0   PtfmYaw     - Initial or fixed yaw rotational displacement of platform
(degrees)
---------------------- TURBINE CONFIGURATION ----------------------------------
        3   NumBl       - Number of blades (-)
       63   TipRad      - The distance from the rotor apex to the blade tip (meters)
      1.5   HubRad      - The distance from the rotor apex to the blade root (meters)
     -2.5   PreCone(1)  - Blade 1 cone angle (degrees)
     -2.5   PreCone(2)  - Blade 2 cone angle (degrees)
     -2.5   PreCone(3)  - Blade 3 cone angle (degrees) [unused for 2 blades]
        0   HubCM       - Distance from rotor apex to hub mass [positive
downwind] (meters)
        0   UndSling    - Undersling length [distance from teeter pin to the rotor
apex] (meters) [unused for 3 blades]
        0   Delta3      - Delta-3 angle for teetering rotors (degrees) [unused for 3
blades]
        0   AzimB1Up    - Azimuth value to use for I/O when blade 1 points up
(degrees)
   -5.0191   OverHang    - Distance from yaw axis to rotor apex [3 blades] or
teeter pin [2 blades] (meters)
    1.912   ShftGagL    - Distance from rotor apex [3 blades] or teeter pin [2
blades] to shaft strain gages [positive for upwind rotors] (meters)
       -5   ShftTilt    - Rotor shaft tilt angle (degrees)
      1.9   NacCMxn     - Downwind distance from the tower-top to the nacelle
CM (meters)
        0   NacCMyn     - Lateral  distance from the tower-top to the nacelle CM
(meters)
     1.75   NacCMzn     - Vertical distance from the tower-top to the nacelle CM
(meters)
```

Appendix A: FAST Input Files

```
  -3.09528   NcIMUxn     - Downwind distance from the tower-top to the nacelle IMU (meters)
         0   NcIMUyn     - Lateral  distance from the tower-top to the nacelle IMU (meters)
   2.23336   NcIMUzn     - Vertical distance from the tower-top to the nacelle IMU (meters)
   1.96256   Twr2Shft    - Vertical distance from the tower-top to the rotor shaft (meters)
      87.6   TowerHt     - Height of tower above ground level [onshore] or MSL [offshore] (meters)
         0   TowerBsHt   - Height of tower base above ground level [onshore] or MSL [offshore] (meters)
         0   PtfmCMxt    - Downwind distance from the ground level [onshore] or MSL [offshore] to the platform CM (meters)
         0   PtfmCMyt    - Lateral distance from the ground level [onshore] or MSL [offshore] to the platform CM (meters)
         0   PtfmCMzt    - Vertical distance from the ground level [onshore] or MSL [offshore] to the platform CM (meters)
         0   PtfmRefzt   - Vertical distance from the ground level [onshore] or MSL [offshore] to the platform reference point (meters)
---------------------- MASS AND INERTIA ----------------------------------------
         0   TipMass(1)  - Tip-brake mass, blade 1 (kg)
         0   TipMass(2)  - Tip-brake mass, blade 2 (kg)
         0   TipMass(3)  - Tip-brake mass, blade 3 (kg) [unused for 2 blades]
     56780   HubMass     - Hub mass (kg)
    115926   HubIner     - Hub inertia about rotor axis [3 blades] or teeter axis [2 blades] (kg m^2)
   534.116   GenIner     - Generator inertia about HSS (kg m^2)
    240000   NacMass     - Nacelle mass (kg)
2.60789E+06   NacYIner    - Nacelle inertia about yaw axis (kg m^2)
         0   YawBrMass   - Yaw bearing mass (kg)
         0   PtfmMass    - Platform mass (kg)
         0   PtfmRIner   - Platform inertia for roll tilt rotation about the platform CM (kg m^2)
         0   PtfmPIner   - Platform inertia for pitch tilt rotation about the platform CM (kg m^2)
         0   PtfmYIner   - Platform inertia for yaw rotation about the platform CM (kg m^2)
---------------------- BLADE ---------------------------------------------------
        17   BldNodes    - Number of blade nodes (per blade) used for analysis (-)
"NRELOffshrBsline5MW_Blade2.dat"    BldFile(1)  - Name of file containing properties for blade 1 (quoted string)
"NRELOffshrBsline5MW_Blade2.dat"    BldFile(2)  - Name of file containing properties for blade 2 (quoted string)
```

Appendix A: FAST Input Files

```
"NRELOffshrBsline5MW_Blade2.dat"    BldFile(3)  - Name of file containing properties for blade 3 (quoted string) [unused for 2 blades]
---------------------- ROTOR-TEETER ---------------------------------------------
         0   TeetMod     - Rotor-teeter spring/damper model {0: none, 1: standard, 2: user-defined from routine UserTeet} (switch) [unused for 3 blades]
         0   TeetDmpP    - Rotor-teeter damper position (degrees) [used only for 2 blades and when TeetMod=1]
         0   TeetDmp     - Rotor-teeter damping constant (N-m/(rad/s)) [used only for 2 blades and when TeetMod=1]
         0   TeetCDmp    - Rotor-teeter rate-independent Coulomb-damping moment (N-m) [used only for 2 blades and when TeetMod=1]
         0   TeetSStP    - Rotor-teeter soft-stop position (degrees) [used only for 2 blades and when TeetMod=1]
         0   TeetHStP    - Rotor-teeter hard-stop position (degrees) [used only for 2 blades and when TeetMod=1]
         0   TeetSSSp    - Rotor-teeter soft-stop linear-spring constant (N-m/rad) [used only for 2 blades and when TeetMod=1]
         0   TeetHSSp    - Rotor-teeter hard-stop linear-spring constant (N-m/rad) [used only for 2 blades and when TeetMod=1]
---------------------- DRIVETRAIN -----------------------------------------------
       100   GBoxEff     - Gearbox efficiency (%)
        97   GBRatio     - Gearbox ratio (-)
8.67637E+08   DTTorSpr    - Drivetrain torsional spring (N-m/rad)
  6.215E+06   DTTorDmp    - Drivetrain torsional damper (N-m/(rad/s))
---------------------- FURLING --------------------------------------------------
False         Furling     - Read in additional model properties for furling turbine (flag) [must currently be FALSE)
"unused"      FurlFile    - Name of file containing furling properties (quoted string) [unused when Furling=False]
---------------------- TOWER ----------------------------------------------------
        20   TwrNodes    - Number of tower nodes used for analysis (-)
"NRELOffshrBsline5MW_Onshore_ElastoDyn_Tower.dat"    TwrFile     - Name of file containing tower properties (quoted string)
---------------------- OUTPUT ---------------------------------------------------
True          SumPrint    - Print summary data to "<RootName>.sum" (flag)
         1   OutFile     - Switch to determine where output will be placed: {1: in module output file only; 2: in glue code output file only; 3: both} (currently unused)
True          TabDelim    - Use tab delimiters in text tabular output file? (flag) (currently unused)
"ES10.3E2"    OutFmt      - Format used for text tabular output (except time). Resulting field should be 10 characters. (quoted string) (currently unused)
         0   TStart      - Time to begin tabular output (s) (currently unused)
         1   DecFact     - Decimation factor for tabular output {1: output every time step} (-) (currently unused)
```

Appendix A: FAST Input Files

```
        0   NTwGages    - Number of tower nodes that have strain gages for output [0 to 9] (-)
       10,       19,       28   TwrGagNd    - List of tower nodes that have strain gages [1 to TwrNodes] (-) [unused if NTwGages=0]
        3   NBlGages    - Number of blade nodes that have strain gages for output [0 to 9] (-)
        5,        9,       13   BldGagNd    - List of blade nodes that have strain gages [1 to BldNodes] (-) [unused if NBlGages=0]
          OutList     - The next line(s) contains a list of output parameters.  See OutListParameters.xlsx for a listing of available output channels, (-)
"OoPDefl1"              - Blade 1 out-of-plane and in-plane deflections and tip twist
"IPDefl1"               - Blade 1 out-of-plane and in-plane deflections and tip twist
"TwstDefl1"             - Blade 1 out-of-plane and in-plane deflections and tip twist
"BldPitch1"             - Blade 1 pitch angle
"Azimuth"               - Blade 1 azimuth angle
"RotSpeed"              - Low-speed shaft and high-speed shaft speeds
"GenSpeed"              - Low-speed shaft and high-speed shaft speeds
"TTDspFA"               - Tower fore-aft and side-to-side displacements and top twist
"TTDspSS"               - Tower fore-aft and side-to-side displacements and top twist
"TTDspTwst"             - Tower fore-aft and side-to-side displacements and top twist
"Spn2MLxb1"             - Blade 1 local edgewise and flapwise bending moments at span station 2 (approx. 50% span)
"Spn2MLyb1"             - Blade 1 local edgewise and flapwise bending moments at span station 2 (approx. 50% span)
"RootFxb1"              - Out-of-plane shear, in-plane shear, and axial forces at the root of blade 1
"RootFyb1"              - Out-of-plane shear, in-plane shear, and axial forces at the root of blade 1
"RootFzb1"              - Out-of-plane shear, in-plane shear, and axial forces at the root of blade 1
"RootMxb1"              - In-plane bending, out-of-plane bending, and pitching moments at the root of blade 1
"RootMyb1"              - In-plane bending, out-of-plane bending, and pitching moments at the root of blade 1
"RootMzb1"              - In-plane bending, out-of-plane bending, and pitching moments at the root of blade 1
"RotTorq"               - Rotor torque and low-speed shaft 0- and 90-bending moments at the main bearing
"LSSGagMya"             - Rotor torque and low-speed shaft 0- and 90-bending moments at the main bearing
"LSSGagMza"             - Rotor torque and low-speed shaft 0- and 90-bending moments at the main bearing
```

```
"YawBrTDxt"
"YawBrTDyt"
"YawBrTDxp"
"YawBrTDyp"
"RotThrust"
"YawBrFxp"              - Fore-aft shear, side-to-side shear, and vertical forces at the
top of the tower (not rotating with nacelle yaw)
"YawBrFyp"              - Fore-aft shear, side-to-side shear, and vertical forces at
the top of the tower (not rotating with nacelle yaw)
"YawBrFzp"              - Fore-aft shear, side-to-side shear, and vertical forces at the
top of the tower (not rotating with nacelle yaw)
"YawBrMxp"              - Side-to-side bending, fore-aft bending, and yaw
moments at the top of the tower (not rotating with nacelle yaw)
"YawBrMyp"              - Side-to-side bending, fore-aft bending, and yaw
moments at the top of the tower (not rotating with nacelle yaw)
"YawBrMzp"              - Side-to-side bending, fore-aft bending, and yaw
moments at the top of the tower (not rotating with nacelle yaw)
"TwrBsFxt"              - Fore-aft shear, side-to-side shear, and vertical forces at the
base of the tower (mudline)
"TwrBsFyt"              - Fore-aft shear, side-to-side shear, and vertical forces at the
base of the tower (mudline)
"TwrBsFzt"              - Fore-aft shear, side-to-side shear, and vertical forces at the
base of the tower (mudline)
"TwrBsMxt"              - Side-to-side bending, fore-aft bending, and yaw moments
at the base of the tower (mudline)
"TwrBsMyt"              - Side-to-side bending, fore-aft bending, and yaw moments
at the base of the tower (mudline)
"TwrBsMzt"              - Side-to-side bending, fore-aft bending, and yaw moments
at the base of the tower (mudline)
END of input file (the word "END" must appear in the first 3 columns of this last
OutList line)
---------------------------------------------------------------------------
```

A.3 Wind File

```
------- InflowWind v3.01.* INPUT FILE ------------------------------------------------------
------------------
12 m/s turbulent winds on 31x31 FF grid and tower for FAST CertTests #18, #19,
#21, #22, #23, and #24
---------------------------------------------------------------------------------------------
----
False        Echo          - Echo input data to <RootName>.ech (flag)
         1   WindType      - switch for wind file type (1=steady; 2=uniform; 3=binary
TurbSim FF; 4=binary Bladed-style FF; 5=HAWC format; 6=User defined)
```

Appendix A: FAST Input Files

```
        0   PropagationDir - Direction of wind propagation (meteoroligical rotation
from aligned with X (positive rotates towards -Y) -- degrees)
        1   NWindVel       - Number of points to output the wind velocity    (0 to 9)
        0   WindVxiList    - List of coordinates in the inertial X direction (m)
        0   WindVyiList    - List of coordinates in the inertial Y direction (m)
       87.6   WindVziList    - List of coordinates in the inertial Z direction (m)
================== Parameters for Steady Wind Conditions [used only for
WindType = 1] =========================
       11.4   HWindSpeed     - Horizontal windspeed                            (m/s)
       87.6   RefHt          - Reference height for horizontal wind speed      (m)
      0.2   PLexp          - Power law exponent                              (-)
================== Parameters for Uniform wind file   [used only for
WindType = 2] ============================
"Wind/90m_8mps_twr.bts"    Filename       - Filename of time series data for
uniform wind field.      (-)
       87.6   RefHt          - Reference height for horizontal wind speed      (m)
    125.88   RefLength      - Reference length for linear horizontal and vertical
sheer (-)
================== Parameters for Binary TurbSim Full-Field files   [used only
for WindType = 3] ==============
"Wind/90m_8mps_twr.bts"    Filename       - Name of the Full field wind file to
use (.bts)
================== Parameters for Binary Bladed-style Full-Field files   [used
only for WindType = 4] =========
"Wind/90m_8mps_twr"    FilenameRoot   - Rootname of the full-field wind file to
use (.wnd, .sum)
False          TowerFile      - Have tower file (.twr) (flag)
================== Parameters for HAWC-format binary files  [Only used with
WindType = 5] ====================
"wasp\Output\basic_5u.bin"    FileName_u     - name of the file containing the
u-component fluctuating wind (.bin)
"wasp\Output\basic_5v.bin"    FileName_v     - name of the file containing the
v-component fluctuating wind (.bin)
"wasp\Output\basic_5w.bin"    FileName_w     - name of the file containing the
w-component fluctuating wind (.bin)
       64   nx             - number of grids in the x direction (in the 3 files above) (-)
       32   ny             - number of grids in the y direction (in the 3 files above) (-)
       32   nz             - number of grids in the z direction (in the 3 files above) (-)
       16   dx             - distance (in meters) between points in the x direction     (m)
        3   dy           - distance (in meters) between points in the y direction     (m)
        3   dz           - distance (in meters) between points in the z direction     (m)
       90   RefHt          - reference height; the height (in meters) of the vertical
center of the grid (m)
 ------------  Scaling parameters for turbulence   ----------------------------------------
--------------
```

```
        1   ScaleMethod    - Turbulence scaling method   [0 = none, 1 = direct
scaling, 2 = calculate scaling factor based on a desired standard deviation]
        1   SFx            - Turbulence scaling factor for the x direction (-)
[ScaleMethod=1]
        1   SFy            - Turbulence scaling factor for the y direction (-)
[ScaleMethod=1]
        1   SFz            - Turbulence scaling factor for the z direction (-)
[ScaleMethod=1]
       12   SigmaFx        - Turbulence standard deviation to calculate scaling from
in x direction (m/s)    [ScaleMethod=2]
        8   SigmaFy        - Turbulence standard deviation to calculate scaling from
in y direction (m/s)    [ScaleMethod=2]
        2   SigmaFz        - Turbulence standard deviation to calculate scaling from
in z direction (m/s)    [ScaleMethod=2]
  ----------   Mean wind profile parameters (added to HAWC-format files)   ------
---------------------------
        5   URef           - Mean u-component wind speed at the reference height
(m/s)
        2   WindProfile    - Wind profile type (0=constant;1=logarithmic,2=power
law)
      0.2   PLExp          - Power law exponent (-) (used for PL wind profile type
only)
     0.03   Z0             - Surface roughness length (m) (used for LG wind profile
type only)
====================== OUTPUT
================================================
False       SumPrint     - Print summary data to <RootName>.IfW.sum (flag)
           OutList      - The next line(s) contains a list of output parameters.  See
OutListParameters.xlsx for a listing of available output channels, (-)
"Wind1VelX"              X-direction wind velocity at point WindList(1)
"Wind1VelY"              Y-direction wind velocity at point WindList(1)
"Wind1VelZ"              Z-direction wind velocity at point WindList(1)
END of input file (the word "END" must appear in the first 3 columns of this last
OutList line)
---------------------------------------------------------------------------------
```

A.4 AeroDyn Input File

```
------- AERODYN v15.03.* INPUT FILE ------------------------------------------------
NREL 5.0 MW offshore baseline aerodynamic input properties.
======  General Options
================================================================================
=====
False       Echo             - Echo the input to "<rootname>.AD.ech"?  (flag)
```

Appendix A: FAST Input Files

```
"default"     DTAero          - Time interval for aerodynamic calculations {or
"default"} (s)
         1   WakeMod         - Type of wake/induction model (switch) {0=none,
1=BEMT}
         1   AFAeroMod       - Type of blade airfoil aerodynamics model (switch)
{1=steady model, 2=Beddoes-Leishman unsteady model}
         1   TwrPotent       - Type tower influence on wind based on potential flow
around the tower (switch) {0=none, 1=baseline potential flow, 2=potential flow
with Bak correction}
False        TwrShadow       – Calculate tower influence on wind based on
downstream tower shadow? (flag)
True         TwrAero         - Calculate tower aerodynamic loads? (flag)
False        FrozenWake      - Assume frozen wake during linearization? (flag)
[used only when WakeMod=1 and when linearizing]
======  Environmental Conditions
===========================================================================
     1.225   AirDens         - Air density (kg/m^3)
 1.464E-05   KinVisc         - Kinematic air viscosity (m^2/s)
       335   SpdSound        - Speed of sound (m/s)
======  Blade-Element/Momentum Theory Options
================================================== [used only when
WakeMod=1]
         2   SkewMod         - Type of skewed-wake correction model (switch)
{1=uncoupled, 2=Pitt/Peters, 3=coupled} [used only when WakeMod=1]
True         TipLoss         - Use the Prandtl tip-loss model? (flag) [used only
when WakeMod=1]
True         HubLoss         - Use the Prandtl hub-loss model? (flag) [used only
when WakeMod=1]
true         TanInd          - Include tangential induction in BEMT calculations?
(flag) [used only when WakeMod=1]
False        AIDrag          - Include the drag term in the axial-induction
calculation? (flag) [used only when WakeMod=1]
False        TIDrag          - Include the drag term in the tangential-induction
calculation? (flag) [used only when WakeMod=1 and TanInd=TRUE]
"Default"    IndToler        - Convergence tolerance for BEMT nonlinear solve
residual equation {or "default"} (-) [used only when WakeMod=1]
       100   MaxIter         - Maximum number of iteration steps (-) [used only
when WakeMod=1]
======  Beddoes-Leishman Unsteady Airfoil Aerodynamics Options
==================================== [used only when AFAeroMod=2]
         3   UAMod           - Unsteady Aero Model Switch (switch) {1=Baseline
model (Original), 2=Gonzalez's variant (changes in Cn,Cc,Cm),
3=Minemma/Pierce variant (changes in Cc and Cm)} [used only when
AFAeroMod=2]
```

Appendix A: FAST Input Files

```
True        FLookup         - Flag to indicate whether a lookup for f' will be
calculated (TRUE) or whether best-fit exponential equations will be used
(FALSE); if FALSE S1-S4 must be provided in airfoil input files (flag) [used only
when AFAeroMod=2]
======  Airfoil Information
==========================================================================
==
        1   InCol_Alfa      - The column in the airfoil tables that contains the angle
of attack (-)
        2   InCol_Cl        - The column in the airfoil tables that contains the lift
coefficient (-)
        3   InCol_Cd        - The column in the airfoil tables that contains the drag
coefficient (-)
        4   InCol_Cm        - The column in the airfoil tables that contains the
pitching-moment coefficient; use zero if there is no Cm column (-)
        0   InCol_Cpmin     - The column in the airfoil tables that contains the
Cpmin coefficient; use zero if there is no Cpmin column (-)
        8   NumAFfiles      - Number of airfoil files used (-)
"Airfoils/Cylinder1.dat"    AFNames         - Airfoil file names (NumAFfiles
lines) (quoted strings)
"Airfoils/Cylinder2.dat"
"Airfoils/DU40_A17.dat"
"Airfoils/DU35_A17.dat"
"Airfoils/DU30_A17.dat"
"Airfoils/DU25_A17.dat"
"Airfoils/DU21_A17.dat"
"Airfoils/NACA64_A17.dat"
======  Rotor/Blade Properties
============================================================================
True        UseBlCm         - Include aerodynamic pitching moment in
calculations?  (flag)
"NRELOffshrBsline5MW_AeroDyn_blade.dat"    ADBlFile(1)      - Name of file
containing distributed aerodynamic properties for Blade #1 (-)
"NRELOffshrBsline5MW_AeroDyn_blade.dat"    ADBlFile(2)      - Name of file
containing distributed aerodynamic properties for Blade #2 (-) [unused if NumBl
< 2]
"NRELOffshrBsline5MW_AeroDyn_blade.dat"    ADBlFile(3)      - Name of file
containing distributed aerodynamic properties for Blade #3 (-) [unused if NumBl
< 3]
======  Tower Influence and Aerodynamics
========================================================== [used only
when TwrPotent/=0, TwrShadow=True, or TwrAero=True]
       12   NumTwrNds       - Number of tower nodes used in the analysis  (-)
[used only when TwrPotent/=0, TwrShadow=True, or TwrAero=True]
TwrElev       TwrDiam       TwrCd
```

```
(m)            (m)          (-)
0.0000000E+00  6.0000000E+00  1.0000000E+00
8.5261000E+00  5.7870000E+00  1.0000000E+00
1.7053000E+01  5.5740000E+00  1.0000000E+00
2.5579000E+01  5.3610000E+00  1.0000000E+00
3.4105000E+01  5.1480000E+00  1.0000000E+00
4.2633000E+01  4.9350000E+00  1.0000000E+00
5.1158000E+01  4.7220000E+00  1.0000000E+00
5.9685000E+01  4.5090000E+00  1.0000000E+00
6.8211000E+01  4.2960000E+00  1.0000000E+00
7.6738000E+01  4.0830000E+00  1.0000000E+00
8.5268000E+01  3.8700000E+00  1.0000000E+00
8.7600000E+01  3.8700000E+00  1.0000000E+00
======  Outputs
======================================================================
============
True         SumPrint          - Generate a summary file listing input options and
interpolated properties to "<rootname>.AD.sum"?  (flag)
        0   NBlOuts           - Number of blade node outputs [0 - 9] (-)
        1,        9,       19   BlOutNd           - Blade nodes whose values will be
output  (-)
        0   NTwOuts           - Number of tower node outputs [0 - 9]  (-)
        1,        2,        6   TwOutNd           - Tower nodes whose values will be
output  (-)
                OutList           - The next line(s) contains a list of output parameters.
See OutListParameters.xlsx for a listing of available output channels, (-)
END of input file (the word "END" must appear in the first 3 columns of this last
OutList line)
---------------------------------------------------------------------------------
```

A.5 Blade Input File

```
------- ELASTODYN V1.00.* INDIVIDUAL BLADE INPUT FILE --------------------------
NREL 5.0 MW offshore baseline blade input properties.
---------------------- BLADE PARAMETERS ----------------------------------------
       49   NBlInpSt    - Number of blade input stations (-)
  0.477465   BldFlDmp(1) - Blade flap mode #1 structural damping in percent of critical
(%)
  0.477465   BldFlDmp(2) - Blade flap mode #2 structural damping in percent of critical
(%)
  0.477465   BldEdDmp(1) - Blade edge mode #1 structural damping in percent of critical
(%)
---------------------- BLADE ADJUSTMENT FACTORS --------------------------------
        1   FlStTunr(1) - Blade flapwise modal stiffness tuner, 1st mode (-)
        1   FlStTunr(2) - Blade flapwise modal stiffness tuner, 2nd mode (-)
```

Appendix A: FAST Input Files

```
   1.04536   AdjBlMs     - Factor to adjust blade mass density (-)  !bjj: value for
AD14=1.04536; value for AD15=1.057344 (it would be nice to enter the requested blade
mass instead of a factor here)
         1   AdjFlSt     - Factor to adjust blade flap stiffness (-)
         1   AdjEdSt     - Factor to adjust blade edge stiffness (-)
---------------------- DISTRIBUTED BLADE PROPERTIES ----------------------------
   BlFract      PitchAxis      StrcTwst       BMassDen        FlpStff        EdgStff
     (-)            (-)          (deg)          (kg/m)         (Nm^2)         (Nm^2)
0.0000000E+00  2.5000000E-01  1.3308000E+01  6.7893500E+02  1.8110000E+10
1.8113600E+10
3.2500000E-03  2.5000000E-01  1.3308000E+01  6.7893500E+02  1.8110000E+10
1.8113600E+10
1.9510000E-02  2.5049000E-01  1.3308000E+01  7.7336300E+02  1.9424900E+10
1.9558600E+10
3.5770000E-02  2.5490000E-01  1.3308000E+01  7.4055000E+02  1.7455900E+10
1.9497800E+10
5.2030000E-02  2.6716000E-01  1.3308000E+01  7.4004200E+02  1.5287400E+10
1.9788800E+10
6.8290000E-02  2.7941000E-01  1.3308000E+01  5.9249600E+02  1.0782400E+10
1.4858500E+10
8.4550000E-02  2.9167000E-01  1.3308000E+01  4.5027500E+02  7.2297200E+09
1.0220600E+10
1.0081000E-01  3.0392000E-01  1.3308000E+01  4.2405400E+02  6.3095400E+09
9.1447000E+09
1.1707000E-01  3.1618000E-01  1.3308000E+01  4.0063800E+02  5.5283600E+09
8.0631600E+09
1.3335000E-01  3.2844000E-01  1.3308000E+01  3.8206200E+02  4.9800600E+09
6.8844400E+09
1.4959000E-01  3.4069000E-01  1.3308000E+01  3.9965500E+02  4.9368400E+09
7.0091800E+09
1.6585000E-01  3.5294000E-01  1.3308000E+01  4.2632100E+02  4.6916600E+09
7.1676800E+09
1.8211000E-01  3.6519000E-01  1.3181000E+01  4.1682000E+02  3.9494600E+09
7.2716600E+09
1.9837000E-01  3.7500000E-01  1.2848000E+01  4.0618600E+02  3.3865200E+09
7.0817000E+09
2.1465000E-01  3.7500000E-01  1.2192000E+01  3.8142000E+02  2.9337400E+09
6.2445300E+09
2.3089000E-01  3.7500000E-01  1.1561000E+01  3.5282200E+02  2.5689600E+09
5.0489600E+09
2.4715000E-01  3.7500000E-01  1.1072000E+01  3.4947700E+02  2.3886500E+09
4.9484900E+09
2.6341000E-01  3.7500000E-01  1.0792000E+01  3.4653800E+02  2.2719900E+09
4.8080200E+09
2.9595000E-01  3.7500000E-01  1.0232000E+01  3.3933300E+02  2.0500500E+09
4.5014000E+09
3.2846000E-01  3.7500000E-01  9.6720000E+00  3.3000400E+02  1.8282500E+09
4.2440700E+09
3.6098000E-01  3.7500000E-01  9.1100000E+00  3.2199000E+02  1.5887100E+09
3.9952800E+09
```

Appendix A: FAST Input Files

3.9350000E-01 3.7500000E-01 8.5340000E+00 3.1382000E+02 1.3619300E+09
3.7507600E+09
4.2602000E-01 3.7500000E-01 7.9320000E+00 2.9473400E+02 1.1023800E+09
3.4471400E+09
4.5855000E-01 3.7500000E-01 7.3210000E+00 2.8712000E+02 8.7580000E+08
3.1390700E+09
4.9106000E-01 3.7500000E-01 6.7110000E+00 2.6334300E+02 6.8130000E+08
2.7342400E+09
5.2358000E-01 3.7500000E-01 6.1220000E+00 2.5320700E+02 5.3472000E+08
2.5548700E+09
5.5610000E-01 3.7500000E-01 5.5460000E+00 2.4166600E+02 4.0890000E+08
2.3340300E+09
5.8862000E-01 3.7500000E-01 4.9710000E+00 2.2063800E+02 3.1454000E+08
1.8287300E+09
6.2115000E-01 3.7500000E-01 4.4010000E+00 2.0029300E+02 2.3863000E+08
1.5841000E+09
6.5366000E-01 3.7500000E-01 3.8340000E+00 1.7940400E+02 1.7588000E+08
1.3233600E+09
6.8618000E-01 3.7500000E-01 3.3320000E+00 1.6509400E+02 1.2601000E+08
1.1836800E+09
7.1870000E-01 3.7500000E-01 2.8900000E+00 1.5441100E+02 1.0726000E+08
1.0201600E+09
7.5122000E-01 3.7500000E-01 2.5030000E+00 1.3893500E+02 9.0880000E+07
7.9781000E+08
7.8376000E-01 3.7500000E-01 2.1160000E+00 1.2955500E+02 7.6310000E+07
7.0961000E+08
8.1626000E-01 3.7500000E-01 1.7300000E+00 1.0726400E+02 6.1050000E+07
5.1819000E+08
8.4878000E-01 3.7500000E-01 1.3420000E+00 9.8776000E+01 4.9480000E+07
4.5487000E+08
8.8130000E-01 3.7500000E-01 9.5400000E-01 9.0248000E+01 3.9360000E+07
3.9512000E+08
8.9756000E-01 3.7500000E-01 7.6000000E-01 8.3001000E+01 3.4670000E+07
3.5372000E+08
9.1382000E-01 3.7500000E-01 5.7400000E-01 7.2906000E+01 3.0410000E+07
3.0473000E+08
9.3008000E-01 3.7500000E-01 4.0400000E-01 6.8772000E+01 2.6520000E+07
2.8142000E+08
9.3821000E-01 3.7500000E-01 3.1900000E-01 6.6264000E+01 2.3840000E+07
2.6171000E+08
9.4636000E-01 3.7500000E-01 2.5300000E-01 5.9340000E+01 1.9630000E+07
1.5881000E+08
9.5447000E-01 3.7500000E-01 2.1600000E-01 5.5914000E+01 1.6000000E+07
1.3788000E+08
9.6260000E-01 3.7500000E-01 1.7800000E-01 5.2484000E+01 1.2830000E+07
1.1879000E+08
9.7073000E-01 3.7500000E-01 1.4000000E-01 4.9114000E+01 1.0080000E+07
1.0163000E+08
9.7886000E-01 3.7500000E-01 1.0100000E-01 4.5818000E+01 7.5500000E+06
8.5070000E+07

```
9.8699000E-01  3.7500000E-01  6.2000000E-02  4.1669000E+01  4.6000000E+06
6.4260000E+07
9.9512000E-01  3.7500000E-01  2.3000000E-02  1.1453000E+01  2.5000000E+05
6.6100000E+06
1.0000000E+00  3.7500000E-01  0.0000000E+00  1.0319000E+01  1.7000000E+05
5.0100000E+06
---------------------- BLADE MODE SHAPES ----------------------------------------
    0.0622   BldFl1Sh(2) - Flap mode 1, coeff of x^2
    1.7254   BldFl1Sh(3) -          , coeff of x^3
   -3.2452   BldFl1Sh(4) -          , coeff of x^4
    4.7131   BldFl1Sh(5) -          , coeff of x^5
   -2.2555   BldFl1Sh(6) -          , coeff of x^6
   -0.5809   BldFl2Sh(2) - Flap mode 2, coeff of x^2
    1.2067   BldFl2Sh(3) -          , coeff of x^3
  -15.5349   BldFl2Sh(4) -          , coeff of x^4
   29.7347   BldFl2Sh(5) -          , coeff of x^5
  -13.8255   BldFl2Sh(6) -          , coeff of x^6
    0.3627   BldEdgSh(2) - Edge mode 1, coeff of x^2
    2.5337   BldEdgSh(3) -          , coeff of x^3
   -3.5772   BldEdgSh(4) -          , coeff of x^4
     2.376   BldEdgSh(5) -          , coeff of x^5
   -0.6952   BldEdgSh(6) -          , coeff of x^6
```

A.6 Tower Input File

```
------- ELASTODYN V1.00.* TOWER INPUT FILE ------------------------------------
NREL 5.0 MW offshore baseline tripod tower with flexible Tripod SubStructure
(however SS cantilevered at seabed).
---------------------- TOWER PARAMETERS ----------------------------------------
        17   NTwInpSt    - Number of input stations to specify tower geometry
         1   TwrFADmp(1) - Tower 1st fore-aft mode structural damping ratio (%)
         1   TwrFADmp(2) - Tower 2nd fore-aft mode structural damping ratio (%)
         1   TwrSSDmp(1) - Tower 1st side-to-side mode structural damping ratio
(%)
         1   TwrSSDmp(2) - Tower 2nd side-to-side mode structural damping ratio
(%)
---------------------- TOWER ADJUSTMUNT FACTORS --------------------------------
         1   FAStTunr(1) - Tower fore-aft modal stiffness tuner, 1st mode (-)
         1   FAStTunr(2) - Tower fore-aft modal stiffness tuner, 2nd mode (-)
         1   SSStTunr(1) - Tower side-to-side stiffness tuner, 1st mode (-)
         1   SSStTunr(2) - Tower side-to-side stiffness tuner, 2nd mode (-)
         1   AdjTwMa     - Factor to adjust tower mass density (-)
         1   AdjFASt     - Factor to adjust tower fore-aft stiffness (-)
         1   AdjSSSt     - Factor to adjust tower side-to-side stiffness (-)
---------------------- DISTRIBUTED TOWER PROPERTIES ----------------------------
HtFract      TMassDen        TwFAStif      TwSSStif
(-)          (kg/m)          (Nm^2)        (Nm^2)
```

Appendix A: FAST Input Files

```
0.000000E+00  6.966874E+03    7.437527E+11   7.437527E+11
4.510309E-02  6.966874E+03    7.437527E+11   7.437527E+11
1.030928E-01  4.473005E+03    4.805433E+11   4.805433E+11
1.610825E-01  4.390907E+03    4.696476E+11   4.696476E+11
2.255155E-01  4.300408E+03    4.577864E+11   4.577864E+11
2.899485E-01  4.209528E+03    4.458233E+11   4.458233E+11
3.543814E-01  4.119805E+03    4.342413E+11   4.342413E+11
4.188144E-01  4.029744E+03    4.225684E+11   4.225684E+11
4.832474E-01  3.940783E+03    4.112605E+11   4.112605E+11
5.476804E-01  3.852218E+03    4.000876E+11   4.000876E+11
6.121134E-01  3.763343E+03    3.888361E+11   3.888361E+11
6.765464E-01  3.675554E+03    3.779331E+11   3.779331E+11
7.409794E-01  3.588146E+03    3.671609E+11   3.671609E+11
8.054124E-01  3.500471E+03    3.563236E+11   3.563236E+11
8.698454E-01  3.413839E+03    3.458157E+11   3.458157E+11
9.342784E-01  3.326969E+03    3.352515E+11   3.352515E+11
1.000000E+00  3.241113E+03    3.250043E+11   3.250043E+11
---------------------- TOWER FORE-AFT MODE SHAPES -----------------------------
   0.9690    TwFAM1Sh(2) - Mode 1, coefficient of x^2 term
   1.7994    TwFAM1Sh(3) -       , coefficient of x^3 term
  -3.8923    TwFAM1Sh(4) -       , coefficient of x^4 term
   3.0866    TwFAM1Sh(5) -       , coefficient of x^5 term
  -0.9627    TwFAM1Sh(6) -       , coefficient of x^6 term
  -0.6346    TwFAM2Sh(2) - Mode 2, coefficient of x^2 term
   1.3523    TwFAM2Sh(3) -       , coefficient of x^3 term
   2.0272    TwFAM2Sh(4) -       , coefficient of x^4 term
  -2.4770    TwFAM2Sh(5) -       , coefficient of x^5 term
   0.7321    TwFAM2Sh(6) -       , coefficient of x^6 term
---------------------- TOWER SIDE-TO-SIDE MODE SHAPES --------------------------
   0.8758    TwSSM1Sh(2) - Mode 1, coefficient of x^2 term
   1.7209    TwSSM1Sh(3) -       , coefficient of x^3 term
  -3.5321    TwSSM1Sh(4) -       , coefficient of x^4 term
   2.8130    TwSSM1Sh(5) -       , coefficient of x^5 term
  -0.8776    TwSSM1Sh(6) -       , coefficient of x^6 term
  -0.6759    TwSSM2Sh(2) - Mode 2, coefficient of x^2 term
   1.2071    TwSSM2Sh(3) -       , coefficient of x^3 term
   2.2450    TwSSM2Sh(4) -       , coefficient of x^4 term
  -2.5177    TwSSM2Sh(5) -       , coefficient of x^5 term
   0.7414    TwSSM2Sh(6) -       , coefficient of x^6 term
```

Appendix A: FAST Input Files

A.7. Airfoil-Data Input File

A.7.1. Cylinder 1

```
! ------------ AirfoilInfo v1.01.x Input File ----------------------------------
! Round root section with a Cd of 0.50
! Made by Jason Jonkman
! note that this file uses Marshall Buhl's new input file processing; start all comment lines with !
! ------------------------------------------------------------------------------
"DEFAULT"     InterpOrd        ! Interpolation order to use for quasi-steady table lookup {1=linear; 3=cubic spline; "default"} [default=3]
         1   NonDimArea       ! The non-dimensional area of the airfoil (area/chord^2) (set to 1.0 if unsure or unneeded)
@"Cylinder1_coords.txt"    NumCoords        ! The number of coordinates in the airfoil shape file.  Set to zero if coordinates not included.
         1   NumTabs          ! Number of airfoil tables in this file.  Each table must have lines for Re and Ctrl.
! ------------------------------------------------------------------------------
! data for table 1
! ------------------------------------------------------------------------------
      0.75   Re               ! Reynolds number in millions
         0   Ctrl             ! Control setting (must be 0 for current AirfoilInfo)
True         InclUAdata       ! Is unsteady aerodynamics data included in this table? If TRUE, then include 30 UA coefficients below this line
!.....................................
         0   alpha0           ! 0-lift angle of attack, depends on airfoil.
         0   alpha1           ! Angle of attack at f=0.7, (approximately the stall angle) for AOA>alpha0. (deg)
         0   alpha2           ! Angle of attack at f=0.7, (approximately the stall angle) for AOA<alpha0. (deg)
         0   eta_e            ! Recovery factor in the range [0.85 - 0.95] used only for UAMOD=1, it is set to 1 in the code when flookup=True. (-)
         0   C_nalpha         ! Slope of the 2D normal force coefficient curve. (1/rad)
         3   T_f0             ! Initial value of the time constant associated with Df in the expression of Df and f''. [default = 3]
         6   T_V0             ! Initial value of the time constant associated with the vortex lift decay process; it is used in the expression of Cvn. It depends on Re,M, and airfoil class. [default = 6]
       1.7   T_p              ! Boundary-layer,leading edge pressure gradient time constant in the expression of Dp. It should be tuned based on airfoil experimental data. [default = 1.7]
        11   T_VL             ! Initial value of the time constant associated with the vortex advection process; it represents the non-dimensional time in semi-chords, needed for a vortex to travel from LE to trailing edge (TE); it is used in the expression of Cvn. It depends on Re, M (weakly), and airfoil. [valid range = 6 - 13, default = 11]
      0.14   b1               ! Constant in the expression of phi_alpha^c and phi_q^c.  This value is relatively insensitive for thin airfoils, but may be different for turbine airfoils. [from experimental results, defaults to 0.14]
      0.53   b2               ! Constant in the expression of phi_alpha^c and phi_q^c.  This value is relatively insensitive for thin airfoils, but may be different for turbine airfoils. [from experimental results, defaults to 0.53]
         5   b5               ! Constant in the expression of K'''_q,Cm_q^nc, and k_m,q.  [from  experimental results, defaults to 5]
       0.3   A1               ! Constant in the expression of phi_alpha^c and phi_q^c.  This value is relatively insensitive for thin airfoils, but may be different for turbine airfoils. [from experimental results, defaults to 0.3]
```

```
      0.7   A2              ! Constant in the expression of phi_alpha^c and phi_q^c.  This value is
relatively insensitive for thin airfoils, but may be different for turbine airfoils. [from experimental
results, defaults to 0.7]
        1   A5              ! Constant in the expression of K'''_q,Cm_q^nc, and k_m,q. [from experimental
results, defaults to 1]
        0   S1              ! Constant in the f curve best-fit for alpha0<=AOA<=alpha1; by definition it
depends on the airfoil. [ignored if UAMod<>1]
        0   S2              ! Constant in the f curve best-fit for        AOA> alpha1; by definition it depends
on the airfoil. [ignored if UAMod<>1]
        0   S3              ! Constant in the f curve best-fit for alpha2<=AOA< alpha0; by definition it
depends on the airfoil. [ignored if UAMod<>1]
        0   S4              ! Constant in the f curve best-fit for        AOA< alpha2; by definition it depends
on the airfoil. [ignored if UAMod<>1]
        0   Cn1             ! Critical value of C0n at leading edge separation. It should be extracted from
airfoil data at a given Mach and Reynolds number. It can be calculated from the static value of Cn at
either the break in the pitching moment or the loss of chord force at the onset of stall. It is close to the
condition of maximum lift of the airfoil at low Mach numbers.
        0   Cn2             ! As Cn1 for negative AOAs.
     0.19   St_sh            ! Strouhal's shedding frequency constant.  [default = 0.19]
      0.5   Cd0             ! 2D drag coefficient value at 0-lift.
        0   Cm0             ! 2D pitching moment coefficient about 1/4-chord location, at 0-lift, positive if
nose up. [If the aerodynamics coefficients table does not include a column for Cm, this needs to be
set to 0.0]
        0   k0              ! Constant in the \hat(x)_cp curve best-fit; = (\hat(x)_AC-0.25).  [ignored if
UAMod<>1]
        0   k1              ! Constant in the \hat(x)_cp curve best-fit.  [ignored if UAMod<>1]
        0   k2              ! Constant in the \hat(x)_cp curve best-fit.  [ignored if UAMod<>1]
        0   k3              ! Constant in the \hat(x)_cp curve best-fit.  [ignored if UAMod<>1]
        0   k1_hat          ! Constant in the expression of Cc due to leading edge vortex effects.  [ignored
if UAMod<>1]
      0.2   x_cp_bar        ! Constant in the expression of \hat(x)_cp^v. [ignored if UAMod<>1, default
= 0.2]
"DEFAULT"     UACutout        ! Angle of attack above which unsteady aerodynamics are disabled
(deg). [Specifying the string "Default" sets UACutout to 45 degrees]
"DEFAULT"     filtCutOff      ! Cut-off frequency (-3 dB corner frequency) for low-pass filtering the
AoA input to UA, as well as the 1st and 2nd derivatives (Hz) [default = 20]
!.....................................
! Table of aerodynamics coefficients
        3   NumAlf           ! Number of data lines in the following table
!    Alpha      Cl      Cd       Cm
!    (deg)      (-)     (-)      (-)
  -180.00      0.000   0.5000     0.0
     0.00      0.000   0.5000     0.0
   180.00      0.000   0.5000     0.0
! ------------------------------------------------------------------------------
```

A.7.2. Cylinder 2

```
! ------------ AirfoilInfo v1.01.x Input File ----------------------------------
! Round root section with a Cd of 0.35
! Made by Jason Jonkman
! note that this file uses Marshall Buhl's new input file processing; start all comment lines with !
! ------------------------------------------------------------------------------
```

Appendix A: FAST Input Files

```
"DEFAULT"     InterpOrd        ! Interpolation order to use for quasi-steady table lookup {1=linear;
3=cubic spline; "default"} [default=3]
        1   NonDimArea       ! The non-dimensional area of the airfoil (area/chord^2) (set to 1.0 if
unsure or unneeded)
@"Cylinder2_coords.txt"    NumCoords        ! The number of coordinates in the airfoil shape file.  Set
to zero if coordinates not included.
! ......... x-y coordinates are next if NumCoords > 0 .............
        1   NumTabs          ! Number of airfoil tables in this file.  Each table must have lines for Re and
Ctrl.
! ------------------------------------------------------------------------------
! data for table 1
! ------------------------------------------------------------------------------
      0.75   Re               ! Reynolds number in millions
         0   Ctrl             ! Control setting (must be 0 for current AirfoilInfo)
True         InclUAdata       ! Is unsteady aerodynamics data included in this table? If TRUE, then
include 30 UA coefficients below this line
!.........................................
         0   alpha0           ! 0-lift angle of attack, depends on airfoil.
         0   alpha1           ! Angle of attack at f=0.7, (approximately the stall angle) for AOA>alpha0.
(deg)
         0   alpha2           ! Angle of attack at f=0.7, (approximately the stall angle) for AOA<alpha0.
(deg)
         0   eta_e            ! Recovery factor in the range [0.85 - 0.95] used only for UAMOD=1, it is set to 1
in the code when flookup=True. (-)
         0   C_nalpha         ! Slope of the 2D normal force coefficient curve. (1/rad)
         3   T_f0             ! Initial value of the time constant associated with Df in the expression of Df and
f''. [default = 3]
         6   T_V0             ! Initial value of the time constant associated with the vortex lift decay process;
it is used in the expression of Cvn. It depends on Re,M, and airfoil class. [default = 6]
       1.7   T_p              ! Boundary-layer,leading edge pressure gradient time constant in the
expression of Dp. It should be tuned based on airfoil experimental data. [default = 1.7]
        11   T_VL             ! Initial value of the time constant associated with the vortex advection
process; it represents the non-dimensional time in semi-chords, needed for a vortex to travel from LE
to trailing edge (TE); it is used in the expression of Cvn. It depends on Re, M (weakly), and airfoil.
[valid range = 6 - 13, default = 11]
      0.14   b1               ! Constant in the expression of phi_alpha^c and phi_q^c.  This value is
relatively insensitive for thin airfoils, but may be different for turbine airfoils. [from experimental
results, defaults to 0.14]
      0.53   b2               ! Constant in the expression of phi_alpha^c and phi_q^c.  This value is
relatively insensitive for thin airfoils, but may be different for turbine airfoils. [from experimental
results, defaults to 0.53]
         5   b5               ! Constant in the expression of K'''_q,Cm_q^nc, and k_m,q.  [from  experimental
results, defaults to 5]
       0.3   A1               ! Constant in the expression of phi_alpha^c and phi_q^c.  This value is
relatively insensitive for thin airfoils, but may be different for turbine airfoils. [from experimental
results, defaults to 0.3]
       0.7   A2               ! Constant in the expression of phi_alpha^c and phi_q^c.  This value is
relatively insensitive for thin airfoils, but may be different for turbine airfoils. [from experimental
results, defaults to 0.7]
         1   A5               ! Constant in the expression of K'''_q,Cm_q^nc, and k_m,q. [from experimental
results, defaults to 1]
         0   S1               ! Constant in the f curve best-fit for alpha0<=AOA<=alpha1; by definition it
depends on the airfoil. [ignored if UAMod<>1]
         0   S2               ! Constant in the f curve best-fit for         AOA> alpha1; by definition it depends
on the airfoil. [ignored if UAMod<>1]
```

```
      0   S3              ! Constant in the f curve best-fit for alpha2<=AOA< alpha0; by definition it
depends on the airfoil. [ignored if UAMod<>1]
      0   S4              ! Constant in the f curve best-fit for        AOA< alpha2; by definition it depends
on the airfoil. [ignored if UAMod<>1]
      0   Cn1             ! Critical value of C0n at leading edge separation. It should be extracted from
airfoil data at a given Mach and Reynolds number. It can be calculated from the static value of Cn at
either the break in the pitching moment or the loss of chord force at the onset of stall. It is close to the
condition of maximum lift of the airfoil at low Mach numbers.
      0   Cn2             ! As Cn1 for negative AOAs.
    0.19  St_sh           ! Strouhal's shedding frequency constant.  [default = 0.19]
    0.35  Cd0             ! 2D drag coefficient value at 0-lift.
      0   Cm0             ! 2D pitching moment coefficient about 1/4-chord location, at 0-lift, positive if
nose up. [If the aerodynamics coefficients table does not include a column for Cm, this needs to be
set to 0.0]
      0   k0              ! Constant in the \hat(x)_cp curve best-fit; = (\hat(x)_AC-0.25).  [ignored if
UAMod<>1]
      0   k1              ! Constant in the \hat(x)_cp curve best-fit.  [ignored if UAMod<>1]
      0   k2              ! Constant in the \hat(x)_cp curve best-fit.  [ignored if UAMod<>1]
      0   k3              ! Constant in the \hat(x)_cp curve best-fit.  [ignored if UAMod<>1]
      0   k1_hat          ! Constant in the expression of Cc due to leading edge vortex effects.  [ignored
if UAMod<>1]
    0.2   x_cp_bar        ! Constant in the expression of \hat(x)_cp^v. [ignored if UAMod<>1, default
= 0.2]
"DEFAULT"    UACutout     ! Angle of attack above which unsteady aerodynamics are disabled
(deg). [Specifying the string "Default" sets UACutout to 45 degrees]
"DEFAULT"    filtCutOff   ! Cut-off frequency (-3 dB corner frequency) for low-pass filtering the
AoA input to UA, as well as the 1st and 2nd derivatives (Hz) [default = 20]
!.....
! Table of aerodynamics coefficients
      3   NumAlf          ! Number of data lines in the following table
!   Alpha     Cl     Cd       Cm
!   (deg)     (-)    (-)      (-)
 -180.00     0.000  0.3500    0.0
    0.00     0.000  0.3500    0.0
  180.00     0.000  0.3500    0.0
! ------------------------------------------------------------------------------
```

A.7.3. DU21-A17

```
! ------------ AirfoilInfo v1.01.x Input File ----------------------------------
! DU21 airfoil with an aspect ratio of 17.  Original -180 to 180deg Cl, Cd, and Cm versus AOA data
taken from Appendix A of DOWEC document 10046_009.pdf (numerical values obtained from Koert
Lindenburg of ECN).
! Cl and Cd values corrected for rotational stall delay and Cd values corrected using the Viterna
method for 0 to 90deg AOA by Jason Jonkman using AirfoilPrep_v2p0.xls.
! note that this file uses Marshall Buhl's new input file processing; start all comment lines with !
! ------------------------------------------------------------------------------
"DEFAULT"    InterpOrd    ! Interpolation order to use for quasi-steady table lookup {1=linear;
3=cubic spline; "default"} [default=3]
      1   NonDimArea     ! The non-dimensional area of the airfoil (area/chord^2) (set to 1.0 if
unsure or unneeded)
@"DU21_A17_coords.txt"    NumCoords     ! The number of coordinates in the airfoil shape file.  Set
to zero if coordinates not included.
```

Appendix A: FAST Input Files

```
        1   NumTabs         ! Number of airfoil tables in this file.  Each table must have lines for Re and
Ctrl.
! ------------------------------------------------------------------------------
! data for table 1
! ------------------------------------------------------------------------------
     0.75   Re              ! Reynolds number in millions
        0   Ctrl            ! Control setting (must be 0 for current AirfoilInfo)
True        InclUAdata      ! Is unsteady aerodynamics data included in this table? If TRUE, then
include 30 UA coefficients below this line
!.....................................
     -4.2   alpha0          ! 0-lift angle of attack, depends on airfoil.
        8   alpha1          ! Angle of attack at f=0.7, (approximately the stall angle) for AOA>alpha0.
(deg)
       -8   alpha2          ! Angle of attack at f=0.7, (approximately the stall angle) for AOA<alpha0.
(deg)
        1   eta_e           ! Recovery factor in the range [0.85 - 0.95] used only for UAMOD=1, it is set to 1
in the code when flookup=True. (-)
   6.2047   C_nalpha        ! Slope of the 2D normal force coefficient curve. (1/rad)
        3   T_f0            ! Initial value of the time constant associated with Df in the expression of Df and
f''. [default = 3]
        6   T_V0            ! Initial value of the time constant associated with the vortex lift decay process;
it is used in the expression of Cvn. It depends on Re,M, and airfoil class. [default = 6]
      1.7   T_p             ! Boundary-layer,leading edge pressure gradient time constant in the
expression of Dp. It should be tuned based on airfoil experimental data. [default = 1.7]
       11   T_VL            ! Initial value of the time constant associated with the vortex advection
process; it represents the non-dimensional time in semi-chords, needed for a vortex to travel from LE
to trailing edge (TE); it is used in the expression of Cvn. It depends on Re, M (weakly), and airfoil.
[valid range = 6 - 13, default = 11]
     0.14   b1              ! Constant in the expression of phi_alpha^c and phi_q^c.  This value is
relatively insensitive for thin airfoils, but may be different for turbine airfoils. [from experimental
results, defaults to 0.14]
     0.53   b2              ! Constant in the expression of phi_alpha^c and phi_q^c.  This value is
relatively insensitive for thin airfoils, but may be different for turbine airfoils. [from experimental
results, defaults to 0.53]
        5   b5              ! Constant in the expression of K'''_q,Cm_q^nc, and k_m,q.  [from  experimental
results, defaults to 5]
      0.3   A1              ! Constant in the expression of phi_alpha^c and phi_q^c.  This value is
relatively insensitive for thin airfoils, but may be different for turbine airfoils. [from experimental
results, defaults to 0.3]
      0.7   A2              ! Constant in the expression of phi_alpha^c and phi_q^c.  This value is
relatively insensitive for thin airfoils, but may be different for turbine airfoils. [from experimental
results, defaults to 0.7]
        1   A5              ! Constant in the expression of K'''_q,Cm_q^nc, and k_m,q. [from experimental
results, defaults to 1]
        0   S1              ! Constant in the f curve best-fit for alpha0<=AOA<=alpha1; by definition it
depends on the airfoil. [ignored if UAMod<>1]
        0   S2              ! Constant in the f curve best-fit for        AOA> alpha1; by definition it depends
on the airfoil. [ignored if UAMod<>1]
        0   S3              ! Constant in the f curve best-fit for alpha2<=AOA< alpha0; by definition it
depends on the airfoil. [ignored if UAMod<>1]
        0   S4              ! Constant in the f curve best-fit for        AOA< alpha2; by definition it depends
on the airfoil. [ignored if UAMod<>1]
   1.4144   Cn1             ! Critical value of C0n at leading edge separation. It should be extracted from
airfoil data at a given Mach and Reynolds number. It can be calculated from the static value of Cn at
either the break in the pitching moment or the loss of chord force at the onset of stall. It is close to the
condition of maximum lift of the airfoil at low Mach numbers.
```

Appendix A: FAST Input Files

```
   -0.5324   Cn2             ! As Cn1 for negative AOAs.
      0.19   St_sh           ! Strouhal's shedding frequency constant.  [default = 0.19]
     0.006   Cd0             ! 2D drag coefficient value at 0-lift.
    -0.121   Cm0             ! 2D pitching moment coefficient about 1/4-chord location, at 0-lift, positive if
nose up. [If the aerodynamics coefficients table does not include a column for Cm, this needs to be
set to 0.0]
         0   k0              ! Constant in the \hat(x)_cp curve best-fit; = (\hat(x)_AC-0.25).  [ignored if
UAMod<>1]
         0   k1              ! Constant in the \hat(x)_cp curve best-fit.  [ignored if UAMod<>1]
         0   k2              ! Constant in the \hat(x)_cp curve best-fit.  [ignored if UAMod<>1]
         0   k3              ! Constant in the \hat(x)_cp curve best-fit.  [ignored if UAMod<>1]
         0   k1_hat          ! Constant in the expression of Cc due to leading edge vortex effects.  [ignored
if UAMod<>1]
       0.2   x_cp_bar        ! Constant in the expression of \hat(x)_cp^v. [ignored if UAMod<>1, default
= 0.2]
"DEFAULT"     UACutout       ! Angle of attack above which unsteady aerodynamics are disabled
(deg). [Specifying the string "Default" sets UACutout to 45 degrees]
"DEFAULT"     filtCutOff     ! Cut-off frequency (-3 dB corner frequency) for low-pass filtering the
AoA input to UA, as well as the 1st and 2nd derivatives (Hz) [default = 20]
!.....................................
! Table of aerodynamics coefficients
       142   NumAlf          ! Number of data lines in the following table
!    Alpha      Cl      Cd       Cm
!    (deg)      (-)     (-)      (-)
   -180.00    0.000   0.0185   0.0000
   -175.00    0.394   0.0332   0.1978
   -170.00    0.788   0.0945   0.3963
   -160.00    0.670   0.2809   0.2738
   -155.00    0.749   0.3932   0.3118
   -150.00    0.797   0.5112   0.3413
   -145.00    0.818   0.6309   0.3636
   -140.00    0.813   0.7485   0.3799
   -135.00    0.786   0.8612   0.3911
   -130.00    0.739   0.9665   0.3980
   -125.00    0.675   1.0625   0.4012
   -120.00    0.596   1.1476   0.4014
   -115.00    0.505   1.2206   0.3990
   -110.00    0.403   1.2805   0.3943
   -105.00    0.294   1.3265   0.3878
   -100.00    0.179   1.3582   0.3796
    -95.00    0.060   1.3752   0.3700
    -90.00   -0.060   1.3774   0.3591
    -85.00   -0.179   1.3648   0.3471
    -80.00   -0.295   1.3376   0.3340
    -75.00   -0.407   1.2962   0.3199
    -70.00   -0.512   1.2409   0.3049
    -65.00   -0.608   1.1725   0.2890
    -60.00   -0.693   1.0919   0.2722
    -55.00   -0.764   1.0002   0.2545
    -50.00   -0.820   0.8990   0.2359
    -45.00   -0.857   0.7900   0.2163
    -40.00   -0.875   0.6754   0.1958
    -35.00   -0.869   0.5579   0.1744
    -30.00   -0.838   0.4405   0.1520
    -25.00   -0.791   0.3256   0.1262
    -24.00   -0.794   0.3013   0.1170
```

Appendix A: FAST Input Files

-23.00	-0.805	0.2762	0.1059
-22.00	-0.821	0.2506	0.0931
-21.00	-0.843	0.2246	0.0788
-20.00	-0.869	0.1983	0.0631
-19.00	-0.899	0.1720	0.0464
-18.00	-0.931	0.1457	0.0286
-17.00	-0.964	0.1197	0.0102
-16.00	-0.999	0.0940	-0.0088
-15.00	-1.033	0.0689	-0.0281
-14.50	-1.050	0.0567	-0.0378
-12.01	-0.953	0.0271	-0.0349
-11.00	-0.900	0.0303	-0.0361
-9.98	-0.827	0.0287	-0.0464
-8.12	-0.536	0.0124	-0.0821
-7.62	-0.467	0.0109	-0.0924
-7.11	-0.393	0.0092	-0.1015
-6.60	-0.323	0.0083	-0.1073
-6.50	-0.311	0.0089	-0.1083
-6.00	-0.245	0.0082	-0.1112
-5.50	-0.178	0.0074	-0.1146
-5.00	-0.113	0.0069	-0.1172
-4.50	-0.048	0.0065	-0.1194
-4.00	0.016	0.0063	-0.1213
-3.50	0.080	0.0061	-0.1232
-3.00	0.145	0.0058	-0.1252
-2.50	0.208	0.0057	-0.1268
-2.00	0.270	0.0057	-0.1282
-1.50	0.333	0.0057	-0.1297
-1.00	0.396	0.0057	-0.1310
-0.50	0.458	0.0057	-0.1324
0.00	0.521	0.0057	-0.1337
0.50	0.583	0.0057	-0.1350
1.00	0.645	0.0058	-0.1363
1.50	0.706	0.0058	-0.1374
2.00	0.768	0.0059	-0.1385
2.50	0.828	0.0061	-0.1395
3.00	0.888	0.0063	-0.1403
3.50	0.948	0.0066	-0.1406
4.00	0.996	0.0071	-0.1398
4.50	1.046	0.0079	-0.1390
5.00	1.095	0.0090	-0.1378
5.50	1.145	0.0103	-0.1369
6.00	1.192	0.0113	-0.1353
6.50	1.239	0.0122	-0.1338
7.00	1.283	0.0131	-0.1317
7.50	1.324	0.0139	-0.1291
8.00	1.358	0.0147	-0.1249
8.50	1.385	0.0158	-0.1213
9.00	1.403	0.0181	-0.1177
9.50	1.401	0.0211	-0.1142
10.00	1.358	0.0255	-0.1103
10.50	1.313	0.0301	-0.1066
11.00	1.287	0.0347	-0.1032
11.50	1.274	0.0401	-0.1002
12.00	1.272	0.0468	-0.0971
12.50	1.273	0.0545	-0.0940

13.00	1.273	0.0633	-0.0909
13.50	1.273	0.0722	-0.0883
14.00	1.272	0.0806	-0.0865
14.50	1.273	0.0900	-0.0854
15.00	1.275	0.0987	-0.0849
15.50	1.281	0.1075	-0.0847
16.00	1.284	0.1170	-0.0850
16.50	1.296	0.1270	-0.0858
17.00	1.306	0.1368	-0.0869
17.50	1.308	0.1464	-0.0883
18.00	1.308	0.1562	-0.0901
18.50	1.308	0.1664	-0.0922
19.00	1.308	0.1770	-0.0949
19.50	1.307	0.1878	-0.0980
20.00	1.311	0.1987	-0.1017
20.50	1.325	0.2100	-0.1059
21.00	1.324	0.2214	-0.1105
22.00	1.277	0.2499	-0.1172
23.00	1.229	0.2786	-0.1239
24.00	1.182	0.3077	-0.1305
25.00	1.136	0.3371	-0.1370
26.00	1.093	0.3664	-0.1433
28.00	1.017	0.4246	-0.1556
30.00	0.962	0.4813	-0.1671
32.00	0.937	0.5356	-0.1778
35.00	0.947	0.6127	-0.1923
40.00	0.950	0.7396	-0.2154
45.00	0.928	0.8623	-0.2374
50.00	0.884	0.9781	-0.2583
55.00	0.821	1.0846	-0.2782
60.00	0.740	1.1796	-0.2971
65.00	0.646	1.2617	-0.3149
70.00	0.540	1.3297	-0.3318
75.00	0.425	1.3827	-0.3476
80.00	0.304	1.4202	-0.3625
85.00	0.179	1.4423	-0.3763
90.00	0.053	1.4512	-0.3890
95.00	-0.073	1.4480	-0.4004
100.00	-0.198	1.4294	-0.4105
105.00	-0.319	1.3954	-0.4191
110.00	-0.434	1.3464	-0.4260
115.00	-0.541	1.2829	-0.4308
120.00	-0.637	1.2057	-0.4333
125.00	-0.720	1.1157	-0.4330
130.00	-0.787	1.0144	-0.4294
135.00	-0.836	0.9033	-0.4219
140.00	-0.864	0.7845	-0.4098
145.00	-0.869	0.6605	-0.3922
150.00	-0.847	0.5346	-0.3682
155.00	-0.795	0.4103	-0.3364
160.00	-0.711	0.2922	-0.2954
170.00	-0.788	0.0969	-0.3966
175.00	-0.394	0.0334	-0.1978
180.00	0.000	0.0185	0.0000

A.7.4. DU25-A17

```
! ------------ AirfoilInfo v1.01.x Input File ----------------------------------
! DU25 airfoil with an aspect ratio of 17.  Original -180 to 180deg Cl, Cd, and Cm versus AOA data
taken from Appendix A of DOWEC document 10046_009.pdf (numerical values obtained from Koert
Lindenburg of ECN).
! Cl and Cd values corrected for rotational stall delay and Cd values corrected using the Viterna
method for 0 to 90deg AOA by Jason Jonkman using AirfoilPrep_v2p0.xls.
! note that this file uses Marshall Buhl's new input file processing; start all comment lines with !
! ------------------------------------------------------------------------
"DEFAULT"     InterpOrd       ! Interpolation order to use for quasi-steady table lookup {1=linear;
3=cubic spline; "default"} [default=3]
        1   NonDimArea       ! The non-dimensional area of the airfoil (area/chord^2) (set to 1.0 if
unsure or unneeded)
@"DU25_A17_coords.txt"    NumCoords       ! The number of coordinates in the airfoil shape file.  Set
to zero if coordinates not included.
        1   NumTabs         ! Number of airfoil tables in this file.  Each table must have lines for Re and
Ctrl.
! ------------------------------------------------------------------------
! data for table 1
! ------------------------------------------------------------------------
      0.75   Re              ! Reynolds number in millions
         0   Ctrl            ! Control setting (must be 0 for current AirfoilInfo)
True          InclUAdata      ! Is unsteady aerodynamics data included in this table? If TRUE, then
include 30 UA coefficients below this line
!.....................................
      -3.2   alpha0          ! 0-lift angle of attack, depends on airfoil.
       8.5   alpha1          ! Angle of attack at f=0.7, (approximately the stall angle) for AOA>alpha0.
(deg)
      -8.5   alpha2          ! Angle of attack at f=0.7, (approximately the stall angle) for AOA<alpha0.
(deg)
         1   eta_e           ! Recovery factor in the range [0.85 - 0.95] used only for UAMOD=1, it is set to 1
in the code when flookup=True. (-)
    6.4462   C_nalpha        ! Slope of the 2D normal force coefficient curve. (1/rad)
         3   T_f0            ! Initial value of the time constant associated with Df in the expression of Df and
f''. [default = 3]
         6   T_V0            ! Initial value of the time constant associated with the vortex lift decay process;
it is used in the expression of Cvn. It depends on Re,M, and airfoil class. [default = 6]
       1.7   T_p             ! Boundary-layer,leading edge pressure gradient time constant in the
expression of Dp. It should be tuned based on airfoil experimental data. [default = 1.7]
        11   T_VL            ! Initial value of the time constant associated with the vortex advection
process; it represents the non-dimensional time in semi-chords, needed for a vortex to travel from LE
to trailing edge (TE); it is used in the expression of Cvn. It depends on Re, M (weakly), and airfoil.
[valid range = 6 - 13, default = 11]
      0.14   b1              ! Constant in the expression of phi_alpha^c and phi_q^c.  This value is
relatively insensitive for thin airfoils, but may be different for turbine airfoils. [from experimental
results, defaults to 0.14]
      0.53   b2              ! Constant in the expression of phi_alpha^c and phi_q^c.  This value is
relatively insensitive for thin airfoils, but may be different for turbine airfoils. [from experimental
results, defaults to 0.53]
         5   b5              ! Constant in the expression of K'''_q,Cm_q^nc, and k_m,q.  [from  experimental
results, defaults to 5]
       0.3   A1              ! Constant in the expression of phi_alpha^c and phi_q^c.  This value is
relatively insensitive for thin airfoils, but may be different for turbine airfoils. [from experimental
results, defaults to 0.3]
```

Appendix A: FAST Input Files

```
      0.7   A2              ! Constant in the expression of phi_alpha^c and phi_q^c.  This value is relatively insensitive for thin airfoils, but may be different for turbine airfoils. [from experimental results, defaults to 0.7]
        1   A5              ! Constant in the expression of K'''_q,Cm_q^nc, and k_m,q. [from experimental results, defaults to 1]
        0   S1              ! Constant in the f curve best-fit for alpha0<=AOA<=alpha1; by definition it depends on the airfoil. [ignored if UAMod<>1]
        0   S2              ! Constant in the f curve best-fit for        AOA> alpha1; by definition it depends on the airfoil. [ignored if UAMod<>1]
        0   S3              ! Constant in the f curve best-fit for alpha2<=AOA< alpha0; by definition it depends on the airfoil. [ignored if UAMod<>1]
        0   S4              ! Constant in the f curve best-fit for        AOA< alpha2; by definition it depends on the airfoil. [ignored if UAMod<>1]
   1.4336   Cn1             ! Critical value of C0n at leading edge separation. It should be extracted from airfoil data at a given Mach and Reynolds number. It can be calculated from the static value of Cn at either the break in the pitching moment or the loss of chord force at the onset of stall. It is close to the condition of maximum lift of the airfoil at low Mach numbers.
  -0.6873   Cn2             ! As Cn1 for negative AOAs.
     0.19   St_sh           ! Strouhal's shedding frequency constant.  [default = 0.19]
    0.006   Cd0             ! 2D drag coefficient value at 0-lift.
    -0.12   Cm0             ! 2D pitching moment coefficient about 1/4-chord location, at 0-lift, positive if nose up. [If the aerodynamics coefficients table does not include a column for Cm, this needs to be set to 0.0]
        0   k0              ! Constant in the \hat(x)_cp curve best-fit; = (\hat(x)_AC-0.25).  [ignored if UAMod<>1]
        0   k1              ! Constant in the \hat(x)_cp curve best-fit.  [ignored if UAMod<>1]
        0   k2              ! Constant in the \hat(x)_cp curve best-fit.  [ignored if UAMod<>1]
        0   k3              ! Constant in the \hat(x)_cp curve best-fit.  [ignored if UAMod<>1]
        0   k1_hat          ! Constant in the expression of Cc due to leading edge vortex effects.  [ignored if UAMod<>1]
      0.2   x_cp_bar        ! Constant in the expression of \hat(x)_cp^v. [ignored if UAMod<>1, default = 0.2]
"DEFAULT"     UACutout      ! Angle of attack above which unsteady aerodynamics are disabled (deg). [Specifying the string "Default" sets UACutout to 45 degrees]
"DEFAULT"     filtCutOff    ! Cut-off frequency (-3 dB corner frequency) for low-pass filtering the AoA input to UA, as well as the 1st and 2nd derivatives (Hz) [default = 20]
!.....................................
! Table of aerodynamics coefficients
      140   NumAlf          ! Number of data lines in the following table
!    Alpha      Cl      Cd       Cm
!    (deg)      (-)     (-)      (-)
   -180.00    0.000   0.0202   0.0000
   -175.00    0.368   0.0324   0.1845
   -170.00    0.735   0.0943   0.3701
   -160.00    0.695   0.2848   0.2679
   -155.00    0.777   0.4001   0.3046
   -150.00    0.828   0.5215   0.3329
   -145.00    0.850   0.6447   0.3540
   -140.00    0.846   0.7660   0.3693
   -135.00    0.818   0.8823   0.3794
   -130.00    0.771   0.9911   0.3854
   -125.00    0.705   1.0905   0.3878
   -120.00    0.624   1.1787   0.3872
   -115.00    0.530   1.2545   0.3841
   -110.00    0.426   1.3168   0.3788
   -105.00    0.314   1.3650   0.3716
```

Appendix A: FAST Input Files

-100.00	0.195	1.3984	0.3629
-95.00	0.073	1.4169	0.3529
-90.00	-0.050	1.4201	0.3416
-85.00	-0.173	1.4081	0.3292
-80.00	-0.294	1.3811	0.3159
-75.00	-0.409	1.3394	0.3017
-70.00	-0.518	1.2833	0.2866
-65.00	-0.617	1.2138	0.2707
-60.00	-0.706	1.1315	0.2539
-55.00	-0.780	1.0378	0.2364
-50.00	-0.839	0.9341	0.2181
-45.00	-0.879	0.8221	0.1991
-40.00	-0.898	0.7042	0.1792
-35.00	-0.893	0.5829	0.1587
-30.00	-0.862	0.4616	0.1374
-25.00	-0.803	0.3441	0.1154
-24.00	-0.792	0.3209	0.1101
-23.00	-0.789	0.2972	0.1031
-22.00	-0.792	0.2730	0.0947
-21.00	-0.801	0.2485	0.0849
-20.00	-0.815	0.2237	0.0739
-19.00	-0.833	0.1990	0.0618
-18.00	-0.854	0.1743	0.0488
-17.00	-0.879	0.1498	0.0351
-16.00	-0.905	0.1256	0.0208
-15.00	-0.932	0.1020	0.0060
-14.00	-0.959	0.0789	-0.0091
-13.00	-0.985	0.0567	-0.0243
-12.01	-0.953	0.0271	-0.0349
-11.00	-0.900	0.0303	-0.0361
-9.98	-0.827	0.0287	-0.0464
-8.98	-0.753	0.0271	-0.0534
-8.47	-0.691	0.0264	-0.0650
-7.45	-0.555	0.0114	-0.0782
-6.42	-0.413	0.0094	-0.0904
-5.40	-0.271	0.0086	-0.1006
-5.00	-0.220	0.0073	-0.1107
-4.50	-0.152	0.0071	-0.1135
-4.00	-0.084	0.0070	-0.1162
-3.50	-0.018	0.0069	-0.1186
-3.00	0.049	0.0068	-0.1209
-2.50	0.115	0.0068	-0.1231
-2.00	0.181	0.0068	-0.1252
-1.50	0.247	0.0067	-0.1272
-1.00	0.312	0.0067	-0.1293
-0.50	0.377	0.0067	-0.1311
0.00	0.444	0.0065	-0.1330
0.50	0.508	0.0065	-0.1347
1.00	0.573	0.0066	-0.1364
1.50	0.636	0.0067	-0.1380
2.00	0.701	0.0068	-0.1396
2.50	0.765	0.0069	-0.1411
3.00	0.827	0.0070	-0.1424
3.50	0.890	0.0071	-0.1437
4.00	0.952	0.0073	-0.1448
4.50	1.013	0.0076	-0.1456

Appendix A: FAST Input Files

5.00	1.062	0.0079	-0.1445
6.00	1.161	0.0099	-0.1419
6.50	1.208	0.0117	-0.1403
7.00	1.254	0.0132	-0.1382
7.50	1.301	0.0143	-0.1362
8.00	1.336	0.0153	-0.1320
8.50	1.369	0.0165	-0.1276
9.00	1.400	0.0181	-0.1234
9.50	1.428	0.0211	-0.1193
10.00	1.442	0.0262	-0.1152
10.50	1.427	0.0336	-0.1115
11.00	1.374	0.0420	-0.1081
11.50	1.316	0.0515	-0.1052
12.00	1.277	0.0601	-0.1026
12.50	1.250	0.0693	-0.1000
13.00	1.246	0.0785	-0.0980
13.50	1.247	0.0888	-0.0969
14.00	1.256	0.1000	-0.0968
14.50	1.260	0.1108	-0.0973
15.00	1.271	0.1219	-0.0981
15.50	1.281	0.1325	-0.0992
16.00	1.289	0.1433	-0.1006
16.50	1.294	0.1541	-0.1023
17.00	1.304	0.1649	-0.1042
17.50	1.309	0.1754	-0.1064
18.00	1.315	0.1845	-0.1082
18.50	1.320	0.1953	-0.1110
19.00	1.330	0.2061	-0.1143
19.50	1.343	0.2170	-0.1179
20.00	1.354	0.2280	-0.1219
20.50	1.359	0.2390	-0.1261
21.00	1.360	0.2536	-0.1303
22.00	1.325	0.2814	-0.1375
23.00	1.288	0.3098	-0.1446
24.00	1.251	0.3386	-0.1515
25.00	1.215	0.3678	-0.1584
26.00	1.181	0.3972	-0.1651
28.00	1.120	0.4563	-0.1781
30.00	1.076	0.5149	-0.1904
32.00	1.056	0.5720	-0.2017
35.00	1.066	0.6548	-0.2173
40.00	1.064	0.7901	-0.2418
45.00	1.035	0.9190	-0.2650
50.00	0.980	1.0378	-0.2867
55.00	0.904	1.1434	-0.3072
60.00	0.810	1.2333	-0.3265
65.00	0.702	1.3055	-0.3446
70.00	0.582	1.3587	-0.3616
75.00	0.456	1.3922	-0.3775
80.00	0.326	1.4063	-0.3921
85.00	0.197	1.4042	-0.4057
90.00	0.072	1.3985	-0.4180
95.00	-0.050	1.3973	-0.4289
100.00	-0.170	1.3810	-0.4385
105.00	-0.287	1.3498	-0.4464
110.00	-0.399	1.3041	-0.4524

```
   115.00   -0.502   1.2442  -0.4563
   120.00   -0.596   1.1709  -0.4577
   125.00   -0.677   1.0852  -0.4563
   130.00   -0.743   0.9883  -0.4514
   135.00   -0.792   0.8818  -0.4425
   140.00   -0.821   0.7676  -0.4288
   145.00   -0.826   0.6481  -0.4095
   150.00   -0.806   0.5264  -0.3836
   155.00   -0.758   0.4060  -0.3497
   160.00   -0.679   0.2912  -0.3065
   170.00   -0.735   0.0995  -0.3706
   175.00   -0.368   0.0356  -0.1846
   180.00    0.000   0.0202   0.0000
```

A.7.5. DU30-A17

```
! ------------ AirfoilInfo v1.01.x Input File ----------------------------------
! DU30 airfoil with an aspect ratio of 17.  Original -180 to 180deg Cl, Cd, and Cm versus AOA data
taken from Appendix A of DOWEC document 10046_009.pdf (numerical values obtained from Koert
Lindenburg of ECN).
! Cl and Cd values corrected for rotational stall delay and Cd values corrected using the Viterna
method for 0 to 90deg AOA by Jason Jonkman using AirfoilPrep_v2p0.xls.
! note that this file uses Marshall Buhl's new input file processing; start all comment lines with !
! ------------------------------------------------------------------------------
"DEFAULT"     InterpOrd        ! Interpolation order to use for quasi-steady table lookup {1=linear;
3=cubic spline; "default"} [default=3]
         1   NonDimArea       ! The non-dimensional area of the airfoil (area/chord^2) (set to 1.0 if
unsure or unneeded)
@"DU30_A17_coords.txt"    NumCoords        ! The number of coordinates in the airfoil shape file.  Set
to zero if coordinates not included.
         1   NumTabs          ! Number of airfoil tables in this file.  Each table must have lines for Re and
Ctrl.
! ------------------------------------------------------------------------------
! data for table 1
! ------------------------------------------------------------------------------
      0.75   Re               ! Reynolds number in millions
         0   Ctrl             ! Control setting (must be 0 for current AirfoilInfo)
True          InclUAdata       ! Is unsteady aerodynamics data included in this table? If TRUE, then
include 30 UA coefficients below this line
!.....................................
      -2.2   alpha0           ! 0-lift angle of attack, depends on airfoil.
         9   alpha1           ! Angle of attack at f=0.7, (approximately the stall angle) for AOA>alpha0.
(deg)
        -9   alpha2           ! Angle of attack at f=0.7, (approximately the stall angle) for AOA<alpha0.
(deg)
         1   eta_e            ! Recovery factor in the range [0.85 - 0.95] used only for UAMOD=1, it is set to 1
in the code when flookup=True. (-)
    7.3326   C_nalpha         ! Slope of the 2D normal force coefficient curve. (1/rad)
         3   T_f0             ! Initial value of the time constant associated with Df in the expression of Df and
f''. [default = 3]
         6   T_V0             ! Initial value of the time constant associated with the vortex lift decay process;
it is used in the expression of Cvn. It depends on Re,M, and airfoil class. [default = 6]
       1.7   T_p              ! Boundary-layer,leading edge pressure gradient time constant in the
expression of Dp. It should be tuned based on airfoil experimental data. [default = 1.7]
```

Appendix A: FAST Input Files

```
      11   T_VL            ! Initial value of the time constant associated with the vortex advection process; it represents the non-dimensional time in semi-chords, needed for a vortex to travel from LE to trailing edge (TE); it is used in the expression of Cvn. It depends on Re, M (weakly), and airfoil. [valid range = 6 - 13, default = 11]
    0.14   b1              ! Constant in the expression of phi_alpha^c and phi_q^c.  This value is relatively insensitive for thin airfoils, but may be different for turbine airfoils. [from experimental results, defaults to 0.14]
    0.53   b2              ! Constant in the expression of phi_alpha^c and phi_q^c.  This value is relatively insensitive for thin airfoils, but may be different for turbine airfoils. [from experimental results, defaults to 0.53]
       5   b5              ! Constant in the expression of K'''_q,Cm_q^nc, and k_m,q.  [from  experimental results, defaults to 5]
     0.3   A1              ! Constant in the expression of phi_alpha^c and phi_q^c.  This value is relatively insensitive for thin airfoils, but may be different for turbine airfoils. [from experimental results, defaults to 0.3]
     0.7   A2              ! Constant in the expression of phi_alpha^c and phi_q^c.  This value is relatively insensitive for thin airfoils, but may be different for turbine airfoils. [from experimental results, defaults to 0.7]
       1   A5              ! Constant in the expression of K'''_q,Cm_q^nc, and k_m,q. [from experimental results, defaults to 1]
       0   S1              ! Constant in the f curve best-fit for alpha0<=AOA<=alpha1; by definition it depends on the airfoil. [ignored if UAMod<>1]
       0   S2              ! Constant in the f curve best-fit for        AOA> alpha1; by definition it depends on the airfoil. [ignored if UAMod<>1]
       0   S3              ! Constant in the f curve best-fit for alpha2<=AOA< alpha0; by definition it depends on the airfoil. [ignored if UAMod<>1]
       0   S4              ! Constant in the f curve best-fit for        AOA< alpha2; by definition it depends on the airfoil. [ignored if UAMod<>1]
   1.449   Cn1             ! Critical value of C0n at leading edge separation. It should be extracted from airfoil data at a given Mach and Reynolds number. It can be calculated from the static value of Cn at either the break in the pitching moment or the loss of chord force at the onset of stall. It is close to the condition of maximum lift of the airfoil at low Mach numbers.
  -0.6138   Cn2             ! As Cn1 for negative AOAs.
    0.19   St_sh           ! Strouhal's shedding frequency constant.  [default = 0.19]
   0.008   Cd0             ! 2D drag coefficient value at 0-lift.
   -0.09   Cm0             ! 2D pitching moment coefficient about 1/4-chord location, at 0-lift, positive if nose up. [If the aerodynamics coefficients table does not include a column for Cm, this needs to be set to 0.0]
       0   k0              ! Constant in the \hat(x)_cp curve best-fit; = (\hat(x)_AC-0.25).  [ignored if UAMod<>1]
       0   k1              ! Constant in the \hat(x)_cp curve best-fit.  [ignored if UAMod<>1]
       0   k2              ! Constant in the \hat(x)_cp curve best-fit.  [ignored if UAMod<>1]
       0   k3              ! Constant in the \hat(x)_cp curve best-fit.  [ignored if UAMod<>1]
       0   k1_hat          ! Constant in the expression of Cc due to leading edge vortex effects.  [ignored if UAMod<>1]
     0.2   x_cp_bar        ! Constant in the expression of \hat(x)_cp^v. [ignored if UAMod<>1, default = 0.2]
"DEFAULT"    UACutout        ! Angle of attack above which unsteady aerodynamics are disabled (deg). [Specifying the string "Default" sets UACutout to 45 degrees]
"DEFAULT"    filtCutOff      ! Cut-off frequency (-3 dB corner frequency) for low-pass filtering the AoA input to UA, as well as the 1st and 2nd derivatives (Hz) [default = 20]
!.....................................
! Table of aerodynamics coefficients
     143   NumAlf          ! Number of data lines in the following table
!   Alpha     Cl     Cd       Cm
!   (deg)     (-)    (-)      (-)
```

Appendix A: FAST Input Files

-180.00	0.000	0.0267	0.0000
-175.00	0.274	0.0370	0.1379
-170.00	0.547	0.0968	0.2778
-160.00	0.685	0.2876	0.2740
-155.00	0.766	0.4025	0.3118
-150.00	0.816	0.5232	0.3411
-145.00	0.836	0.6454	0.3631
-140.00	0.832	0.7656	0.3791
-135.00	0.804	0.8807	0.3899
-130.00	0.756	0.9882	0.3965
-125.00	0.690	1.0861	0.3994
-120.00	0.609	1.1730	0.3992
-115.00	0.515	1.2474	0.3964
-110.00	0.411	1.3084	0.3915
-105.00	0.300	1.3552	0.3846
-100.00	0.182	1.3875	0.3761
-95.00	0.061	1.4048	0.3663
-90.00	-0.061	1.4070	0.3551
-85.00	-0.183	1.3941	0.3428
-80.00	-0.302	1.3664	0.3295
-75.00	-0.416	1.3240	0.3153
-70.00	-0.523	1.2676	0.3001
-65.00	-0.622	1.1978	0.2841
-60.00	-0.708	1.1156	0.2672
-55.00	-0.781	1.0220	0.2494
-50.00	-0.838	0.9187	0.2308
-45.00	-0.877	0.8074	0.2113
-40.00	-0.895	0.6904	0.1909
-35.00	-0.889	0.5703	0.1696
-30.00	-0.858	0.4503	0.1475
-25.00	-0.832	0.3357	0.1224
-24.00	-0.852	0.3147	0.1156
-23.00	-0.882	0.2946	0.1081
-22.00	-0.919	0.2752	0.1000
-21.00	-0.963	0.2566	0.0914
-20.00	-1.013	0.2388	0.0823
-19.00	-1.067	0.2218	0.0728
-18.00	-1.125	0.2056	0.0631
-17.00	-1.185	0.1901	0.0531
-16.00	-1.245	0.1754	0.0430
-15.25	-1.290	0.1649	0.0353
-14.24	-1.229	0.1461	0.0240
-13.24	-1.148	0.1263	0.0100
-12.22	-1.052	0.1051	-0.0090
-11.22	-0.965	0.0886	-0.0230
-10.19	-0.867	0.0740	-0.0336
-9.70	-0.822	0.0684	-0.0375
-9.18	-0.769	0.0605	-0.0440
-8.18	-0.756	0.0270	-0.0578
-7.19	-0.690	0.0180	-0.0590
-6.65	-0.616	0.0166	-0.0633
-6.13	-0.542	0.0152	-0.0674
-6.00	-0.525	0.0117	-0.0732
-5.50	-0.451	0.0105	-0.0766
-5.00	-0.382	0.0097	-0.0797
-4.50	-0.314	0.0092	-0.0825

Appendix A: FAST Input Files

-4.00	-0.251	0.0091	-0.0853
-3.50	-0.189	0.0089	-0.0884
-3.00	-0.120	0.0089	-0.0914
-2.50	-0.051	0.0088	-0.0942
-2.00	0.017	0.0088	-0.0969
-1.50	0.085	0.0088	-0.0994
-1.00	0.152	0.0088	-0.1018
-0.50	0.219	0.0088	-0.1041
0.00	0.288	0.0087	-0.1062
0.50	0.354	0.0087	-0.1086
1.00	0.421	0.0088	-0.1107
1.50	0.487	0.0089	-0.1129
2.00	0.554	0.0090	-0.1149
2.50	0.619	0.0091	-0.1168
3.00	0.685	0.0092	-0.1185
3.50	0.749	0.0093	-0.1201
4.00	0.815	0.0095	-0.1218
4.50	0.879	0.0096	-0.1233
5.00	0.944	0.0097	-0.1248
5.50	1.008	0.0099	-0.1260
6.00	1.072	0.0101	-0.1270
6.50	1.135	0.0103	-0.1280
7.00	1.197	0.0107	-0.1287
7.50	1.256	0.0112	-0.1289
8.00	1.305	0.0125	-0.1270
9.00	1.390	0.0155	-0.1207
9.50	1.424	0.0171	-0.1158
10.00	1.458	0.0192	-0.1116
10.50	1.488	0.0219	-0.1073
11.00	1.512	0.0255	-0.1029
11.50	1.533	0.0307	-0.0983
12.00	1.549	0.0370	-0.0949
12.50	1.558	0.0452	-0.0921
13.00	1.470	0.0630	-0.0899
13.50	1.398	0.0784	-0.0885
14.00	1.354	0.0931	-0.0885
14.50	1.336	0.1081	-0.0902
15.00	1.333	0.1239	-0.0928
15.50	1.326	0.1415	-0.0963
16.00	1.329	0.1592	-0.1006
16.50	1.326	0.1743	-0.1042
17.00	1.321	0.1903	-0.1084
17.50	1.331	0.2044	-0.1125
18.00	1.333	0.2186	-0.1169
18.50	1.340	0.2324	-0.1215
19.00	1.362	0.2455	-0.1263
19.50	1.382	0.2584	-0.1313
20.00	1.398	0.2689	-0.1352
20.50	1.426	0.2814	-0.1406
21.00	1.437	0.2943	-0.1462
22.00	1.418	0.3246	-0.1516
23.00	1.397	0.3557	-0.1570
24.00	1.376	0.3875	-0.1623
25.00	1.354	0.4198	-0.1676
26.00	1.332	0.4524	-0.1728
28.00	1.293	0.5183	-0.1832

```
 30.00   1.265   0.5843  -0.1935
 32.00   1.253   0.6492  -0.2039
 35.00   1.264   0.7438  -0.2193
 40.00   1.258   0.8970  -0.2440
 45.00   1.217   1.0402  -0.2672
 50.00   1.146   1.1686  -0.2891
 55.00   1.049   1.2779  -0.3097
 60.00   0.932   1.3647  -0.3290
 65.00   0.799   1.4267  -0.3471
 70.00   0.657   1.4621  -0.3641
 75.00   0.509   1.4708  -0.3799
 80.00   0.362   1.4544  -0.3946
 85.00   0.221   1.4196  -0.4081
 90.00   0.092   1.3938  -0.4204
 95.00  -0.030   1.3943  -0.4313
100.00  -0.150   1.3798  -0.4408
105.00  -0.267   1.3504  -0.4486
110.00  -0.379   1.3063  -0.4546
115.00  -0.483   1.2481  -0.4584
120.00  -0.578   1.1763  -0.4597
125.00  -0.660   1.0919  -0.4582
130.00  -0.727   0.9962  -0.4532
135.00  -0.777   0.8906  -0.4441
140.00  -0.807   0.7771  -0.4303
145.00  -0.815   0.6581  -0.4109
150.00  -0.797   0.5364  -0.3848
155.00  -0.750   0.4157  -0.3508
160.00  -0.673   0.3000  -0.3074
170.00  -0.547   0.1051  -0.2786
175.00  -0.274   0.0388  -0.1380
180.00   0.000   0.0267   0.0000
```

A.7.6. DU35-A17

```
! ------------ AirfoilInfo v1.01.x Input File ----------------------------------
! DU35 airfoil with an aspect ratio of 17.  Original -180 to 180deg Cl, Cd, and Cm versus AOA data
taken from Appendix A of DOWEC document 10046_009.pdf (numerical values obtained from Koert
Lindenburg of ECN).
! Cl and Cd values corrected for rotational stall delay and Cd values corrected using the Viterna
method for 0 to 90deg AOA by Jason Jonkman using AirfoilPrep_v2p0.xls.
! note that this file uses Marshall Buhl's new input file processing; start all comment lines with !
! ------------------------------------------------------------------------------
"DEFAULT"     InterpOrd        ! Interpolation order to use for quasi-steady table lookup {1=linear;
3=cubic spline; "default"} [default=3]
        1   NonDimArea       ! The non-dimensional area of the airfoil (area/chord^2) (set to 1.0 if
unsure or unneeded)
@"DU35_A17_coords.txt"    NumCoords        ! The number of coordinates in the airfoil shape file.  Set
to zero if coordinates not included.
        1   NumTabs          ! Number of airfoil tables in this file.  Each table must have lines for Re and
Ctrl.
! ------------------------------------------------------------------------------
! data for table 1
! ------------------------------------------------------------------------------
      0.75   Re               ! Reynolds number in millions
```

Appendix A: FAST Input Files

```
        0   Ctrl            ! Control setting (must be 0 for current AirfoilInfo)
True        InclUAdata      ! Is unsteady aerodynamics data included in this table? If TRUE, then include 30 UA coefficients below this line
!.....................................
     -1.2   alpha0          ! 0-lift angle of attack, depends on airfoil.
     11.5   alpha1          ! Angle of attack at f=0.7, (approximately the stall angle) for AOA>alpha0. (deg)
    -11.5   alpha2          ! Angle of attack at f=0.7, (approximately the stall angle) for AOA<alpha0. (deg)
        1   eta_e           ! Recovery factor in the range [0.85 - 0.95] used only for UAMOD=1, it is set to 1 in the code when flookup=True. (-)
   7.1838   C_nalpha        ! Slope of the 2D normal force coefficient curve. (1/rad)
        3   T_f0            ! Initial value of the time constant associated with Df in the expression of Df and f''. [default = 3]
        6   T_V0            ! Initial value of the time constant associated with the vortex lift decay process; it is used in the expression of Cvn. It depends on Re,M, and airfoil class. [default = 6]
      1.7   T_p             ! Boundary-layer,leading edge pressure gradient time constant in the expression of Dp. It should be tuned based on airfoil experimental data. [default = 1.7]
       11   T_VL            ! Initial value of the time constant associated with the vortex advection process; it represents the non-dimensional time in semi-chords, needed for a vortex to travel from LE to trailing edge (TE); it is used in the expression of Cvn. It depends on Re, M (weakly), and airfoil. [valid range = 6 - 13, default = 11]
     0.14   b1              ! Constant in the expression of phi_alpha^c and phi_q^c.  This value is relatively insensitive for thin airfoils, but may be different for turbine airfoils. [from experimental results, defaults to 0.14]
     0.53   b2              ! Constant in the expression of phi_alpha^c and phi_q^c.  This value is relatively insensitive for thin airfoils, but may be different for turbine airfoils. [from experimental results, defaults to 0.53]
        5   b5              ! Constant in the expression of K'''_q,Cm_q^nc, and k_m,q.  [from  experimental results, defaults to 5]
      0.3   A1              ! Constant in the expression of phi_alpha^c and phi_q^c.  This value is relatively insensitive for thin airfoils, but may be different for turbine airfoils. [from experimental results, defaults to 0.3]
      0.7   A2              ! Constant in the expression of phi_alpha^c and phi_q^c.  This value is relatively insensitive for thin airfoils, but may be different for turbine airfoils. [from experimental results, defaults to 0.7]
        1   A5              ! Constant in the expression of K'''_q,Cm_q^nc, and k_m,q. [from experimental results, defaults to 1]
        0   S1              ! Constant in the f curve best-fit for alpha0<=AOA<=alpha1; by definition it depends on the airfoil. [ignored if UAMod<>1]
        0   S2              ! Constant in the f curve best-fit for        AOA> alpha1; by definition it depends on the airfoil. [ignored if UAMod<>1]
        0   S3              ! Constant in the f curve best-fit for alpha2<=AOA< alpha0; by definition it depends on the airfoil. [ignored if UAMod<>1]
        0   S4              ! Constant in the f curve best-fit for        AOA< alpha2; by definition it depends on the airfoil. [ignored if UAMod<>1]
   1.6717   Cn1             ! Critical value of C0n at leading edge separation. It should be extracted from airfoil data at a given Mach and Reynolds number. It can be calculated from the static value of Cn at either the break in the pitching moment or the loss of chord force at the onset of stall. It is close to the condition of maximum lift of the airfoil at low Mach numbers.
  -0.3075   Cn2             ! As Cn1 for negative AOAs.
     0.19   St_sh           ! Strouhal's shedding frequency constant.  [default = 0.19]
    0.012   Cd0             ! 2D drag coefficient value at 0-lift.
    -0.07   Cm0             ! 2D pitching moment coefficient about 1/4-chord location, at 0-lift, positive if nose up. [If the aerodynamics coefficients table does not include a column for Cm, this needs to be set to 0.0]
```

Appendix A: FAST Input Files

```
      0   k0              ! Constant in the \hat(x)_cp curve best-fit; = (\hat(x)_AC-0.25).  [ignored if
UAMod<>1]
      0   k1              ! Constant in the \hat(x)_cp curve best-fit.  [ignored if UAMod<>1]
      0   k2              ! Constant in the \hat(x)_cp curve best-fit.  [ignored if UAMod<>1]
      0   k3              ! Constant in the \hat(x)_cp curve best-fit.  [ignored if UAMod<>1]
      0   k1_hat          ! Constant in the expression of Cc due to leading edge vortex effects.  [ignored
if UAMod<>1]
    0.2   x_cp_bar        ! Constant in the expression of \hat(x)_cp^v. [ignored if UAMod<>1, default
= 0.2]
"DEFAULT"     UACutout        ! Angle of attack above which unsteady aerodynamics are disabled
(deg). [Specifying the string "Default" sets UACutout to 45 degrees]
"DEFAULT"     filtCutOff      ! Cut-off frequency (-3 dB corner frequency) for low-pass filtering the
AoA input to UA, as well as the 1st and 2nd derivatives (Hz) [default = 20]
!.....................................
! Table of aerodynamics coefficients
    135   NumAlf          ! Number of data lines in the following table
!   Alpha     Cl     Cd       Cm
!   (deg)     (-)    (-)      (-)
  -180.00   0.000  0.0407   0.0000
  -175.00   0.223  0.0507   0.0937
  -170.00   0.405  0.1055   0.1702
  -160.00   0.658  0.2982   0.2819
  -155.00   0.733  0.4121   0.3213
  -150.00   0.778  0.5308   0.3520
  -145.00   0.795  0.6503   0.3754
  -140.00   0.787  0.7672   0.3926
  -135.00   0.757  0.8785   0.4046
  -130.00   0.708  0.9819   0.4121
  -125.00   0.641  1.0756   0.4160
  -120.00   0.560  1.1580   0.4167
  -115.00   0.467  1.2280   0.4146
  -110.00   0.365  1.2847   0.4104
  -105.00   0.255  1.3274   0.4041
  -100.00   0.139  1.3557   0.3961
   -95.00   0.021  1.3692   0.3867
   -90.00  -0.098  1.3680   0.3759
   -85.00  -0.216  1.3521   0.3639
   -80.00  -0.331  1.3218   0.3508
   -75.00  -0.441  1.2773   0.3367
   -70.00  -0.544  1.2193   0.3216
   -65.00  -0.638  1.1486   0.3054
   -60.00  -0.720  1.0660   0.2884
   -55.00  -0.788  0.9728   0.2703
   -50.00  -0.840  0.8705   0.2512
   -45.00  -0.875  0.7611   0.2311
   -40.00  -0.889  0.6466   0.2099
   -35.00  -0.880  0.5299   0.1876
   -30.00  -0.846  0.4141   0.1641
   -25.00  -0.784  0.3030   0.1396
   -24.00  -0.768  0.2817   0.1345
   -23.00  -0.751  0.2608   0.1294
   -22.00  -0.733  0.2404   0.1243
   -21.00  -0.714  0.2205   0.1191
   -20.00  -0.693  0.2011   0.1139
   -19.00  -0.671  0.1822   0.1086
   -18.00  -0.648  0.1640   0.1032
```

-17.00	-0.624	0.1465	0.0975
-16.00	-0.601	0.1300	0.0898
-15.00	-0.579	0.1145	0.0799
-14.00	-0.559	0.1000	0.0682
-13.00	-0.539	0.0867	0.0547
-12.00	-0.519	0.0744	0.0397
-11.00	-0.499	0.0633	0.0234
-10.00	-0.480	0.0534	0.0060
-5.54	-0.385	0.0245	-0.0800
-5.04	-0.359	0.0225	-0.0800
-4.54	-0.360	0.0196	-0.0800
-4.04	-0.355	0.0174	-0.0800
-3.54	-0.307	0.0162	-0.0800
-3.04	-0.246	0.0144	-0.0800
-3.00	-0.240	0.0240	-0.0623
-2.50	-0.163	0.0188	-0.0674
-2.00	-0.091	0.0160	-0.0712
-1.50	-0.019	0.0137	-0.0746
-1.00	0.052	0.0118	-0.0778
-0.50	0.121	0.0104	-0.0806
0.00	0.196	0.0094	-0.0831
0.50	0.265	0.0096	-0.0863
1.00	0.335	0.0098	-0.0895
1.50	0.404	0.0099	-0.0924
2.00	0.472	0.0100	-0.0949
2.50	0.540	0.0102	-0.0973
3.00	0.608	0.0103	-0.0996
3.50	0.674	0.0104	-0.1016
4.00	0.742	0.0105	-0.1037
4.50	0.809	0.0107	-0.1057
5.00	0.875	0.0108	-0.1076
5.50	0.941	0.0109	-0.1094
6.00	1.007	0.0110	-0.1109
6.50	1.071	0.0113	-0.1118
7.00	1.134	0.0115	-0.1127
7.50	1.198	0.0117	-0.1138
8.00	1.260	0.0120	-0.1144
8.50	1.318	0.0126	-0.1137
9.00	1.368	0.0133	-0.1112
9.50	1.422	0.0143	-0.1100
10.00	1.475	0.0156	-0.1086
10.50	1.523	0.0174	-0.1064
11.00	1.570	0.0194	-0.1044
11.50	1.609	0.0227	-0.1013
12.00	1.642	0.0269	-0.0980
12.50	1.675	0.0319	-0.0953
13.00	1.700	0.0398	-0.0925
13.50	1.717	0.0488	-0.0896
14.00	1.712	0.0614	-0.0864
14.50	1.703	0.0786	-0.0840
15.50	1.671	0.1173	-0.0830
16.00	1.649	0.1377	-0.0848
16.50	1.621	0.1600	-0.0880
17.00	1.598	0.1814	-0.0926
17.50	1.571	0.2042	-0.0984
18.00	1.549	0.2316	-0.1052

```
 19.00   1.544   0.2719  -0.1158
 19.50   1.549   0.2906  -0.1213
 20.00   1.565   0.3085  -0.1248
 21.00   1.565   0.3447  -0.1317
 22.00   1.563   0.3820  -0.1385
 23.00   1.558   0.4203  -0.1452
 24.00   1.552   0.4593  -0.1518
 25.00   1.546   0.4988  -0.1583
 26.00   1.539   0.5387  -0.1647
 28.00   1.527   0.6187  -0.1770
 30.00   1.522   0.6978  -0.1886
 32.00   1.529   0.7747  -0.1994
 35.00   1.544   0.8869  -0.2148
 40.00   1.529   1.0671  -0.2392
 45.00   1.471   1.2319  -0.2622
 50.00   1.376   1.3747  -0.2839
 55.00   1.249   1.4899  -0.3043
 60.00   1.097   1.5728  -0.3236
 65.00   0.928   1.6202  -0.3417
 70.00   0.750   1.6302  -0.3586
 75.00   0.570   1.6031  -0.3745
 80.00   0.396   1.5423  -0.3892
 85.00   0.237   1.4598  -0.4028
 90.00   0.101   1.4041  -0.4151
 95.00  -0.022   1.4053  -0.4261
100.00  -0.143   1.3914  -0.4357
105.00  -0.261   1.3625  -0.4437
110.00  -0.374   1.3188  -0.4498
115.00  -0.480   1.2608  -0.4538
120.00  -0.575   1.1891  -0.4553
125.00  -0.659   1.1046  -0.4540
130.00  -0.727   1.0086  -0.4492
135.00  -0.778   0.9025  -0.4405
140.00  -0.809   0.7883  -0.4270
145.00  -0.818   0.6684  -0.4078
150.00  -0.800   0.5457  -0.3821
155.00  -0.754   0.4236  -0.3484
160.00  -0.677   0.3066  -0.3054
170.00  -0.417   0.1085  -0.1842
175.00  -0.229   0.0510  -0.1013
180.00   0.000   0.0407   0.0000
```

A.7.7. DU40-A17

```
! ------------ AirfoilInfo v1.01.x Input File ----------------------------------
! DU40 airfoil with an aspect ratio of 17.  Original -180 to 180deg Cl, Cd, and Cm versus AOA data
taken from Appendix A of DOWEC document 10046_009.pdf (numerical values obtained from Koert
Lindenburg of ECN).
! Cl and Cd values corrected for rotational stall delay and Cd values corrected using the Viterna
method for 0 to 90deg AOA by Jason Jonkman using AirfoilPrep_v2p0.xls.
! note that this file uses Marshall Buhl's new input file processing; start all comment lines with !
! ------------------------------------------------------------------------
"DEFAULT"     InterpOrd        ! Interpolation order to use for quasi-steady table lookup {1=linear;
3=cubic spline; "default"} [default=3]
```

Appendix A: FAST Input Files

```
      1   NonDimArea       ! The non-dimensional area of the airfoil (area/chord^2) (set to 1.0 if
unsure or unneeded)
@"DU40_A17_coords.txt"    NumCoords        ! The number of coordinates in the airfoil shape file.  Set
to zero if coordinates not included.
      1   NumTabs          ! Number of airfoil tables in this file.  Each table must have lines for Re and
Ctrl.
! ------------------------------------------------------------------------------
! data for table 1
! ------------------------------------------------------------------------------
    0.75   Re              ! Reynolds number in millions
      0   Ctrl             ! Control setting (must be 0 for current AirfoilInfo)
True        InclUAdata       ! Is unsteady aerodynamics data included in this table? If TRUE, then
include 30 UA coefficients below this line
!.....................................
    -3.2   alpha0          ! 0-lift angle of attack, depends on airfoil.
      9   alpha1           ! Angle of attack at f=0.7, (approximately the stall angle) for AOA>alpha0.
(deg)
     -9   alpha2           ! Angle of attack at f=0.7, (approximately the stall angle) for AOA<alpha0.
(deg)
      1   eta_e            ! Recovery factor in the range [0.85 - 0.95] used only for UAMOD=1, it is set to 1
in the code when flookup=True. (-)
 7.4888   C_nalpha         ! Slope of the 2D normal force coefficient curve. (1/rad)
      3   T_f0             ! Initial value of the time constant associated with Df in the expression of Df and
f''. [default = 3]
      6   T_V0             ! Initial value of the time constant associated with the vortex lift decay process;
it is used in the expression of Cvn. It depends on Re,M, and airfoil class. [default = 6]
    1.7   T_p              ! Boundary-layer,leading edge pressure gradient time constant in the
expression of Dp. It should be tuned based on airfoil experimental data. [default = 1.7]
     11   T_VL             ! Initial value of the time constant associated with the vortex advection
process; it represents the non-dimensional time in semi-chords, needed for a vortex to travel from LE
to trailing edge (TE); it is used in the expression of Cvn. It depends on Re, M (weakly), and airfoil.
[valid range = 6 - 13, default = 11]
    0.14   b1              ! Constant in the expression of phi_alpha^c and phi_q^c.  This value is
relatively insensitive for thin airfoils, but may be different for turbine airfoils. [from experimental
results, defaults to 0.14]
    0.53   b2              ! Constant in the expression of phi_alpha^c and phi_q^c.  This value is
relatively insensitive for thin airfoils, but may be different for turbine airfoils. [from experimental
results, defaults to 0.53]
      5   b5               ! Constant in the expression of K'''_q,Cm_q^nc, and k_m,q.  [from  experimental
results, defaults to 5]
     0.3   A1              ! Constant in the expression of phi_alpha^c and phi_q^c.  This value is
relatively insensitive for thin airfoils, but may be different for turbine airfoils. [from experimental
results, defaults to 0.3]
     0.7   A2              ! Constant in the expression of phi_alpha^c and phi_q^c.  This value is
relatively insensitive for thin airfoils, but may be different for turbine airfoils. [from experimental
results, defaults to 0.7]
      1   A5               ! Constant in the expression of K'''_q,Cm_q^nc, and k_m,q. [from experimental
results, defaults to 1]
      0   S1               ! Constant in the f curve best-fit for alpha0<=AOA<=alpha1; by definition it
depends on the airfoil. [ignored if UAMod<>1]
      0   S2               ! Constant in the f curve best-fit for        AOA> alpha1; by definition it depends
on the airfoil. [ignored if UAMod<>1]
      0   S3               ! Constant in the f curve best-fit for alpha2<=AOA< alpha0; by definition it
depends on the airfoil. [ignored if UAMod<>1]
      0   S4               ! Constant in the f curve best-fit for        AOA< alpha2; by definition it depends
on the airfoil. [ignored if UAMod<>1]
```

Appendix A: FAST Input Files

```
    1.3519   Cn1             ! Critical value of C0n at leading edge separation. It should be extracted from airfoil data at a given Mach and Reynolds number. It can be calculated from the static value of Cn at either the break in the pitching moment or the loss of chord force at the onset of stall. It is close to the condition of maximum lift of the airfoil at low Mach numbers.
   -0.3226   Cn2             ! As Cn1 for negative AOAs.
       0.19  St_sh           ! Strouhal's shedding frequency constant.  [default = 0.19]
       0.03  Cd0             ! 2D drag coefficient value at 0-lift.
      -0.05  Cm0             ! 2D pitching moment coefficient about 1/4-chord location, at 0-lift, positive if nose up. [If the aerodynamics coefficients table does not include a column for Cm, this needs to be set to 0.0]
          0  k0              ! Constant in the \hat(x)_cp curve best-fit; = (\hat(x)_AC-0.25).  [ignored if UAMod<>1]
          0  k1              ! Constant in the \hat(x)_cp curve best-fit.  [ignored if UAMod<>1]
          0  k2              ! Constant in the \hat(x)_cp curve best-fit.  [ignored if UAMod<>1]
          0  k3              ! Constant in the \hat(x)_cp curve best-fit.  [ignored if UAMod<>1]
          0  k1_hat          ! Constant in the expression of Cc due to leading edge vortex effects.  [ignored if UAMod<>1]
        0.2  x_cp_bar        ! Constant in the expression of \hat(x)_cp^v. [ignored if UAMod<>1, default = 0.2]
"DEFAULT"    UACutout        ! Angle of attack above which unsteady aerodynamics are disabled (deg). [Specifying the string "Default" sets UACutout to 45 degrees]
"DEFAULT"    filtCutOff      ! Cut-off frequency (-3 dB corner frequency) for low-pass filtering the AoA input to UA, as well as the 1st and 2nd derivatives (Hz) [default = 20]
!.....................................
! Table of aerodynamics coefficients
        136  NumAlf          ! Number of data lines in the following table
!   Alpha     Cl     Cd       Cm
!   (deg)     (-)    (-)      (-)
  -180.00    0.000  0.0602   0.0000
  -175.00    0.218  0.0699   0.0934
  -170.00    0.397  0.1107   0.1697
  -160.00    0.642  0.3045   0.2813
  -155.00    0.715  0.4179   0.3208
  -150.00    0.757  0.5355   0.3516
  -145.00    0.772  0.6535   0.3752
  -140.00    0.762  0.7685   0.3926
  -135.00    0.731  0.8777   0.4048
  -130.00    0.680  0.9788   0.4126
  -125.00    0.613  1.0700   0.4166
  -120.00    0.532  1.1499   0.4176
  -115.00    0.439  1.2174   0.4158
  -110.00    0.337  1.2716   0.4117
  -105.00    0.228  1.3118   0.4057
  -100.00    0.114  1.3378   0.3979
   -95.00   -0.002  1.3492   0.3887
   -90.00   -0.120  1.3460   0.3781
   -85.00   -0.236  1.3283   0.3663
   -80.00   -0.349  1.2964   0.3534
   -75.00   -0.456  1.2507   0.3394
   -70.00   -0.557  1.1918   0.3244
   -65.00   -0.647  1.1204   0.3084
   -60.00   -0.727  1.0376   0.2914
   -55.00   -0.792  0.9446   0.2733
   -50.00   -0.842  0.8429   0.2543
   -45.00   -0.874  0.7345   0.2342
   -40.00   -0.886  0.6215   0.2129
```

-35.00	-0.875	0.5067	0.1906
-30.00	-0.839	0.3932	0.1670
-25.00	-0.777	0.2849	0.1422
-24.00	-0.761	0.2642	0.1371
-23.00	-0.744	0.2440	0.1320
-22.00	-0.725	0.2242	0.1268
-21.00	-0.706	0.2049	0.1215
-20.00	-0.685	0.1861	0.1162
-19.00	-0.662	0.1687	0.1097
-18.00	-0.635	0.1533	0.1012
-17.00	-0.605	0.1398	0.0907
-16.00	-0.571	0.1281	0.0784
-15.00	-0.534	0.1183	0.0646
-14.00	-0.494	0.1101	0.0494
-13.00	-0.452	0.1036	0.0330
-12.00	-0.407	0.0986	0.0156
-11.00	-0.360	0.0951	-0.0026
-10.00	-0.311	0.0931	-0.0213
-8.00	-0.208	0.0930	-0.0600
-6.00	-0.111	0.0689	-0.0500
-5.50	-0.090	0.0614	-0.0516
-5.00	-0.072	0.0547	-0.0532
-4.50	-0.065	0.0480	-0.0538
-4.00	-0.054	0.0411	-0.0544
-3.50	-0.017	0.0349	-0.0554
-3.00	0.003	0.0299	-0.0558
-2.50	0.014	0.0255	-0.0555
-2.00	0.009	0.0198	-0.0534
-1.50	0.004	0.0164	-0.0442
-1.00	0.036	0.0147	-0.0469
-0.50	0.073	0.0137	-0.0522
0.00	0.137	0.0113	-0.0573
0.50	0.213	0.0114	-0.0644
1.00	0.292	0.0118	-0.0718
1.50	0.369	0.0122	-0.0783
2.00	0.444	0.0124	-0.0835
2.50	0.514	0.0124	-0.0866
3.00	0.580	0.0123	-0.0887
3.50	0.645	0.0120	-0.0900
4.00	0.710	0.0119	-0.0914
4.50	0.776	0.0122	-0.0933
5.00	0.841	0.0125	-0.0947
5.50	0.904	0.0129	-0.0957
6.00	0.967	0.0135	-0.0967
6.50	1.027	0.0144	-0.0973
7.00	1.084	0.0158	-0.0972
7.50	1.140	0.0174	-0.0972
8.00	1.193	0.0198	-0.0968
8.50	1.242	0.0231	-0.0958
9.00	1.287	0.0275	-0.0948
9.50	1.333	0.0323	-0.0942
10.00	1.368	0.0393	-0.0926
10.50	1.400	0.0475	-0.0908
11.00	1.425	0.0580	-0.0890
11.50	1.449	0.0691	-0.0877
12.00	1.473	0.0816	-0.0870

12.50	1.494	0.0973	-0.0870
13.00	1.513	0.1129	-0.0876
13.50	1.538	0.1288	-0.0886
14.50	1.587	0.1650	-0.0917
15.00	1.614	0.1845	-0.0939
15.50	1.631	0.2052	-0.0966
16.00	1.649	0.2250	-0.0996
16.50	1.666	0.2467	-0.1031
17.00	1.681	0.2684	-0.1069
17.50	1.699	0.2900	-0.1110
18.00	1.719	0.3121	-0.1157
19.00	1.751	0.3554	-0.1242
19.50	1.767	0.3783	-0.1291
20.50	1.798	0.4212	-0.1384
21.00	1.810	0.4415	-0.1416
22.00	1.830	0.4830	-0.1479
23.00	1.847	0.5257	-0.1542
24.00	1.861	0.5694	-0.1603
25.00	1.872	0.6141	-0.1664
26.00	1.881	0.6593	-0.1724
28.00	1.894	0.7513	-0.1841
30.00	1.904	0.8441	-0.1954
32.00	1.915	0.9364	-0.2063
35.00	1.929	1.0722	-0.2220
40.00	1.903	1.2873	-0.2468
45.00	1.820	1.4796	-0.2701
50.00	1.690	1.6401	-0.2921
55.00	1.522	1.7609	-0.3127
60.00	1.323	1.8360	-0.3321
65.00	1.106	1.8614	-0.3502
70.00	0.880	1.8347	-0.3672
75.00	0.658	1.7567	-0.3830
80.00	0.449	1.6334	-0.3977
85.00	0.267	1.4847	-0.4112
90.00	0.124	1.3879	-0.4234
95.00	0.002	1.3912	-0.4343
100.00	-0.118	1.3795	-0.4437
105.00	-0.235	1.3528	-0.4514
110.00	-0.348	1.3114	-0.4573
115.00	-0.453	1.2557	-0.4610
120.00	-0.549	1.1864	-0.4623
125.00	-0.633	1.1041	-0.4606
130.00	-0.702	1.0102	-0.4554
135.00	-0.754	0.9060	-0.4462
140.00	-0.787	0.7935	-0.4323
145.00	-0.797	0.6750	-0.4127
150.00	-0.782	0.5532	-0.3863
155.00	-0.739	0.4318	-0.3521
160.00	-0.664	0.3147	-0.3085
170.00	-0.410	0.1144	-0.1858
175.00	-0.226	0.0702	-0.1022
180.00	0.000	0.0602	0.0000

Appendix A: FAST Input Files

A7.8. NACA64-A17

```
! ------------ AirfoilInfo v1.01.x Input File ----------------------------------
! NACA64 airfoil with an aspect ratio of 17.  Original -180 to 180deg Cl, Cd, and Cm versus AOA
data taken from Appendix A of DOWEC document 10046_009.pdf (numerical values obtained from
Koert Lindenburg of ECN).
! Cl and Cd values corrected for rotational stall delay and Cd values corrected using the Viterna
method for 0 to 90deg AOA by Jason Jonkman using AirfoilPrep_v2p0.xls.
! note that this file uses Marshall Buhl's new input file processing; start all comment lines with !
! ------------------------------------------------------------------------
"DEFAULT"     InterpOrd        ! Interpolation order to use for quasi-steady table lookup {1=linear;
3=cubic spline; "default"} [default=3]
        1   NonDimArea        ! The non-dimensional area of the airfoil (area/chord^2) (set to 1.0 if
unsure or unneeded)
@"NACA64_A17_coords.txt"    NumCoords        ! The number of coordinates in the airfoil shape file.
Set to zero if coordinates not included.
        1   NumTabs          ! Number of airfoil tables in this file.  Each table must have lines for Re and
Ctrl.
! ------------------------------------------------------------------------
! data for table 1
! ------------------------------------------------------------------------
      0.75   Re               ! Reynolds number in millions
         0   Ctrl             ! Control setting (must be 0 for current AirfoilInfo)
True         InclUAdata       ! Is unsteady aerodynamics data included in this table? If TRUE, then
include 30 UA coefficients below this line
!.....................................
    -4.432   alpha0           ! 0-lift angle of attack, depends on airfoil.
         9   alpha1           ! Angle of attack at f=0.7, (approximately the stall angle) for AOA>alpha0.
(deg)
        -9   alpha2           ! Angle of attack at f=0.7, (approximately the stall angle) for AOA<alpha0.
(deg)
         1   eta_e            ! Recovery factor in the range [0.85 - 0.95] used only for UAMOD=1, it is set to 1
in the code when flookup=True. (-)
    6.0031   C_nalpha         ! Slope of the 2D normal force coefficient curve. (1/rad)
"Default"     T_f0             ! Initial value of the time constant associated with Df in the expression of Df
and f". [default = 3]
"Default"     T_V0             ! Initial value of the time constant associated with the vortex lift decay
process; it is used in the expression of Cvn. It depends on Re,M, and airfoil class. [default = 6]
"Default"     T_p              ! Boundary-layer,leading edge pressure gradient time constant in the
expression of Dp. It should be tuned based on airfoil experimental data. [default = 1.7]
"Default"     T_VL             ! Initial value of the time constant associated with the vortex advection
process; it represents the non-dimensional time in semi-chords, needed for a vortex to travel from LE
to trailing edge (TE); it is used in the expression of Cvn. It depends on Re, M (weakly), and airfoil.
[valid range = 6 - 13, default = 11]
"Default"     b1               ! Constant in the expression of phi_alpha^c and phi_q^c.  This value is
relatively insensitive for thin airfoils, but may be different for turbine airfoils. [from experimental
results, defaults to 0.14]
"Default"     b2               ! Constant in the expression of phi_alpha^c and phi_q^c.  This value is
relatively insensitive for thin airfoils, but may be different for turbine airfoils. [from experimental
results, defaults to 0.53]
"Default"     b5               ! Constant in the expression of K'''_q,Cm_q^nc, and k_m,q.  [from
experimental results, defaults to 5]
"Default"     A1               ! Constant in the expression of phi_alpha^c and phi_q^c.  This value is
relatively insensitive for thin airfoils, but may be different for turbine airfoils. [from experimental
results, defaults to 0.3]
```

Appendix A: FAST Input Files

```
"Default"     A2              ! Constant in the expression of phi_alpha^c and phi_q^c.  This value is relatively insensitive for thin airfoils, but may be different for turbine airfoils. [from experimental results, defaults to 0.7]
"Default"     A5              ! Constant in the expression of K'"_q,Cm_q^nc, and k_m,q. [from experimental results, defaults to 1]
        0   S1              ! Constant in the f curve best-fit for alpha0<=AOA<=alpha1; by definition it depends on the airfoil. [ignored if UAMod<>1]
        0   S2              ! Constant in the f curve best-fit for        AOA> alpha1; by definition it depends on the airfoil. [ignored if UAMod<>1]
        0   S3              ! Constant in the f curve best-fit for alpha2<=AOA< alpha0; by definition it depends on the airfoil. [ignored if UAMod<>1]
        0   S4              ! Constant in the f curve best-fit for        AOA< alpha2; by definition it depends on the airfoil. [ignored if UAMod<>1]
    1.4073   Cn1             ! Critical value of C0n at leading edge separation. It should be extracted from airfoil data at a given Mach and Reynolds number. It can be calculated from the static value of Cn at either the break in the pitching moment or the loss of chord force at the onset of stall. It is close to the condition of maximum lift of the airfoil at low Mach numbers.
   -0.7945   Cn2             ! As Cn1 for negative AOAs.
      0.19   St_sh           ! Strouhal's shedding frequency constant.  [default = 0.19]
    0.0065   Cd0             ! 2D drag coefficient value at 0-lift.
    -0.088   Cm0             ! 2D pitching moment coefficient about 1/4-chord location, at 0-lift, positive if nose up. [If the aerodynamics coefficients table does not include a column for Cm, this needs to be set to 0.0]
        0   k0              ! Constant in the \hat(x)_cp curve best-fit; = (\hat(x)_AC-0.25).  [ignored if UAMod<>1]
        0   k1              ! Constant in the \hat(x)_cp curve best-fit.  [ignored if UAMod<>1]
        0   k2              ! Constant in the \hat(x)_cp curve best-fit.  [ignored if UAMod<>1]
        0   k3              ! Constant in the \hat(x)_cp curve best-fit.  [ignored if UAMod<>1]
        0   k1_hat          ! Constant in the expression of Cc due to leading edge vortex effects.  [ignored if UAMod<>1]
"Default"     x_cp_bar        ! Constant in the expression of \hat(x)_cp^v. [ignored if UAMod<>1, default = 0.2]
"Default"     UACutout        ! Angle of attack above which unsteady aerodynamics are disabled (deg). [Specifying the string "Default" sets UACutout to 45 degrees]
"DEFAULT"     filtCutOff      ! Cut-off frequency (-3 dB corner frequency) for low-pass filtering the AoA input to UA, as well as the 1st and 2nd derivatives (Hz) [default = 20]
!.....................................
! Table of aerodynamics coefficients
      127   NumAlf          ! Number of data lines in the following table
!   Alpha     Cl     Cd       Cm
!   (deg)     (-)    (-)      (-)
  -180.00    0.000  0.0198   0.0000
  -175.00    0.374  0.0341   0.1880
  -170.00    0.749  0.0955   0.3770
  -160.00    0.659  0.2807   0.2747
  -155.00    0.736  0.3919   0.3130
  -150.00    0.783  0.5086   0.3428
  -145.00    0.803  0.6267   0.3654
  -140.00    0.798  0.7427   0.3820
  -135.00    0.771  0.8537   0.3935
  -130.00    0.724  0.9574   0.4007
  -125.00    0.660  1.0519   0.4042
  -120.00    0.581  1.1355   0.4047
  -115.00    0.491  1.2070   0.4025
  -110.00    0.390  1.2656   0.3981
  -105.00    0.282  1.3104   0.3918
```

Appendix A: FAST Input Files

-100.00	0.169	1.3410	0.3838
-95.00	0.052	1.3572	0.3743
-90.00	-0.067	1.3587	0.3636
-85.00	-0.184	1.3456	0.3517
-80.00	-0.299	1.3181	0.3388
-75.00	-0.409	1.2765	0.3248
-70.00	-0.512	1.2212	0.3099
-65.00	-0.606	1.1532	0.2940
-60.00	-0.689	1.0731	0.2772
-55.00	-0.759	0.9822	0.2595
-50.00	-0.814	0.8820	0.2409
-45.00	-0.850	0.7742	0.2212
-40.00	-0.866	0.6610	0.2006
-35.00	-0.860	0.5451	0.1789
-30.00	-0.829	0.4295	0.1563
-25.00	-0.853	0.3071	0.1156
-24.00	-0.870	0.2814	0.1040
-23.00	-0.890	0.2556	0.0916
-22.00	-0.911	0.2297	0.0785
-21.00	-0.934	0.2040	0.0649
-20.00	-0.958	0.1785	0.0508
-19.00	-0.982	0.1534	0.0364
-18.00	-1.005	0.1288	0.0218
-17.00	-1.082	0.1037	0.0129
-16.00	-1.113	0.0786	-0.0028
-15.00	-1.105	0.0535	-0.0251
-14.00	-1.078	0.0283	-0.0419
-13.50	-1.053	0.0158	-0.0521
-13.00	-1.015	0.0151	-0.0610
-12.00	-0.904	0.0134	-0.0707
-11.00	-0.807	0.0121	-0.0722
-10.00	-0.711	0.0111	-0.0734
-9.00	-0.595	0.0099	-0.0772
-8.00	-0.478	0.0091	-0.0807
-7.00	-0.375	0.0086	-0.0825
-6.00	-0.264	0.0082	-0.0832
-5.00	-0.151	0.0079	-0.0841
-4.00	-0.017	0.0072	-0.0869
-3.00	0.088	0.0064	-0.0912
-2.00	0.213	0.0054	-0.0946
-1.00	0.328	0.0052	-0.0971
0.00	0.442	0.0052	-0.1014
1.00	0.556	0.0052	-0.1076
2.00	0.670	0.0053	-0.1126
3.00	0.784	0.0053	-0.1157
4.00	0.898	0.0054	-0.1199
5.00	1.011	0.0058	-0.1240
6.00	1.103	0.0091	-0.1234
7.00	1.181	0.0113	-0.1184
8.00	1.257	0.0124	-0.1163
8.50	1.293	0.0130	-0.1163
9.00	1.326	0.0136	-0.1160
9.50	1.356	0.0143	-0.1154
10.00	1.382	0.0150	-0.1149
10.50	1.400	0.0267	-0.1145
11.00	1.415	0.0383	-0.1143

Appendix A: FAST Input Files

11.50	1.425	0.0498	-0.1147
12.00	1.434	0.0613	-0.1158
12.50	1.443	0.0727	-0.1165
13.00	1.451	0.0841	-0.1153
13.50	1.453	0.0954	-0.1131
14.00	1.448	0.1065	-0.1112
14.50	1.444	0.1176	-0.1101
15.00	1.445	0.1287	-0.1103
15.50	1.447	0.1398	-0.1109
16.00	1.448	0.1509	-0.1114
16.50	1.444	0.1619	-0.1111
17.00	1.438	0.1728	-0.1097
17.50	1.439	0.1837	-0.1079
18.00	1.448	0.1947	-0.1080
18.50	1.452	0.2057	-0.1090
19.00	1.448	0.2165	-0.1086
19.50	1.438	0.2272	-0.1077
20.00	1.428	0.2379	-0.1099
21.00	1.401	0.2590	-0.1169
22.00	1.359	0.2799	-0.1190
23.00	1.300	0.3004	-0.1235
24.00	1.220	0.3204	-0.1393
25.00	1.168	0.3377	-0.1440
26.00	1.116	0.3554	-0.1486
28.00	1.015	0.3916	-0.1577
30.00	0.926	0.4294	-0.1668
32.00	0.855	0.4690	-0.1759
35.00	0.800	0.5324	-0.1897
40.00	0.804	0.6452	-0.2126
45.00	0.793	0.7573	-0.2344
50.00	0.763	0.8664	-0.2553
55.00	0.717	0.9708	-0.2751
60.00	0.656	1.0693	-0.2939
65.00	0.582	1.1606	-0.3117
70.00	0.495	1.2438	-0.3285
75.00	0.398	1.3178	-0.3444
80.00	0.291	1.3809	-0.3593
85.00	0.176	1.4304	-0.3731
90.00	0.053	1.4565	-0.3858
95.00	-0.074	1.4533	-0.3973
100.00	-0.199	1.4345	-0.4075
105.00	-0.321	1.4004	-0.4162
110.00	-0.436	1.3512	-0.4231
115.00	-0.543	1.2874	-0.4280
120.00	-0.640	1.2099	-0.4306
125.00	-0.723	1.1196	-0.4304
130.00	-0.790	1.0179	-0.4270
135.00	-0.840	0.9064	-0.4196
140.00	-0.868	0.7871	-0.4077
145.00	-0.872	0.6627	-0.3903
150.00	-0.850	0.5363	-0.3665
155.00	-0.798	0.4116	-0.3349
160.00	-0.714	0.2931	-0.2942
170.00	-0.749	0.0971	-0.3771
175.00	-0.374	0.0334	-0.1879
180.00	0.000	0.0198	0.0000

Appendix A: FAST Input Files

A.8. ServoDyn Input File

```
------- SERVODYN v1.05.* INPUT FILE ------------------------------------------
NREL 5.0 MW Baseline Wind Turbine for Use in Offshore Analysis. Properties from Dutch Offshore Wind Energy Converter (DOWEC) 6MW Pre-Design (10046_009.pdf) and REpower 5M 5MW (5m_uk.pdf)
---------------------- SIMULATION CONTROL --------------------------------------
False        Echo        - Echo input data to <RootName>.ech (flag)
"default"    DT          - Communication interval for controllers (s) (or "default")
---------------------- PITCH CONTROL -------------------------------------------
        0  PCMode       - Pitch control mode {0: none, 3: user-defined from routine PitchCntrl, 4: user-defined from Simulink/Labview, 5: user-defined from Bladed-style DLL} (switch)
        0  TPCOn        - Time to enable active pitch control (s) [unused when PCMode=0]
   9999.9  TPitManS(1)  - Time to start override pitch maneuver for blade 1 and end standard pitch control (s)
   9999.9  TPitManS(2)  - Time to start override pitch maneuver for blade 2 and end standard pitch control (s)
   9999.9  TPitManS(3)  - Time to start override pitch maneuver for blade 3 and end standard pitch control (s) [unused for 2 blades]
        2  PitManRat(1) - Pitch rate at which override pitch maneuver heads toward final pitch angle for blade 1 (deg/s)
        2  PitManRat(2) - Pitch rate at which override pitch maneuver heads toward final pitch angle for blade 2 (deg/s)
        2  PitManRat(3) - Pitch rate at which override pitch maneuver heads toward final pitch angle for blade 3 (deg/s) [unused for 2 blades]
        0  BlPitchF(1)  - Blade 1 final pitch for pitch maneuvers (degrees)
        0  BlPitchF(2)  - Blade 2 final pitch for pitch maneuvers (degrees)
        0  BlPitchF(3)  - Blade 3 final pitch for pitch maneuvers (degrees) [unused for 2 blades]
---------------------- GENERATOR AND TORQUE CONTROL ----------------------------
        1  VSContrl     - Variable-speed control mode {0: none, 1: simple VS, 3: user-defined from routine UserVSCont, 4: user-defined from Simulink/Labview, 5: user-defined from Bladed-style DLL} (switch)
        1  GenModel     - Generator model {1: simple, 2: Thevenin, 3: user-defined from routine UserGen} (switch) [used only when VSContrl=0]
     94.4  GenEff       - Generator efficiency [ignored by the Thevenin and user-defined generator models] (%)
True         GenTiStr     - Method to start the generator {T: timed using TimGenOn, F: generator speed using SpdGenOn} (flag)
True         GenTiStp     - Method to stop the generator {T: timed using TimGenOf, F: when generator power = 0} (flag)
   9999.9  SpdGenOn     - Generator speed to turn on the generator for a startup (HSS speed) (rpm) [used only when GenTiStr=False]
        0  TimGenOn     - Time to turn on the generator for a startup (s) [used only when GenTiStr=True]
   9999.9  TimGenOf     - Time to turn off the generator (s) [used only when GenTiStp=True]
---------------------- SIMPLE VARIABLE-SPEED TORQUE CONTROL --------------------
   1173.7  VS_RtGnSp    - Rated generator speed for simple variable-speed generator control (HSS side) (rpm) [used only when VSContrl=1]
  43093.55 VS_RtTq      - Rated generator torque/constant generator torque in Region 3 for simple variable-speed generator control (HSS side) (N-m) [used only when VSContrl=1]
  0.0255764 VS_Rgn2K    - Generator torque constant in Region 2 for simple variable-speed generator control (HSS side) (N-m/rpm^2) [used only when VSContrl=1]
```

Appendix A: FAST Input Files

```
    10   VS_SlPc      - Rated generator slip percentage in Region 2 1/2 for simple variable-speed
generator control (%) [used only when VSContrl=1]
---------------------- SIMPLE INDUCTION GENERATOR ------------------------------
    9999.9   SIG_SlPc     - Rated generator slip percentage (%) [used only when VSContrl=0 and
GenModel=1]
    9999.9   SIG_SySp     - Synchronous (zero-torque) generator speed (rpm) [used only when
VSContrl=0 and GenModel=1]
    9999.9   SIG_RtTq     - Rated torque (N-m) [used only when VSContrl=0 and GenModel=1]
    9999.9   SIG_PORt     - Pull-out ratio (Tpullout/Trated) (-) [used only when VSContrl=0 and
GenModel=1]
---------------------- THEVENIN-EQUIVALENT INDUCTION GENERATOR -----------------
    9999.9   TEC_Freq     - Line frequency [50 or 60] (Hz) [used only when VSContrl=0 and
GenModel=2]
     9998   TEC_NPol     - Number of poles [even integer > 0] (-) [used only when VSContrl=0 and
GenModel=2]
    9999.9   TEC_SRes     - Stator resistance (ohms) [used only when VSContrl=0 and GenModel=2]
    9999.9   TEC_RRes     - Rotor resistance (ohms) [used only when VSContrl=0 and GenModel=2]
    9999.9   TEC_VLL      - Line-to-line RMS voltage (volts) [used only when VSContrl=0 and
GenModel=2]
    9999.9   TEC_SLR      - Stator leakage reactance (ohms) [used only when VSContrl=0 and
GenModel=2]
    9999.9   TEC_RLR      - Rotor leakage reactance (ohms) [used only when VSContrl=0 and
GenModel=2]
    9999.9   TEC_MR       - Magnetizing reactance (ohms) [used only when VSContrl=0 and
GenModel=2]
---------------------- HIGH-SPEED SHAFT BRAKE ---------------------------------
        0   HSSBrMode    - HSS brake model {0: none, 1: simple, 3: user-defined from routine
UserHSSBr, 4: user-defined from Simulink/Labview, 5: user-defined from Bladed-style DLL} (switch)
    9999.9   THSSBrDp     - Time to initiate deployment of the HSS brake (s)
       0.6   HSSBrDT     - Time for HSS-brake to reach full deployment once initiated (sec) [used only
when HSSBrMode=1]
   28116.2   HSSBrTqF     - Fully deployed HSS-brake torque (N-m)
---------------------- NACELLE-YAW CONTROL ------------------------------------
        0   YCMode      - Yaw control mode {0: none, 3: user-defined from routine UserYawCont, 4:
user-defined from Simulink/Labview, 5: user-defined from Bladed-style DLL} (switch)
    9999.9   TYCOn       - Time to enable active yaw control (s) [unused when YCMode=0]
        0   YawNeut     - Neutral yaw position--yaw spring force is zero at this yaw (degrees)
9.02832E+09   YawSpr      - Nacelle-yaw spring constant (N-m/rad)
 1.916E+07   YawDamp     - Nacelle-yaw damping constant (N-m/(rad/s))
    9999.9   TYawManS     - Time to start override yaw maneuver and end standard yaw control (s)
        2   YawManRat    - Yaw maneuver rate (in absolute value) (deg/s)
        0   NacYawF      - Final yaw angle for override yaw maneuvers (degrees)
---------------------- TUNED MASS DAMPER --------------------------------------
False        CompNTMD     - Compute nacelle tuned mass damper {true/false} (flag)
"NRELOffshrBsline5MW_ServoDyn_TMD.dat"    NTMDfile     - Name of the file for nacelle tuned
mass damper (quoted string) [unused when CompNTMD is false]
False        CompTTMD     - Compute tower tuned mass damper {true/false} (flag)
"NRELOffshrBsline5MW_ServoDyn_TMD.dat"    TTMDfile     - Name of the file for tower tuned
mass damper (quoted string) [unused when CompTTMD is false]
---------------------- BLADED INTERFACE ---------------------------------------- [used only with Bladed
Interface]
"ServoData/DISCON_x64.dll"    DLL_FileName - Name/location of the dynamic library {.dll
[Windows] or .so [Linux]} in the Bladed-DLL format (-) [used only with Bladed Interface]
"DISCON.IN"    DLL_InFile   - Name of input file sent to the DLL (-) [used only with Bladed
Interface]
```

Appendix A: FAST Input Files

```
"DISCON"     DLL_ProcName - Name of procedure in DLL to be called (-) [case sensitive; used only
with DLL Interface]
"default"    DLL_DT       - Communication interval for dynamic library (s) (or "default") [used only
with Bladed Interface]
false        DLL_Ramp     - Whether a linear ramp should be used between DLL_DT time steps
[introduces time shift when true] (flag) [used only with Bladed Interface]
   9999.9  BPCutoff     - Cuttoff frequency for low-pass filter on blade pitch from DLL (Hz) [used
only with Bladed Interface]
        0  NacYaw_North - Reference yaw angle of the nacelle when the upwind end points due
North (deg) [used only with Bladed Interface]
        0  Ptch_Cntrl   - Record 28: Use individual pitch control {0: collective pitch; 1: individual pitch
control} (switch) [used only with Bladed Interface]
        0  Ptch_SetPnt  - Record  5: Below-rated pitch angle set-point (deg) [used only with Bladed
Interface]
        0  Ptch_Min     - Record  6: Minimum pitch angle (deg) [used only with Bladed Interface]
        0  Ptch_Max     - Record  7: Maximum pitch angle (deg) [used only with Bladed Interface]
        0  PtchRate_Min - Record  8: Minimum pitch rate (most negative value allowed) (deg/s) [used
only with Bladed Interface]
        0  PtchRate_Max - Record  9: Maximum pitch rate  (deg/s) [used only with Bladed Interface]
        0  Gain_OM      - Record 16: Optimal mode gain (Nm/(rad/s)^2) [used only with Bladed
Interface]
        0  GenSpd_MinOM - Record 17: Minimum generator speed (rpm) [used only with Bladed
Interface]
        0  GenSpd_MaxOM - Record 18: Optimal mode maximum speed (rpm) [used only with
Bladed Interface]
        0  GenSpd_Dem   - Record 19: Demanded generator speed above rated (rpm) [used only with
Bladed Interface]
        0  GenTrq_Dem   - Record 22: Demanded generator torque above rated (Nm) [used only with
Bladed Interface]
        0  GenPwr_Dem   - Record 13: Demanded power (W) [used only with Bladed Interface]
---------------------- BLADED INTERFACE TORQUE-SPEED LOOK-UP TABLE -------------
        0  DLL_NumTrq   - Record 26: No. of points in torque-speed look-up table {0 = none and use
the optimal mode parameters; nonzero = ignore the optimal mode PARAMETERs by setting Record
16 to 0.0} (-) [used only with Bladed Interface]
 GenSpd_TLU   GenTrq_TLU
 (rpm)        (Nm)
---------------------- OUTPUT --------------------------------------------------
True         SumPrint     - Print summary data to <RootName>.sum (flag) (currently unused)
        1  OutFile      - Switch to determine where output will be placed: {1: in module output file only;
2: in glue code output file only; 3: both} (currently unused)
True         TabDelim     - Use tab delimiters in text tabular output file? (flag) (currently unused)
"ES10.3E2"   OutFmt       - Format used for text tabular output (except time).  Resulting field should
be 10 characters. (quoted string) (currently unused)
        0  TStart       - Time to begin tabular output (s) (currently unused)
           OutList      - The next line(s) contains a list of output parameters.  See OutListParameters.xlsx
for a listing of available output channels, (-)
"GenPwr"                - Electrical generator power and torque
"GenTq"                 - Electrical generator power and torque
END of input file (the word "END" must appear in the first 3 columns of this last OutList line)
---------------------------------------------------------------------------------------
```

This page is intentionally left blank.

List of Publications

Peer-reviewed journal articles

1- "Aeroelastic Analysis of a Coplanar Twin-Rotor Wind Turbine", Amr Ismaiel, and Shigeo Yoshida, energies, doi:10.3390/en12101881, 12, 1881, 1-21, 2019.05.

2- "Study of Turbulence Intensity Effect on the Fatigue Lifetime of Wind Turbines", Amr Ismaiel, and Shigeo Yoshida, Evergreen, 5, 1, 25-32, 2018.03.

3- "Fatigue analysis of an optimized HAWT composite blade", Amr Ismaiel, Sayed Metwalli, Basman El-Hadidi, and Shigeo Yoshida, Evergreen, 4, 2/3, 1-6, 2017.09.

4- "System Identification, Fuzzy Control, and Simulation Results for Fixed length Tether of Kite Power System.", Dief T. N., Fechner U., Schmehl R., Yoshida S., Ismaiel A. M., Halawa A. M., Wind Energy Science, 5, 1, pp. 275, 2018.

Peer-reviewed conference articles

1- "Fatigue analysis of an optimized HAWT composite blade", Amr Ismaiel, Sayed Metwalli, Basman El-Hadidi, and Shigeo Yoshida, IEICES III, Fukuoka, Japan.

List of Publications

2- “Verification of equivalent isotropic model for a composite HAWT blade”, Amr Ismaiel, Sayed Metwalli, Basman El-Hadidi, and Shigeo Yoshida, CSS-EEST18, Shanghai, China.

3- “Study of Turbulence Intensity Effect on the Fatigue Lifetime of Wind Turbines”, Amr Ismaiel, and Shigeo Yoshida, IEICES IV, Fukuoka, Japan.

4- “Fluid-Structure Interaction Computations for Wind Turbine Blade”, Halawa A. M., Amr Ismaiel, and Shigeo Yoshida, GRE 2018, Yokohama, Japan.

5- “Wind turbulence effect investigation on fatigue of horizontal axis wind turbine (HAWT)” Amr Ismaiel, and Shigeo Yoshida, CSS-EEST20, Busan, Korea.

Vitae

Amr Ismaiel was born in Cairo, Egypt in October 1990. In 2012, he got his Bachelor of Science degree in Aerospace Engineering from the Faculty of Engineering, Cairo University. Afterwards, he pursued his Master studies in the department of Mechanical Design, Cairo University, majoring in Aeroelasticity and got his Master of Science in Mechanical Engineering in 2016. During the period 2012-2016, he was employed as a teaching assistant in the Mechatronics Department, at the Faculty of Engineering and Technology at Future University in Egypt (FUE). In October 2016, he joined the Earth System Science and Technology (ESST) department in the Interdisciplinary Graduate School of Engineering Sciences (IGSES) at Kyushu University as a PhD student working on aeroelastic modelling and analysis of multi-rotor systems wind turbines.